VIRGINIA POLYTECHNIC INSTITUTE AND STATE UNIVERSITY PRESENTS

THE CASPER

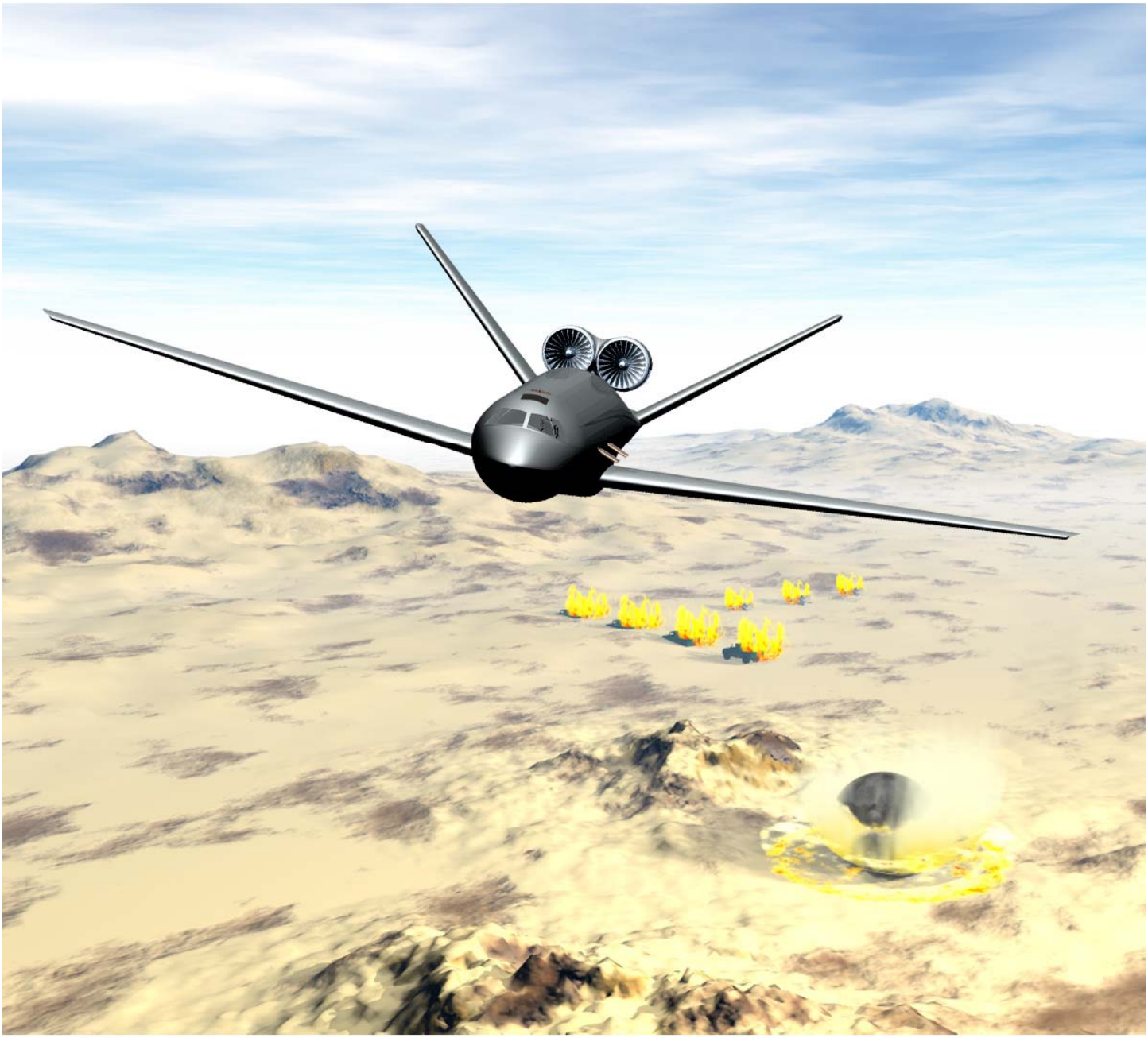

TEAM CASPER

2004/2005 AIAA Undergraduate Design Competition
Virginia Polytechnic and State University
June 10, 2005

Brian Call (223476) Group Leader / Costs	Ian Marley (235169) Performance	Andrew Hopkins (220496) Configuration
Jennifer Klein (225959) Structures / Weights	Rui Chen (223472) Aerodynamics	Jeffery Wilson (254845) Stability and Control / Survivability
Doug Morton (253581) Weapons	Richard Harris (253182) Avionics	Ryan Haac (253681) Weapons Configuration
Thomas Billheimer (254828) Materials	William Mason Faculty Advisor	Mike Cavanaugh Faculty Advisor

Executive Summary

Team Casper presents their self-titled aircraft, the Casper, as a solution to the 2004-2005 AIAA Team Undergraduate Design Competition. The Request for Proposal (RFP) requires a low cost, highly survivable aircraft capable of laying persistent firepower upon low value targets. This report includes estimates of the size, weight, performance, and cost of the new gunship design, as well as a detailed layout.

A comparator aircraft study revealed that all of the existing aircraft that meet the necessary range and cruise requirements far exceeded the 15,000 *lbs* payload requirement by more than 200%. This information confirms the need for an optimized design of a smaller and lighter aircraft. Initial sizing approximations estimated the gross takeoff weight of the Casper to be 89,911 *lbs*.

The Casper has a round cross-sectioned fuselage with low mounted un-swept wings and a rear V-Tail. The majority of the structure is made of aluminum alloys in order to reduce the overall costs of the aircraft, while composites and high-strength alloys will be used for critical structural components. The Casper is powered by two scaled AIAA engines that are mounted on the top of the fuselage, with high-temperature surfaces hidden by the V-Tail and engine nacelles. A standard cockpit system and an integrated modular avionics system, both utilizing Honeywell products, have been selected for use on the Casper.

Using countermeasure systems alone, the Casper meets the survivability requirement stated in the RFP. The probability of kill per encounter, $P_{K/E}$, was determined to be 0.076 for anti-aircraft artillery (AAA) threats and 0.095 for man-portable air defense systems (MANPADS). With the addition of a more protective structure and the aforementioned engine placement and thermal signature reduction, these $P_{K/E}$ values will be further reduced.

The primary weapons on board the Casper are two 40 *mm* Bofors cannons, one GAU-12 gatling gun, and an internal bomb bay capable of carrying three GBU-12 Paveway II guided bombs. The highly adaptable nature of the fuselage and weapons bay allows for the use of available cluster bombs, bomb variants, and nontraditional weapons.

THE CASPER

TYPE: Twin-engine advanced gunship to be operated by the U.S. Military

WINGS: Un-swept, high aspect ratio design

FUSELAGE: Circular, conventional design with modified empennage to allow for placement of engines between a dihedral tail

TAIL: Swept dihedral tail

LANDING GEAR: Dual configuration, tricycle arrangement with titanium struts and shocks

POWERPLANT: 54.5% scaled down version of the AIAA supplied high bypass turbofan engine deck

ACCOMODATIONS: Interior layout allows for adaptation for future missions and weapon systems. The cockpit seats 5 crew members and includes a lavatory.

DIMENSIONS:

Wingspan:	93’-6”
Overall length:	96’-8”
Overall height:	22’-6”
Fuselage diameter:	10’
TOGW:	89911 *lbs*

PERFORMANCE:

Cruise speed:	400 *knots*
Rate of climb:	6380 *fpm*
Design range:	2850 *nm*
Ferry range:	3237 *nm*

Table of Contents

EXECUTIVE SUMMARY ..... **II**

TABLE OF CONTENTS ..... **IV**

INDEX OF FIGURES ..... **VI**

INDEX OF TABLES ..... **VII**

INDEX OF FOLDOUTS ..... **VIII**

INDEX OF ACRONYMS ..... **IX**

INDEX OF SYMBOLS ..... **X**

1. INTRODUCTION AND REQUEST FOR PROPOSAL **1**

1.1 INTRODUCTION 1
1.2 RESPONDING TO THE RFP 1

2. COMPARATOR AIRCRAFT **3**

3. INITIAL SIZING **4**

3.1 PRELIMINARY CONSIDERATIONS 4
3.1.1 Manned Vs. Unmanned *4*
3.1.2 Comparable Aircraft and Weapons Systems *5*
3.2 WEIGHT ESTIMATION 6
3.3 STANDARD CONFIGURATION SIZING 7
3.4 BLENDED WING BODY SIZING 9

4. CONCEPTUAL DESIGNS **10**

4.1 CONCEPT 1 – CONVENTIONAL TRANSPORT 11
4.1.1 High, Aft-Swept Wings *11*
4.1.2 Wing Mounted Engines *12*
4.1.3 Conventional Tail *12*
4.1.4 Payload/Weapons Configuration *12*
4.2 CONCEPT 2 – CONVENTIONAL DESIGN WITH DIHEDRAL 12
4.2.1 V-Tail *13*
4.2.2 Rear Mounted Engines *13*
4.2.3 Payload Weapons Configuration *14*
4.3 CONCEPT 3 - BLENDED WING BODY 14
4.3.1 Aerodynamic Efficiency *15*
4.3.2 Multi-functional Control Surfaces *15*
4.3.3 Winglets *16*
4.3.4 Top-Mounted Engines *16*
4.3.5 Payload Weapons Configuration *16*

5. ARRIVING AT THE PREFERRED CONCEPT **17**

5.1 DECISION MATRIX CATEGORIES 17
5.1.1 Marketability *17*
5.1.2 Maintainability *17*
5.1.3 Takeoff / Landing Durability *18*
5.1.4 Stability and Controllability *18*
5.1.5 Acquisition Costs *18*
5.1.6 Lifetime Cost *18*
5.1.7 Survivability *19*
5.2 DECISION MATRIX RATING SYSTEM 19
5.3 CONCEPT EVALUATIONS 19

5.3.1 Concept 1 ..... *20*
5.3.2 Concept 2 ..... *21*
5.3.3 Concept 3 ..... *22*
5.3.3 Preferred Concept *23*
5.3.4 Progression of Preferred Concept *23*

6. MISSION SYSTEMS **25**

6.1 WEAPONS 25
6.1.1 40 mm Bofors Cannons *26*
6.1.2 GAU-12 25mm Equalizer *27*
6.1.3 GBU-12 Laser Guided Bomb *28*
6.1.4 Weapons Configuration *29*
6.1.5 Investigation of non-traditional weapons *31*
6.2 SURVIVABILITY AND COUNTER-MEASURE SYSTEM 32
6.2.1 Fire Detection & Suppression *33*
6.2.2 Fuel Tank Ullage *33*
6.2.3 Flare Dispensers *33*
6.2.4 Overall $P_{k/e}$ Reduction *34*
6.3 ELECTRONIC SYSTEMS 35
6.3.1 Cockpit *35*
6.3.2 Fly-by-Light *36*
6.3.3 Cockpit Systems *37*
6.3.4 Weapons Console *37*
6.3.5 Hydraulics *37*
6.3.6 Power Systems *38*
6.3.7 Survivability systems *38*
6.3.8 Deicing *38*
6.3.9 Fuel system *39*
6.3.9.1 Fuel Storage 39
6.3.9.2 Mid-Air Refueling 40
6.3.10 Additional Systems *40*

7. MATERIALS AND STRUCTURES **42**

7.1 MATERIALS 42
7.2 V-N DIAGRAM 45
7.2 WING STRUCTURAL LAYOUT 46
7.3 WING STRUCTURAL ANALYSIS 46
7.4 FUSELAGE DESIGN 50
7.5 LANDING GEAR 50
7.5.1 Gear Retraction *52*

8. WEIGHTS AND BALANCE **53**

9. AERODYNAMICS **56**

9.1. AIRFOIL SELECTION 56
9.2. WING GEOMETRY 58
9.3. PREDICTION OF AIRPLANE LIFT 59
9.3.1 Takeoff, Landing and loitering *59*
9.3.2. Cruise *61*
9.4 PREDICTION OF AIRPLANE DRAG POLAR 61
9.4.1 Takeoff, landing and loitering *62*
9.4.2 Cruise *63*

10. STABILITY AND CONTROL **65**

10.1 WING PLACEMENT, TAIL DESIGN AND SIZING 65
10.2 CONTROL SURFACES 65

10.3 Control Deflections for Trim and Takeoff 66
10.4 Stability and Control Derivatives 66
10.5 Dynamic Response 68
10.6 Roll Performance 70
10.7 System Considerations 70

11. PROPULSION 71

11.1 Nacelle Design 71
11.2 Engine Removal 72

12. PERFORMANCE 73

12.1 Takeoff and Landing Performance 73
12.2 Rate of Climb, Ceilings and Time to Climb 75
12.3 Cruise/Range Performance and Level Flight Envelope 79
12.4 Endurance and Loiter 80
12.5 Maneuvering 81
12.6 Performance Summary 81

13. COST ESTIMATION 83

13.1 Research and Development 83
13.2 Average Acquisition Cost 83
13.3 Operational Cost 84
13.4 Cost Summary 85

14. COROLLARY MISSIONS AND AIRCRAFT VARIANTS 86

REFERENCES 87

Index of Figures

Figure 1. Primary mission profile 2
Figure 2. Similar Aircraft Weight Estimation Plot 6
Figure 3. High lift device employments based on lift coefficient and wing sweep 7
Figure 4. Constraint plot showing relationship between T/W and W/S and optimum design point 8
Figure 5. TOGW Carpet Plot 9
Figure 6. Concept evolution 10
Figure 7. Concept 1 layout and sizing 11
Figure 8. Concept 2 layout and sizing 13
Figure 9. Concept 3 layout and sizing 14
Figure 10. Blended wing body control system architecture[5] 15
Figure 11. 40mm Bofors Cannon 26
Figure 12. Dispersion of a 40mm cannon on ship in sea states of 4-5 at a 10,000 ft firing distance 27
Figure 13. GAU-12 25mm Equalizer 28
Figure 14. GBU-12 Laser Guided Bomb 28
Figure 15. Weapons configuration w/ pressurization hood 29
Figure 16. Instantaneous and total target area for 20,000 ft turn radius 30
Figure 17. Instantaneous and total target area for 6,500 ft turn radius 31
Figure 18. General systems layout 35
Figure 19. Three-dimensional cut-away of cockpit layout 36
Figure 20. Weapons console 37
Figure 21. Fuel system layout (bladder tanks are depicted in red and fuel lines for aerial refueling in blue) 39
Figure 22. The Casper in a midair refueling 40
Figure 23. Color-coded layout of primary materials used 42
Figure 24. V-n Diagram showing load factor as a function of airspeed 45
Figure 25. Wing structural layout 46
Figure 26. Shear Force over the semi-span of the wing due to an elliptical lift distribution, n = 3.5 47

FIGURE 27. BENDING MOMENT ACROSS THE SEMI-SPAN OF THE WING DUE TO AN ELLIPTICAL LIFT DISTRIBUTION, N = 3.5 47
FIGURE 28. THEORETICAL REPRESENTATION OF WING BOX 48
FIGURE 29. WING BOX CONSTRAINT DIAGRAM: SHOWS THE OPTIMUM AREA OF THE FLANGE TO BE 10.89 IN^2 49
FIGURE 30. DIAGRAM SHOWING THE INERTIA OF THE WING BOX IS ALWAYS GREATER THAN THE REQUIRED MINIMUM MOMENT OF INERTIA ACROSS THE SPAN OF THE WING. 50
FIGURE 31. MAIN LANDING GEAR EXTENDED 51
FIGURE 32. RETRACTION AND SPECIFICATIONS OF THE NOSE LANDING GEAR 52
FIGURE 33. RETRACTION AND SPECIFICATIONS OF THE MAIN LANDING GEAR 53
FIGURE 34. CG TRAVEL FOR THE DESIGN MISSION 55
FIGURE 35. CG TRAVEL FOR THE FERRY MISSION 56
FIGURE 36. NASA SC(2)-0714 AIRFOIL USED FOR WING 57
FIGURE 37. NASA SC(2)-0012 AIRFOIL FOR V-TAIL 57
FIGURE 38. CRITICAL MACH NUMBER VS. QUARTER-CHORD SWEEP 58
FIGURE 39. HOERNER WINGTIP USED TO REDUCE DRAG 59
FIGURE 40. WING WITH FOWLER FLAPS DEFLECTED 60
FIGURE 41. TRIMMED SUBSONIC AIRPLANE LIFT CURVES 60
FIGURE 42. TRIMMED AIRPLANE LIFT CURVE AT CRUISE MACH NUMBER OF 0.7 61
FIGURE 43. TRIMMED AIRPLANE DRAG POLAR AT TAKEOFF, LANDING AND LOITERING CONDITIONS 63
FIGURE 44. TRIMMED DRAG POLAR AT CRUISE CONDITIONS 64
FIGURE 45. PANELING SCHEME FOR AVL CODE SHOWING WINGS AND V-TAIL 67
FIGURE 46. ROLL PERFORMANCE VS. FLIGHT PHASE GA REQUIREMENT 70
FIGURE 47. NACELLE DESIGN WITH BOTH ENGINES IN A SINGLE HOUSING 71
FIGURE 48. DEMONSTRATION OF ENGINE REMOVAL FROM NACELLE 72
FIGURE 49. MILITARY REQUIREMENTS FOR TAKEOFF ANALYSIS 74
FIGURE 50. MILITARY REQUIREMENTS FOR LANDING ANALYSIS 75
FIGURE 51. HODOGRAM DIAGRAM SHOWING RATE OF CLIMB AT SEA LEVEL 76
FIGURE 52. ABSOLUTE, SERVICE, AND CRUISE CEILING FOR FIRST LEG OF PRIMARY MISSION 77
FIGURE 53. ABSOLUTE, SERVICE, AND CRUISE CEILING FOR RETURN LEG OF PRIMARY MISSION 78
FIGURE 54. PAYLOAD-RANGE DIAGRAM 79
FIGURE 55. 1-G LEVEL FLIGHT ENVELOPE AT MAXIMUM WEIGHT 80
FIGURE 56. BREAKDOWN OF THE CASPER'S R&D COST 83
FIGURE 57. AVERAGE ACQUISITION COST PER AIRCRAFT PRODUCED 84
FIGURE 58. BREAKDOWN OF OPERATIONAL COST 85

Index of Tables

TABLE 1. COMPARATOR AIRCRAFT SPECIFICATIONS 3
TABLE 2. CATEGORY WEIGHTING FOR DECISION MATRIX 19
TABLE 3. DECISION MATRIX EVALUATION FOR CONCEPT 1 20
TABLE 4. DECISION MATRIX EVALUATION FOR CONCEPT 2 21
TABLE 5. DECISION MATRIX EVALUATION FOR CONCEPT 3 22
TABLE 6. EVALUATION RESULTS FROM DECISION MATRIX 23
TABLE 7. CONSIDERED WEAPONS SYSTEMS 25
TABLE 8. OVERALL SURVIVABILITY ESTIMATES 34
TABLE 9. MATERIALS USED (COLOR CODED FOR AIRCRAFT LOCATION ILLUSTRATION) 42
TABLE 10. WEIGHT BREAKDOWN 54
TABLE 11. DETAILED WING GEOMETRY 59
TABLE 12. DRAG COEFFICIENT BREAKDOWN FOR TAKEOFF AND LANDING 62
TABLE 13. CRUISE PARASITE DRAG BY COMPONENT 64
TABLE 14. LIFT TO DRAG RATIO FOR DIFFERENT MISSION SEGMENTS 64
TABLE 15. V-TAIL PLANFORM CHARACTERISTICS 65
TABLE 16. STABILITY AND CONTROL DERIVATIVES 68
TABLE 17. CLASS A DYNAMIC RESPONSE PROPERTIES 69
TABLE 18. CLASS B DYNAMIC RESPONSE PROPERTIES 69
TABLE 19. CLASS C DYNAMIC RESPONSE PROPERTIES 69

TABLE 20. RFP PERFORMANCE REQUIREMENTS 73
TABLE 21. TAKEOFF LENGTH AND BALANCED FIELD LENGTH FOR VARIOUS GROUND SURFACE TYPES....74
TABLE 22. BREAKDOWN OF LANDING FIELD LENGTH FOR VARIOUS GROUND SURFACE TYPES 75
TABLE 23. SUMMARY OF CLIMBING PERFORMANCE AT SEA LEVEL....76
TABLE 24. ABSOLUTE, SERVICE, AND CRUISE CEILING FOR FIRST LEG OF PRIMARY MISSION 77
TABLE 25. ABSOLUTE, SERVICE, AND CRUISE CEILING FOR RETURN LEG OF PRIMARY MISSION 78
TABLE 26. LOITER/ENDURANCE DATA FOR PRIMARY MISSION 80
TABLE 27. 1.5*G* MANEUVERING PERFORMANCE AT 20,000 *FT* AND V=208 *KNOTS* 81
TABLE 28. PERFORMANCE SUMMARY 82
TABLE 29. COST SUMMARY 85

Index of Foldouts

FOLDOUT 1. The Casper General Layout……..……..III
FOLDOUT 2. Casper General Arrangement…..……...24
FOLDOUT 3. Casper Systems Layout…...……..41
FOLDOUT 4. Casper Structural Design…….……...44

Index of Acronyms

AAA	Anti-Aircraft Artillery
AESA	Active Electronically Scanned Arrays
AGM	Air-to-Ground Munitions
AIAA	American Institute of Aeronautics and Astronautics
APU	Auxiliary Power Unit
AVL	Athena Vortex Lattice
BLI	Boundary Layer Ingestion
BFL	Balanced Field Length
BOFI	Bofors Optronic Fire-control Instrument
BWB	Blended Wing Body
CG	Center of Gravity
DAPCA	Development and Procurement Costs of Aircraft
EGPWS	Enhanced Ground Proximity Warning System
EMEDS	Electro-Mechanical Expulsion Deicing System
ETCAS	Enhanced Traffic Collision Awareness System
FAR	Federal Aviation Regulation
FS	Factor of Safety
GNSSU	Global Navigation Satellite Sensor Unit
GPS	Global Positioning System
IIR	Imaging Infrared
IMA	Integrated Modular Avionics
INS	Inertial Navigation System
IR	Infrared
IRCM	Infra-red Countermeasure Systems
JSOW	Joint Stand-Off Weapon
LCD	Liquid Crystal Display
LCOSS	Lead Computing Optical Sight System
MANPADS	Man Portable Air Defense Systems
MSL	Mean Sea Level
RDT&E	Research, Development, Testing and Engineering
RFP	Request for Proposal
SAR	Synthetic Aperture Radar
SC	Supercritical
SFC	Specific Fuel Consumption
SOJ	Stand-off Jamming
STOJ	Stand-Off Jamming
TOGW	Takeoff Gross Weight
UAV	Unmanned Aerial Vehicle
VIA	Versatile Integrated Avionics

Index of Symbols

ε	Washout angle
Γ	Dihedral angle
λ	Taper ratio
$\Lambda_{1/4}$	Quarter-chord wing sweep angle
ρ	Air density
ζ_{SP}	Short period damping coefficient
ω_{SP}	Short period natural frequency
ζ_{Ph}	Phugoid damping coefficient
ω_{Ph}	Phugoid natural frequency
ζ_{DR}	Dutch roll damping coefficient
ω_{DR}	Dutch roll natural frequency
Af	Flange area
AR	Aspect Ratio
b_f	Width of wing box
b_w	Height of wing box
C_D	Drag coefficient
C_{D0}	Parasite drag coefficient
C_{HT}	Horizontal tail volume coefficient
$C_{l\delta rv}$	Rolling moment due to ruddervator deflection derivative
$C_{l\delta a}$	Rolling moment due to aileron derivative
$C_{l\beta}$	Rolling moment due to sideslip derivative
C_{lr}	Rolling moment due to yaw-rate derivative
C_{lp}	Rolling moment due to roll-rate derivative
C_L	Lift coefficient
$C_{L\alpha}$	Lift curve slope
$C_{L\delta rv}$	Lift due to elevator deflection derivative
C_{Lcr}	Critical lift coefficient
C_{Lmax}	Maximum lift coefficient
C_{Lq}	Lift due to pitch rate derivative
C_m	Pitching moment coefficient
$C_{m\alpha}$	Static longitudinal stability derivative
C_{mq}	Pitching moment due to pitch rate derivative
$C_{m\delta rv}$	Pitching moment due to pitch rate derivative
$C_{n\delta rv}$	Yawing moment due to ruddervator derivative
$C_{n\delta a}$	Yawing moment due to aileron derivative
$C_{n\beta}$	Yawing moment due to sideslip derivative
C_{nr}	Yawing moment due to yaw-rate derivative
C_{np}	Yawing moment due to roll-rate derivative
C_{nmax}	Maximum load factor coefficient
C_{nmin}	Minimum load factor coefficient
$C_{Y\beta}$	Side force due to sideslip derivative
C_{Yr}	Side force due to yaw-rate derivative
C_{VT}	Vertical tail volume coefficient
E/ρ	Young's specific modulus
G/ρ	Shear specific modulus
i	Incidence angle
I	Area moment of inertia
L/D	Lift to drag ratio
M_{crit2D}	2-D critical Mach number
M_{crit3D}	3-D critical Mach number
M_{DD}	Drag divergence Mach number
M_{MAX}	Maximum Mach number
P_D	Probably of being detected by enemy
$P_{k/e}$	Probability of kill per encounter
P_{KSS}	Probability of kill by single shot
P_L	Probability of enemy weapon launch
R^2	Correlation coefficient
RC	Rate of climb
S	Planform area
S_2	Landing distance after braking
S_{AIR}	Landing distance before touchdown
S_B	Landing distance before braking
S_{TO}	Takeoff distance
S_{TOG}	Takeoff ground run distance
S_{TOTAL}	Total landing distance
t/c	Thickness ratio
t_f	Thickness of flange
t_w	Thickness of the web
T/W	Thrust to weight ratio
V_{cruise}	Cruise Speed
V_{dive}	Dive Speed
V_{Gmax}	Speed of maximum gust
V_{LOF}	Speed at liftoff
V_{man}	Maneuvering Speed in KEAS
V_{manu}	Maneuvering Speed
V_{STALL}	Stall speed
V_{STO}	Takeoff stall speed
W_{CREW}	Weight of crew
W_E	Empty weight
W_F	Weight of the fuel
W_{PL}	Weight of the payload
W_{tfo}	Weight of trapped fuel and oil
W_{TO}	Takeoff gross weight
W/S	Wing loading

1. Introduction and Request for Proposal

1.1 Introduction

For the 2004-2005 Undergraduate Design Competition, the AIAA has requested a new design for a low cost, highly survivable gunship that can deliver precise and persistent firepower. The primary mission for the design was stated to be the interdiction and destruction of low value targets, including personnel, trucks, light armored vehicles, and small buildings.

1.2 Responding to the RFP

One of the main features mentioned in the RFP is the survivability of the aircraft, specifically against MANPADS and AAA threats. The $P_{K/E}$ must be less than 0.1 for both threats. This means that the aircraft must be able to avoid being hit by these weapons systems, or once hit, be able to survive. The design of the aircraft will incorporate a structure that promotes survivability and will use counter measures to achieve the desired $P_{K/E}$. Another key performance parameter of the gunship design is that it must be able to sustain a load factor of 3.5 with a 1.5 Factor of Safety (FS).

The gunship should be designed to carry a payload of 15,000 *lbs*. This payload includes the armament, ammunition, and weapons but does not include the avionics or sensors. The payload should be designed to maximize lethality, precision, persistence, flexibility and affordability. For this reason, low-cost fire power has been investigated as well as the possibility of non-traditional weapons such as lasers and other non-lethal directed energy weapons.

The primary mission of the designed gunship, as shown in Figure 1, includes a 500 *nm* flight radius, a 4 *hr* time on station, and a payload deployment segment.

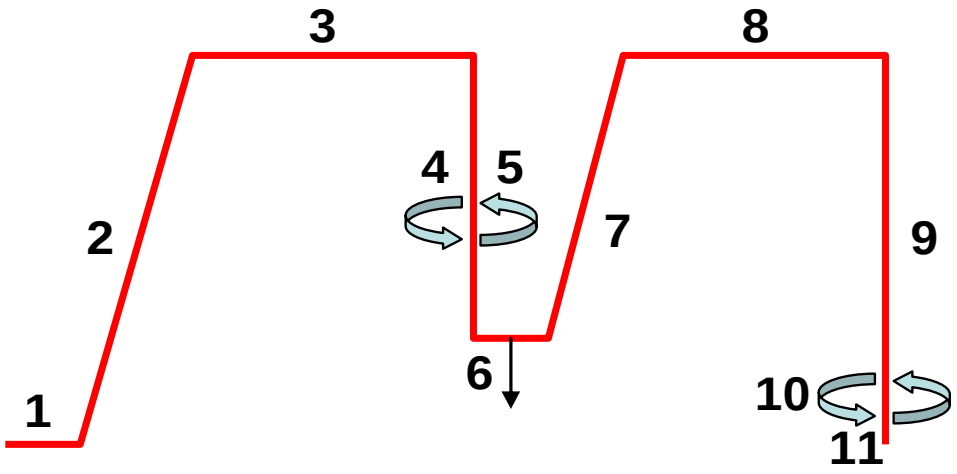

1) **Warm-up and Takeoff**
   a) **Taxi and Warm-up at idle engine power for 20 minutes**
   b) **Takeoff at maximum takeoff power for 2 minutes**
2) **Climb at maximum power and best climb speed to best cruise altitude (Altitude must be greater than 30,000 ft.**
3) **Cruise at best cruise speed and altitude to the target area at least 500 nautical miles away. (Speed must be greater than 400 kts and altitude must be greater than 30,000 ft)**
4) **Loiter at 20,000 ft for at least 4 hours**
5) **Sustain a maneuver of at least 1.5g's at 20,000 ft**
6) **Descend to 10,000 ft to identify target and expend payload.**
7) **Climb at maximum power and best climb speed to best cruise altitude (Altitude must be greater than 30,000 ft)**
8) **Cruise at best cruise speed and altitude back to base. (Speed must be greater than 400 kts and altitude must be greater than 30,000 ft)**
9) **Descend to sea level**
10) **Loiter for 30 minutes at sea level**
11) **Land with a reserve fuel of at least 5% of total mission fuel.**

Figure 1. Primary mission profile

A secondary mission of the gunship is the ferry mission, which is essentially the transportation of the fully loaded aircraft at least 2600*nm*. Although the aircraft must be capable of aerial refueling, both the ferry and design missions must be completed without refueling. The most crucial difference between the ferry mission and the design mission is that the payload is not deployed during the ferry mission. For this reason, the maximum landing weight of the aircraft is an important consideration for the ferry mission. As specified in the RFP, the landing weight is to be no greater than 80% of the total takeoff gross weight (TOGW).

2. Comparator Aircraft

Before beginning the preliminary design of an aircraft to meet the requirements of the RFP, existing aircraft were investigated to determine if the requirements could be met with a currently used platform. The aircraft presented here are the *A-10 Thunderbolt*, *Kawasaki C-1*, *Su-25 Frogfoot*, *AN-72 Coaler*, *Boeing YC-14 Transport*, *McDonnel Douglas YC-15*, *AC-130 Spectre*, *AC-130 Spooky*, and *Boeing C-40*. Specifications for these aircraft are displayed in Table 1.

Table 1. Comparator Aircraft Specifications

Aircraft	AC-130 Spectre	AC-130 Spooky	C-40 / Boeing 737	A-10 Thunderbolt	Kawasaki C-1	Su-25 Frogfoot	Boeing YC-14 Transport	McDonnel Douglas YC-15
Cruise (knts)	291	291	513	282	355	377	390	390
Max Speed (knts)	330	365		365	440	527	438	434
Cruise Altitude (ft)	25,000	25,000		45,000	35,000			
Range (NM)	1,300	1,300	3,000	695	702	675	2,719	2,719
Gross Weight (lbs)	155,000	155,000	171,000	21,500	99,210	21,605	225,000	216,680
Fuel Weight (lbs)	45,900	45,900	57,400	10,700	19,403	8,500	62,736	51,961
Payload (lbs)	41,800	41,800	40,000	16,000	26,235	11,023	34,566	59,341
Wing Span (ft)	132.58	132.58	113.00	57.50	100.42	47.17	129.00	110.33
Wing area (sq. ft)	1,745.00	1,745.00	1,344.00	506.40	1,297.00	362.74	1,762.00	1,740.00
Wing Aspect Ratio	10.10	10.10	9.30	6.54	7.80	7.00	9.44	7.00
Aircraft Length (ft)	97.75	97.75	110.33	53.33	95.1	50.85	131.67	124.25
Total Thrust	19,640 HP	19,640 HP	54000 lbs	18130	29,000 lbs	19,842 lbs	102,000 lbs	64,000 lbs
W/S at MTOGW (lb/sq. ft)	88.8	88.8	127.2	98.8	76.5	146	127.7	124.5
T/W at MTOGW			0.316	0.6	0.3	0.53	0.4	0.3
Cost (million US $)	46.5	72	70	13		8.3		

The RFP states that the proposed aircraft must have a cruise speed of 400 *knots*. Of the aircraft shown in Table 1, only one exceeds this requirement: the *Boeing C-40*, which has a cruise speed of 512 *knots*. The *YC -14*, *YC-15*, *Su-25*, and *C-1* all come very close with cruise speeds of 390, 390, 377, and 355 *knots* respectively. Since an "over-engineered" aircraft is not desired, the *YC-14* and *YC-15* are considered to be the best match to the RFP for this parameter, with differences of only 2.5% from the desired value of cruise speed.

The primary mission requirements for the range of the aircraft are a 500 *nm* radius with a 4 *hr* loiter period, while the secondary ferry mission requires a 2600nm range. The *C-40*, *YC-14*, and *YC-15* all meet this requirement with ranges of 3000, 2700, and 2700 *nm* respectively. The *Su-25* and *C-1* fall well short with ranges of only 675 and 700 *nm* respectively. Although they are fast enough to meet the RFP, these two aircraft can only fly about a quarter of the required distance. Again, the *YC-14* and *YC-15* are the closest matches to the RFP, with maximum ranges similar to the required range value for the ferry mission.

According to the RFP, the required aircraft needs to carry a payload of at least 15,000 *lbs*. All of the aircraft that meet the range and speed requirements far exceed this minimum payload requirement. The *C-40* has nearly three times the payload capacity with a 40,000 *lb* payload, and the *YC-15* carries nearly four times the requirement with a 59,300 *lb* payload. The YC-14 is the closest match to the RFP specifications with a payload of 34,500 *lbs*, more than twice the required capacity.

Clearly, none of the existing aircraft are ideal designs because they do not effectively meet all of the requirements stated in the RFP. The aircraft that most closely matches these specifications is the *Boeing YC-14* transport. This aircraft cruises at 98% of the required speed and has a range equal to the specified value; however, it carries a payload more than twice the required weight. This information confirms the need for an optimized design of a smaller and lighter aircraft.

3. Initial Sizing

To develop concept platforms, initial sizing calculations were made. The initial sizing process consisted of three stages, starting with preliminary considerations, moving to weight estimations, and ending with wing loading and required thrust calculations. The results of this process allowed for the sizing of the initial platforms.

3.1 Preliminary Considerations

Initial considerations concerning the weight of the aircraft included the determination of whether the aircraft will be manned or unmanned, as well as a broad decision as to what types of weapon systems will be employed. These considerations were used as a base for determining what aircraft platforms were ideal for the mission and established initial weight estimates.

3.1.1 Manned Vs. Unmanned

With the advances in technology in the area of autonomous flight in the recent years, particular focus must be paid to the idea of reducing pilot losses in combat situations through the use of Unmanned Aerial Vehicles (UAV). Considerations in the use of UAVs, as opposed to conventional manned aircraft, include the cost of human life, configuration and production concerns, problems arising with operations and logistics, and the moral dilemma associated with unmanned combat vehicles.

One of the primary arguments concerning the use of these advanced technologies is whether or not they are cost-effective. According to a recent report, the costs of using UAVs in hostile territory has increased, and in some cases tripled since inception.[1]

With concern for logistics, issues arise when employing UAV technologies with long range requirements and the need for ground support. The complexity of UAVs requires a larger number of personnel at ground stations in comparison to manned aircraft. In addition, the telemetry signal being sent from the ground has a chance of being lost or jammed over enemy territory, leading to a loss of mission control and the possibility of aircraft destruction. The telemetry signal also requires high bandwidth which current communications systems are just now being able to cope with and the requirement of over-the-horizon communication with an unmanned system would require a satellite uplink. Utilizing these state of the art communications systems leads to inherently expensive development and operational costs. In comparison, for manned aircraft, a pilot is always in control and has increased situational awareness.

As stated in the RFP, survivability is a key driver in the overall design. For enemy weapon detection, an onboard crew would be able to detect all forms of anti-aircraft and small arms fire in a faster and more precise manner than a computer. Current UAVs are typically used in situations where survivability is not a defining factor in the design.[2] With an aircraft designed to be survivable, the benefit of an unmanned aircraft is not significantly greater than a manned system. While no human loss is ideal, the benefits of manned aircraft outweigh those of an unmanned system.

After these considerations, it was decided to proceed with a manned aircraft. The trends in cost and benefits show that an unmanned system of this size is neither cost nor mission effective at this point in time. According to the Department of Defense, in the next 25 years, there are no plans for UAVs of the size indicated by preliminary sizing estimates to perform missions of the type outlined in the RFP.[2]

3.1.2 Comparable Aircraft and Weapons Systems

Preliminary studies of the RFP and comparator aircraft revealed that a jet transport most closely met the requirements of the RFP. Jet transports have typical ranges, payloads, internal volume for weapons, and cruise speeds that meet the requirements for the gunship aircraft. This conclusion stemmed from preliminary decisions for both the weapons systems as well as the crew. The low cost-per-kill requirement limits the use of smart weapons,

therefore larger guns and cannons were chosen as the primary weapons systems. A fuselage modeled after a jet transport is required to support these weapons, which are too large for smaller aircraft. This size fuselage will also be able to support the necessary crew for such an operation. Identifying the characteristics of a jet transport as the most effective means of meeting the RFP requirements provided a basis for initial sizing.

3.2 Weight Estimation

The takeoff gross weight of the aircraft (TOGW) was calculated using the following equation from *Aircraft Design: A Conceptual Approach* by Raymer: [3]

$$W_{TO} = W_E + W_{crew} + W_{tfo} + W_{PL} + W_F$$

where W_{T0} is the TOGW, W_E is the empty weight, W_{crew} is the crew weight, W_{tfo} is the weight of trapped fuel and oil, W_{PL} is the payload weight, and W_F is the weight of the fuel. The payload weight is set by the RFP as 15000 *lbs*, and the W_{tfo} is assumed to be negligible for the initial weight approximation. The weight of the crew was approximated for 5 crew members at 200 *lbs* each. The empty weight is linearly dependent on the TOGW and a correlation was found using existing jet transport aircraft of comparable size. Figure 2 shows the linear correlation between W_E and W_{TO} for tactical transports.

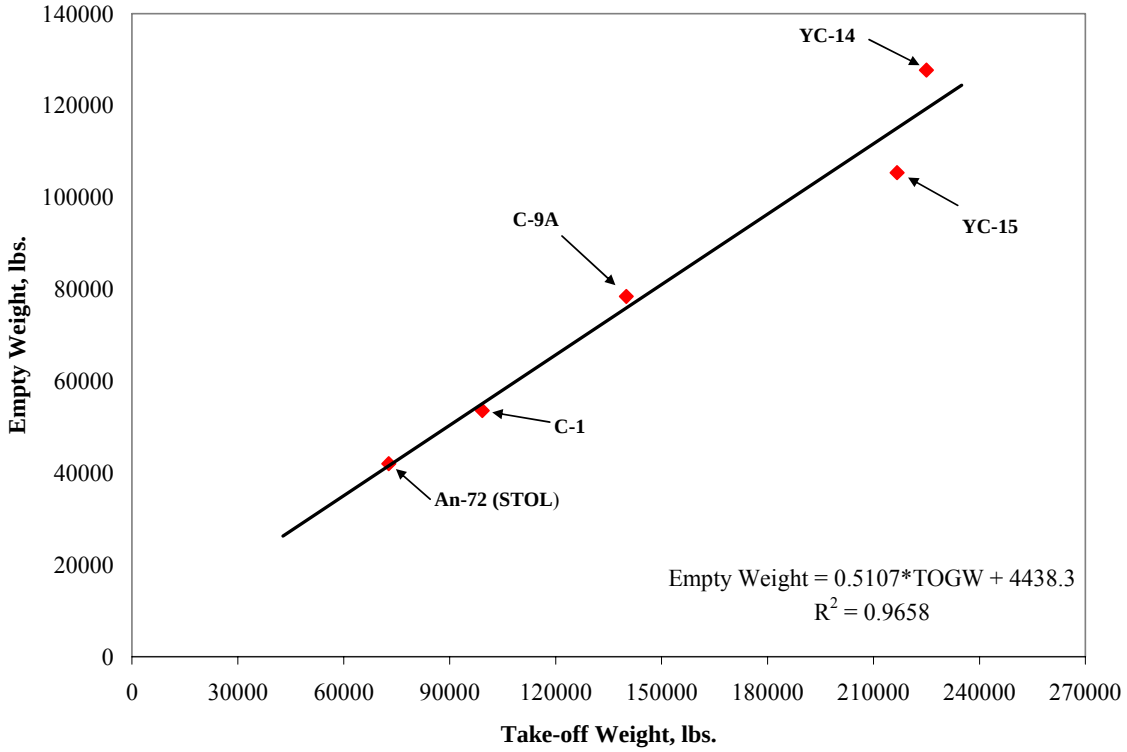

Figure 2. Similar Aircraft Weight Estimation Plot

The line of best fit for the data is shown to be $W_E = 0.5107W_{TO} + 4438.3$. A strong correlation coefficient, R^2, of 0.966 is accurate with data from existing tactical transports.

A fuel fraction method, which takes each segment of the design mission into account, was used to find the weight of the fuel required to complete the mission. The worst case scenario is examined by assuming that the payload was not dropped as stated in the RFP, but was carried throughout the mission. An iterative method was then used to solve the TOGW equation because TOGW appears on both sides of the equation. This was done to estimate the weight for both a standard and a blended wing body (BWB) design. The weight for the standard design was found to be 95,000 *lbs*. For the blended wing body, a 30% increase in the *L/D* ratio was assumed, resulting in a 14.6% reduction in the TOGW.[4] As such, the BWB design ended up with a TOGW of 81,000 *lbs*. However, this is not a particularly accurate estimate of the blended wing body's weight. If it were to be sized properly, comparator aircraft would need to be benchmarked using BWB concepts. Since no comparable blended wing aircraft are available for this analysis, the standard sizing was assumed with the adjusted *L/D*.

3.3 Standard Configuration Sizing

Based on the RFP requirements, performance constraints were used to determine wing loading and thrust to weight ratios. These constraints included requirements for takeoff distance, maneuvering, cruise, landing distance, and rate of climb. The landing constraint required an estimate of the maximum lift coefficient. Figure 3 shows that a C_{Lmax} value of 2.6 is attainable with a minimally swept wing without complicated high lift devices.

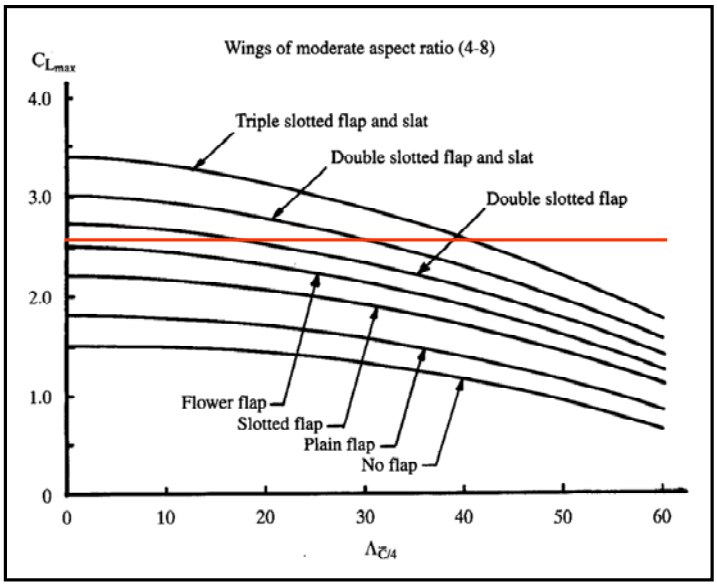

Figure 3. High lift device employments based on lift coefficient and wing sweep[3]

Values for the wing loading, thrust to weight ratio, and a refined TOGW were estimated using constraint diagrams and carpet plots. Performance constraints were used to find relationships between thrust to weight ratio and wing loading for the various RFP requirements. Figure 4 shows the initial constraint plot which was created using direct requirements from the RFP. These requirements include a takeoff distance of 5,000 *ft*, landing over a 50 *ft* obstacle with 40% internal fuel and full payload of 15000 *lbs*, maximum rate of climb, maneuverability requirements, and a minimum cruise ceiling of 30,000 *ft*. The ideal aircraft would have the highest possible wing loading, *W/S*, and the lowest possible thrust to weight ratio, *T/W*. The figure clearly shows that the maneuverability requirements, V_{manu}, and the maximum lift coefficient, C_{Lmax} are the limiting factors in determining the thrust to weight ratio and wing loading. For this constraint diagram, a maneuvering speed of 400 *knots* was assumed.

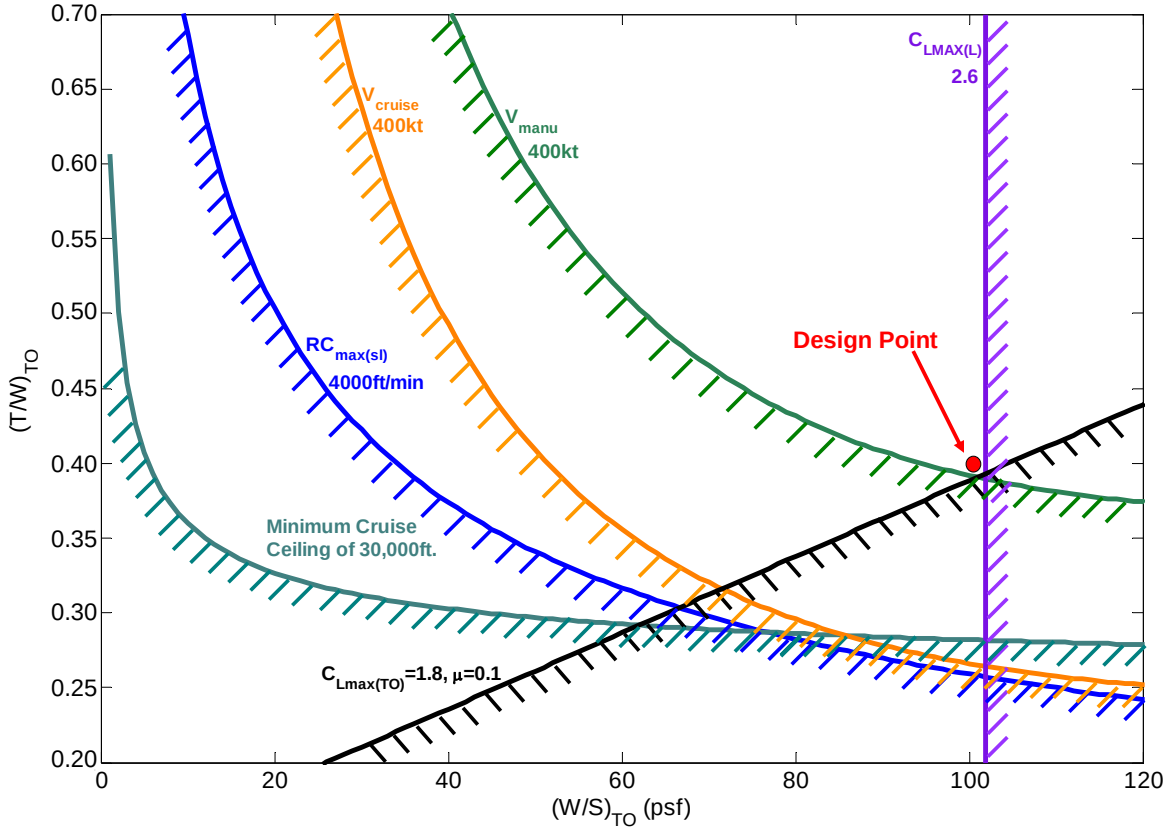

Figure 4. Constraint plot showing relationship between T/W and W/S and optimum design point

With the aforementioned C_{Lmax} of 2.6, an ideal wing loading and thrust to weight ratio was determined using Figure 4. According to the constraints of Figure 4, the most efficient design had a *W/S* of 100 lb/ft^2 and a *T/W* of 0.4. This point is shown on the figure as a red dot.

The relationships between thrust to weight ratio and wing loading used in Figure 4 were also used to determine an optimum TOGW. This optimum value is obtained through the use of a carpet plot. Based on the limiting factors illustrated in Figure 4, the takeoff, landing and maneuvering requirements were used to constrain the carpet plot, as shown in Figure 5.

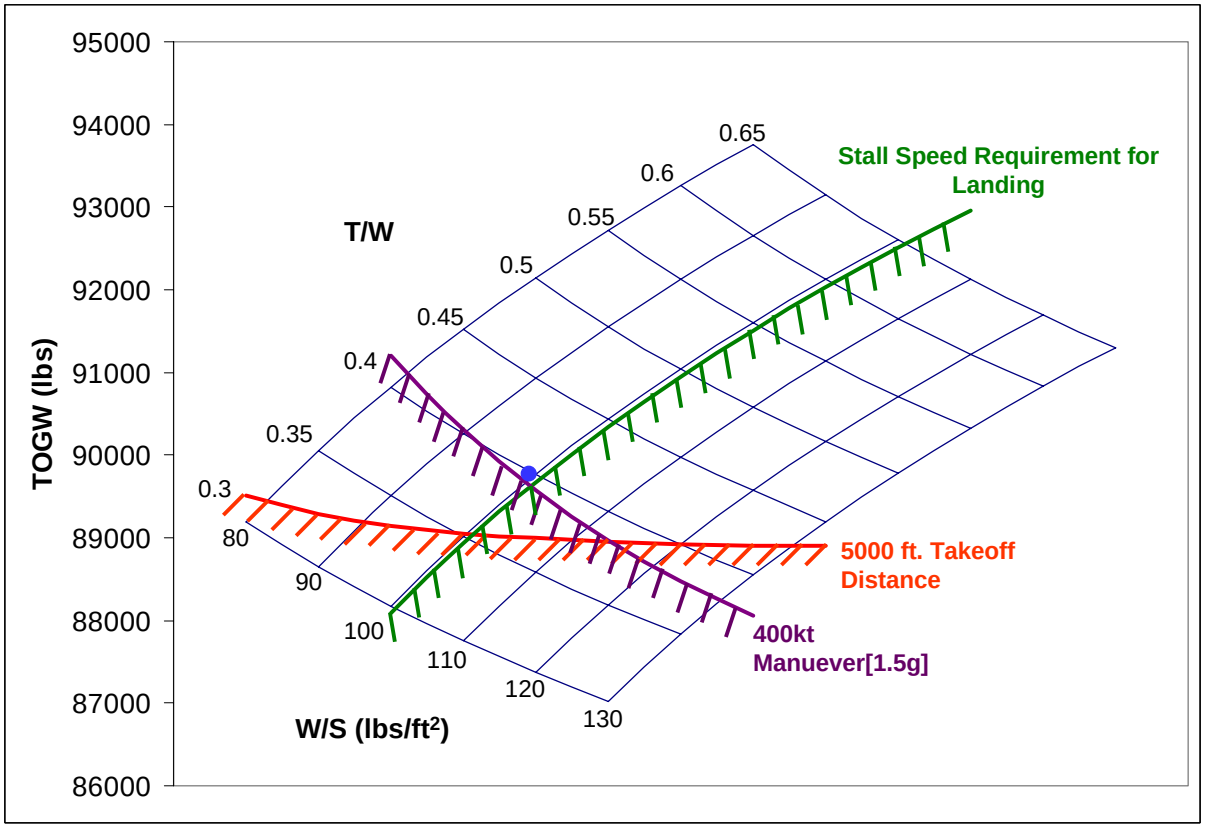

Figure 5. TOGW Carpet Plot

From this carpet plot it is clear that the previously proven wing loading and T/W ratios were accurate. Additionally it is now clear that the aircraft TOGW may be decreased for a standard design to a weight of 90,000 *lbs*. This weight will be the initial design weight for a standard configuration aircraft.

3.4 Blended Wing Body Sizing

As previously mentioned, sizing for the BWB concept was largely based on theory. Weights were estimated using the percentage increase in *L/D* as traditionally found in similar concepts. Estimation of the wing loading and required thrust could not be performed using constraint diagrams and carpet plots, due to the complex nature of the body. Instead, theoretical estimations were made based on extensive research. A wing loading of 65 lb/ft^2 was estimated from a previous study of the BWB performed by I. E. Pambagjo, K. Nakahashi, S. Obayashi,

and K. Matsushima.[4] The thrust to weight ratio of 0.5 was then estimated using the constraint diagram shown in Figure 4. These initial sizing constraints are sufficient to allow for an accurate comparison between the BWB and traditional concepts.

4. Conceptual Designs

Initially, there were six concepts under consideration, ranging from traditional approaches to flying wings, as shown in Figure 6. Preliminary discussion and brief analysis narrowed the decision down to three concepts. These three concepts were chosen for further investigation in order to ensure that the requirements set forth in the RFP were met. Two turbofan engines were used in each design.

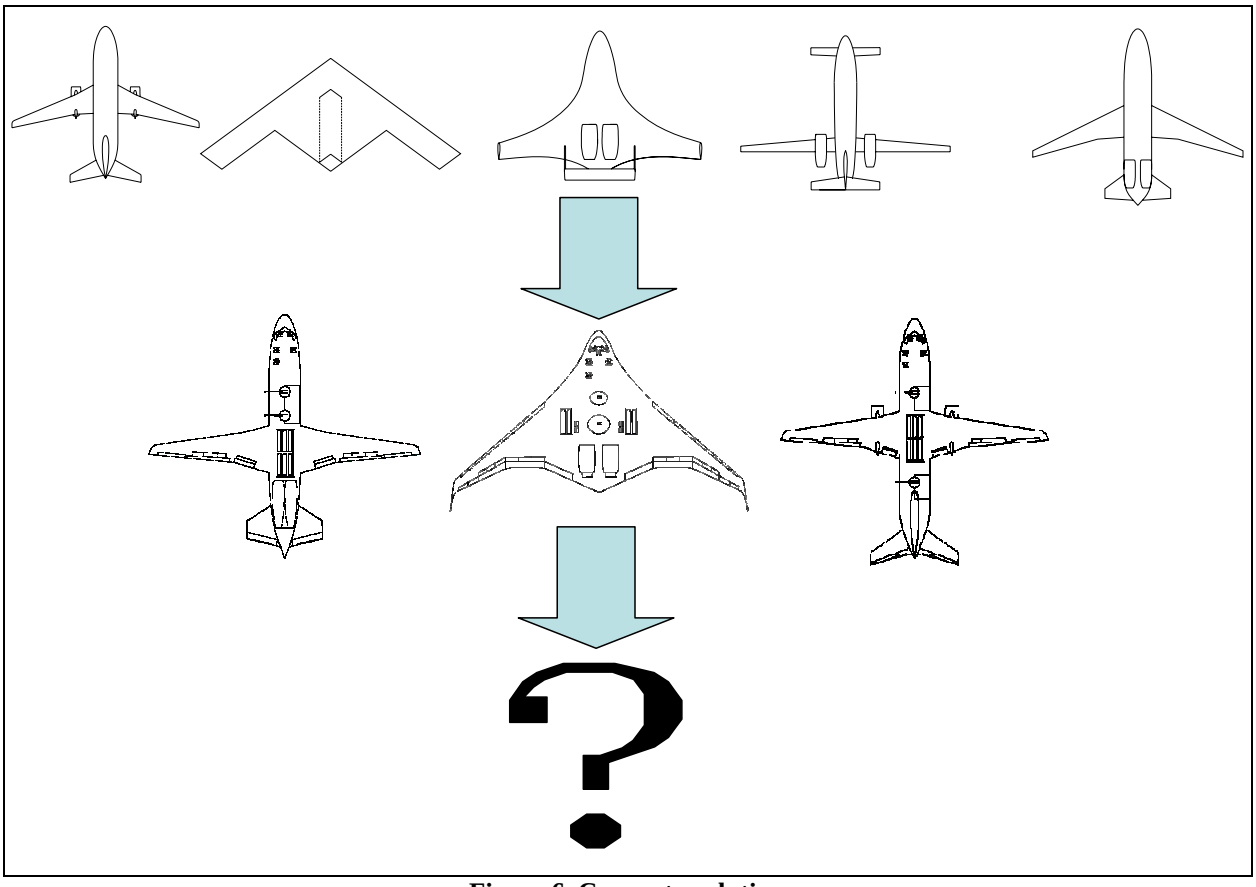

Figure 6. Concept evolution

4.1 Concept 1 – Conventional Transport

Concept 1, as shown in Figure 7, utilizes an already well-established conventional design to increase marketability and ease in maintenance, as well as decreasing time and costs related to production. The distinguishing features of Concept 1 are described in the remainder of this section.

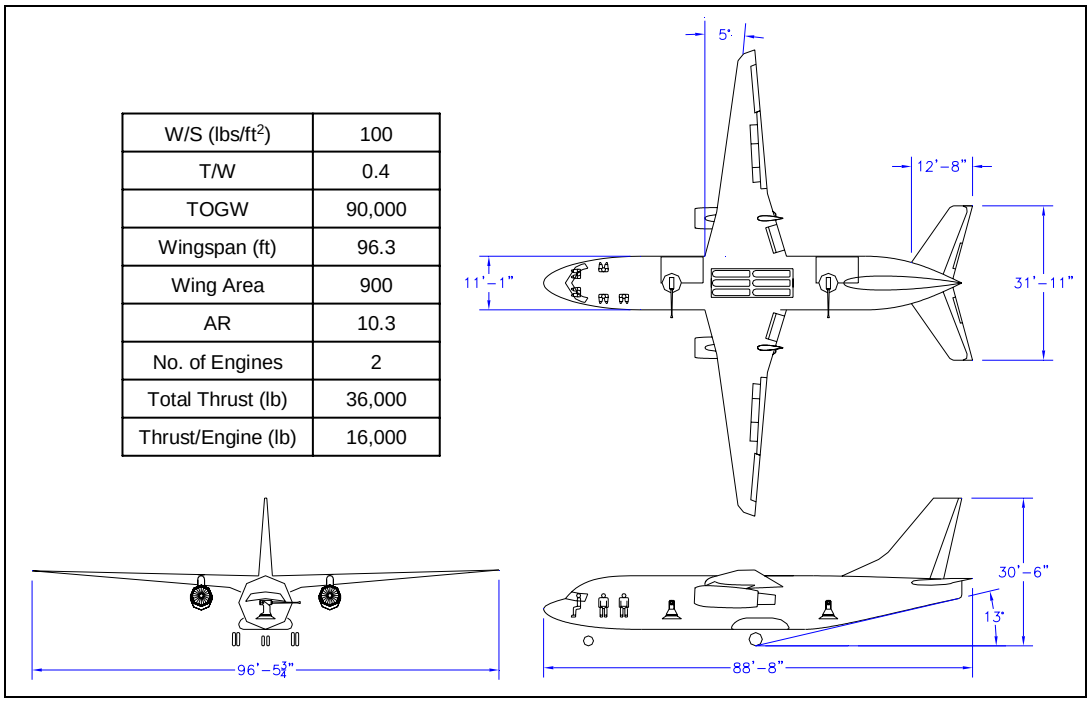

Figure 7. Concept 1 layout and sizing

4.1.1 High, Aft-Swept Wings

The wings of Concept 1 are mounted high on the fuselage to maximize usable fuselage area for side-mounted munitions. With this configuration, the engines have sufficient ground clearance with minimal landing gear length, consequently, reducing the landing gear weight. The increased ground clearance also reduces the ground effects during landing, allowing for shorter landing distance. Additionally the high wings allow larger wing flaps to be used which increases the maximum possible lift coefficient. Both of these characteristics help Concept 1 attain the take-off and landing requirements stated in the RFP. In addition, the structural weight of the aircraft is reduced because the wing box can be mounted on the top of the fuselage. This configuration is in contrast to a wing box passing through the fuselage, which would require stiffeners around the cut-out area.

One disadvantage to the high-wing arrangement is that the landing gear can not retract into the wing. As a result, blisters need to be added to the fuselage to hold the landing gear. To mount the landing gear on the body of

the aircraft, the fuselage needs to be strengthened to sustain the additional loads during landing. The blisters also cause a slight increase to the parasite drag which is undesirable.

4.1.2 Wing Mounted Engines

During the 1940s, Boeing engineers researched the advantages of wing mounted engines for the design of the B-47. With this configuration, it was determined that there is less interference drag, a better center of gravity (CG) location, more usable cabin space at the rear, easier access to engines for maintenance, and less piping required for fuel and bleeds. Structurally, the weight of the engines also provides bending relief from the lift of the wings. Disadvantages include vertical tail sizing and survivability concerns. With wing-mounted engines, the size of the tail must be increased for engine-out operations. Also, the engines are not shielded from ground fire, so the aircraft is less survivable as a whole and may need additional countermeasures.

4.1.3 Conventional Tail

The conventional tail configuration consists of a low horizontal tail and a centrally mounted vertical tail. With this configuration, the roots of both horizontal and vertical surfaces are attached directly to the fuselage. This results in lower vertical fin loads, less potential for difficulties associated with flutter, and fewer problems associated with deep-stall compared to a T-tail design. In addition, the effectiveness of the vertical tail is large because the interference with the fuselage and horizontal tail increases its effective aspect ratio. A disadvantage to this tail configuration is that the local dynamic pressure might be reduced due to the large tail areas being affected by the fuselage flow.

4.1.4 Payload/Weapons Configuration

This design utilizes two Bofors 40 *mm* cannons mounted on the left side of the aircraft to allow the aircraft to circle a target and lay down persistent firepower. The design will also be outfitted with an internal bomb bay, capable of holding a variety of bombs. The purpose of using both cannons and bombs is to meet each target requirement. Placing the internal bomb bay near the CG will reduce CG travel during weapons release.

4.2 Concept 2 – Conventional Design with Dihedral

Concept 2, as shown in Figure 8, has many of the same features as Concept 1, however the engines for Concept 2 are mounted on top of the fuselage and the conventional tail is replaced with a V-Tail. Overall, Concept 2

is a relatively traditional approach with slight modifications to increase durability and survivability. The distinguishing features are described in the remainder of this section.

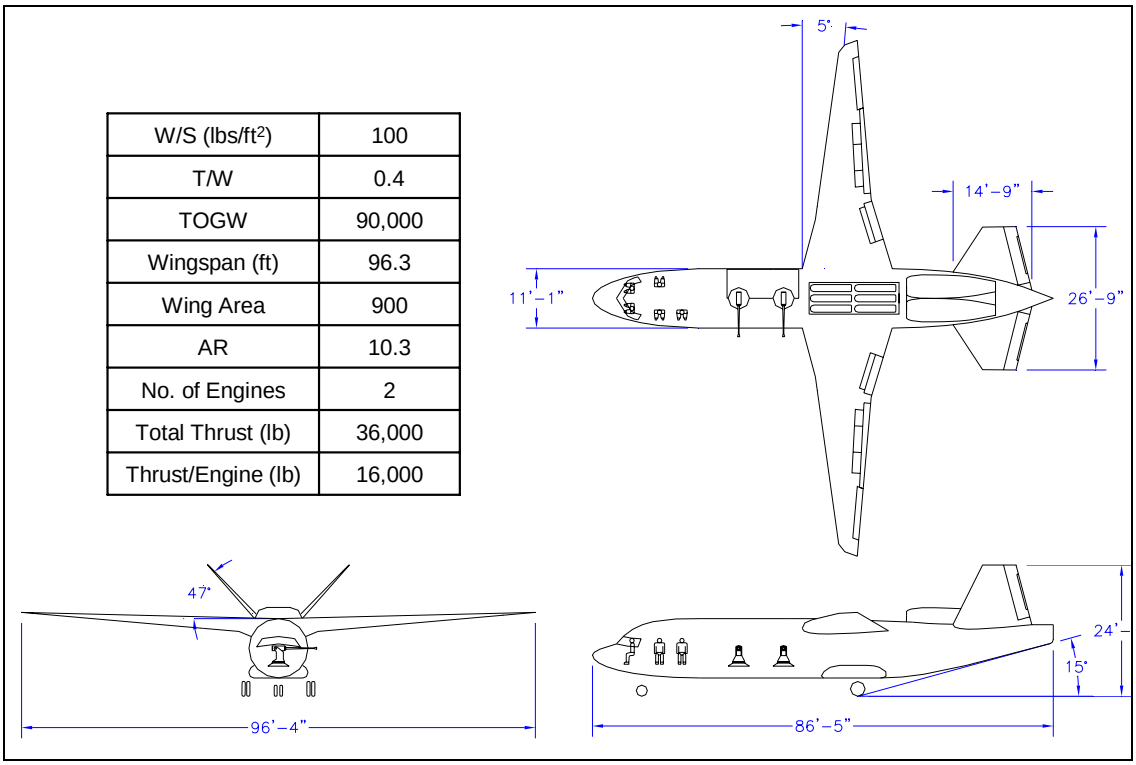

Figure 8. Concept 2 layout and sizing

4.2.1 V-Tail

A V-Tail is designed to have the same wetted area as a conventional tail with horizontal and vertical surfaces, while, at the same time, reducing interference drag. The rudder and elevator control inputs are combined into a "ruddervator," which causes increased complexity in the actuator controls. A disadvantage of using this type of system is encountered in maneuvers involving yaw. In a maneuver, the ruddervators produce a rolling moment in the opposite direction of the yaw moment, an action termed "adverse roll-yaw coupling."[3]

4.2.2 Rear Mounted Engines

Having the engines mounted in the rear of the aircraft between the V-Tail increases the survivability by both blocking the engine exhaust and allowing the engine exhaust to mix with cool air over the upper surface of the fuselage. This, in turn, reduces the overall infrared (IR) signature. In addition, the engines are less likely to be hit by ground fire, as they are shielded by the fuselage and tail sections. The thrust is applied close to the centerline, preventing a large induced yaw moment associated with one engine out. The top mounted engines will, however, create a pitch which will need to be counteracted through the use of control surfaces. Another disadvantage to this

engine placement is the difficulty for repair, as the engines are hard to access. Not separating the engines from one another reduces redundancy by increasing the chances of a total engine out situation.

4.2.3 Payload Weapons Configuration

Similar to the first design, this design contains two Bofors 40 *mm* cannons as well as an internal bomb bay to hold a variety of bombs. The cannons for this design will be mounted in front of the wings to balance the weight of the rear mounted engines. The internal bomb bays will be located as close as possible to the CG to prevent CG travel during weapons release.

4.3 Concept 3 - Blended Wing Body

Concept 3 is shown in Figure 9. This aircraft is very different from the previous two designs and offers a technologically advanced solution to the RFP. This design utilizes the benefits of the blended wing body to provide a more aerodynamically efficient design. The distinguishing characteristics of this aircraft are described in the remainder of this section.

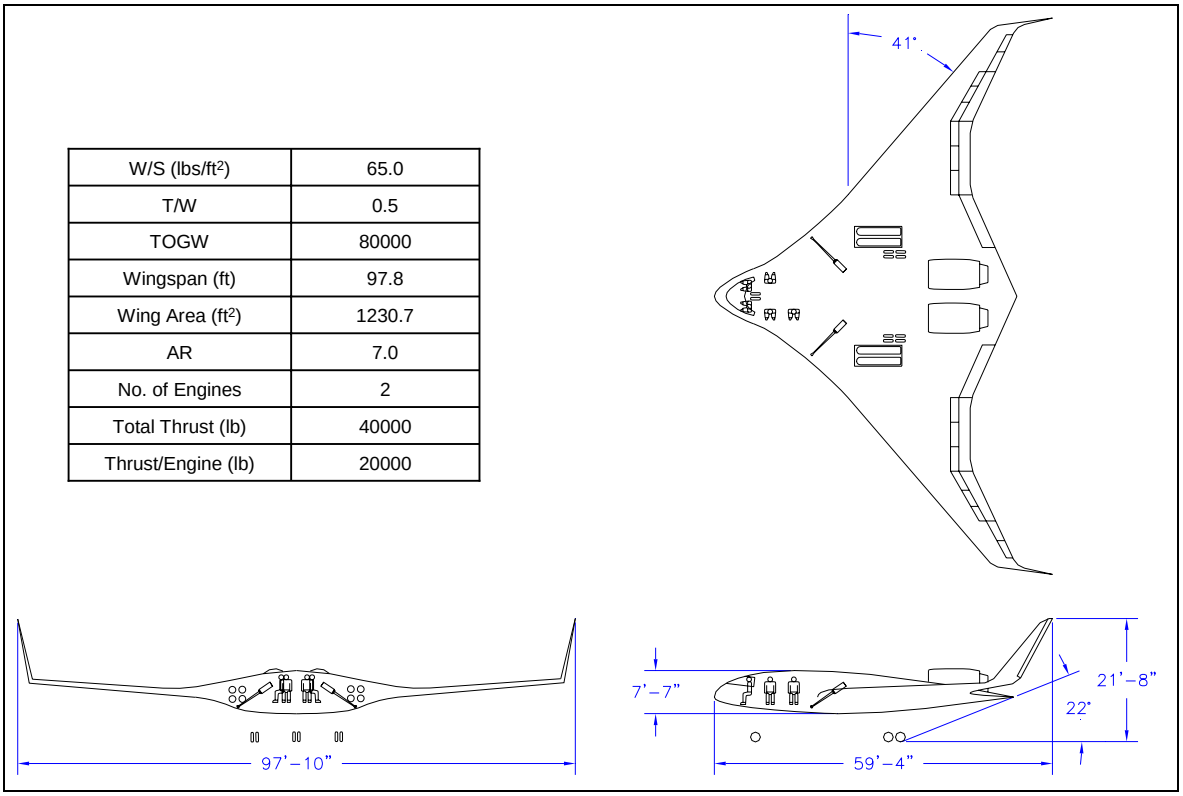

W/S (lbs/ft^2)	65.0
T/W	0.5
TOGW	80000
Wingspan (ft)	97.8
Wing Area (ft^2)	1230.7
AR	7.0
No. of Engines	2
Total Thrust (lb)	40000
Thrust/Engine (lb)	20000

Figure 9. Concept 3 layout and sizing

4.3.1 Aerodynamic Efficiency

Aerodynamic efficiency plays an important role in meeting the mission requirements set forth by the RFP. For performance considerations, aerodynamic efficiency corresponds to a high lift to drag ratio. Theoretically, BWB aircraft have significantly less wetted area, about 33% less than a conventional aircraft with the same payload capacity.[5] Consequently, since friction drag is directly proportional to the wetted area, BWB aircraft have lower parasite drag than conventional aircraft.[6] Also, the streamlined shape and lack of horizontal and vertical tails significantly decreases the interference drag. Taking into account drag reduction, a 20% increase in the overall *L/D*, as compared to more traditional approaches, can be achieved with a BWB design.[7] This increase, in turn, leads to greater fuel efficiency, reducing both the fuel weight and takeoff gross weight.

4.3.2 Multi-functional Control Surfaces

A BWB concept is designed to be statically unstable in order to be aerodynamically efficient. A stable BWB aircraft would require a reduction of the wing loading at the outer tips of the wing, making the aerodynamic span less than the physical span. [8] This reduces aerodynamic efficiency through a reduction in lift. For this reason, the aircraft is naturally designed to be un-stable, and complicated stability augmentation and fly-by-wire systems are required. Figure 10 shows the control surface configuration of a BWB transport.

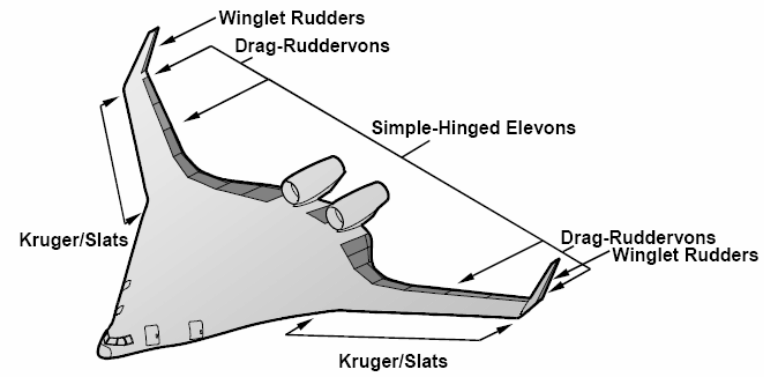

Figure 10. Blended wing body control system architecture[5]

Similar to a flying wing, trailing edge flaps cannot be used with a BWB, because there is no aft tail to trim the aircraft when the flaps are deflected. However, the low wing loading of a BWB design is such that it does not require the use of trailing edge flaps. [5] However, as shown in Figure 10, leading edge slats can be installed, and have the effect of increasing C_{Lmax} at takeoff and landing. Pitch and roll are controlled by inboard elevons and outboard drag-ruddervons (split drag-rudders + elevons). Drag-ruddervons, similar to those used on the *B-2*, are used to

control lateral directional movement of the aircraft. The outboard ruddervons are used to control rotation about all three axes (pitch, roll and yaw). High demand is placed on the ruddervons, especially when stability augmentation is used.[5] This is a disadvantage of having multi-functional control surfaces, as it increases the possibility of encountering control surface saturation. The use of stability augmentation may also cause problems such as poor dynamic stability, and insufficient actuator bandwidth.[8] In addition, having so many control surfaces in high demand requires a substantial amount of power.

4.3.3 Winglets

Concept 3 utilizes winglets for enhanced performance and control, as seen in Figure 9. The effect of using winglets for performance is to increase L/D. The winglet acts as a small wing, cambered and twisted, so that the rotating vortex flow at the wing tip creates lift with a forward component. This forward lift component acts as "negative" drag.[3] Also shown in Figure 9, rudders are employed on the winglets to control lateral movement of the aircraft. For increased control, large winglets and rudders are used.

4.3.4 Top-Mounted Engines

The propulsive efficiency of the BWB can be improved by utilizing boundary layer ingestion (BLI). With the engines mounted aft of the center-body and on top of the fuselage, as shown in Figure 9, boundary layer ingestion can be used to reduce the engine ram drag. This has the effect of increasing the cruise range by approximately 10%.[9] Having the engines configured as described also minimizes the ingestion of foreign objects during takeoff and landing, such as debris from austere airstrips. A disadvantage of using boundary layer ingestion is the possibility of the engines encountering an adverse pressure gradient near the inlet of the engine, causing significant pressure losses. Pressure losses across the boundary layer also cause total pressure and velocity distortions inside the engine, which leads to the stall of compressor blades.[10] Engine placement above the fuselage also has advantages in survivability. The engines are less likely to be hit by ground fire when shielded by the body of the airplane. The thrust also acts through the centerline, reducing the induced yaw moment with one engine out. The heat signature of the aircraft is reduced as air flows over the trailing edge of the body, cooling the exhaust.

4.3.5 Payload Weapons Configuration

Consistent with the first two designs, this design contains two Bofors 40 *mm* cannons and an internal bomb bay. Due to sizing constraints, the cannons are mounted near the front of the aircraft, one on each side. The cannons

could not be mounted on a single side of the aircraft due to the short fuselage length. The bomb bay is located close to the CG to minimize CG travel during weapons release.

5. Arriving at the Preferred Concept

To determine which concept was the best match for meeting the RFP requirements, a decision matrix was created. With this tool, qualitative and quantitative data were used to determine each concept's effectiveness in meeting the requirements. Descriptions of the categories for the decision, ratings, and the method for arriving at the preferred concept are described in the remainder of this section.

5.1 Decision Matrix Categories

The categories used for the decision matrix include marketability, maintainability, take-off and landing durability, stability and controllability, acquisition cost, lifetime cost, and survivability. These concept characteristics were determined to be the key driving factors in the decision because while they are very important for the overall design, they are also independent of each other. Independence of the categories is essential, such that if one concept does not perform well in one area, it will not be penalized twice in the overall decision.

5.1.1 Marketability

Marketability is the ease with which an investment may be bought and sold. For aircraft designs, radically new concepts are traditionally not very marketable because they do not signify a reliable product to the buyer. For designs that require a large investment of time and money, a buyer is more likely to choose a concept that follows traditionally accepted designs as opposed to one that does not. As such, in a case where radical new technologies are not essential to meeting the design requirements, a traditional approach is much more marketable.

5.1.2 Maintainability

Maintainability is the ease with which a product can be kept in a working state over its lifetime. For this design, maintainability is based on the location of the engines, access to the engines, general layout, and whether or not the concept requires the use of advanced technologies. An ideal maintainable concept would be one where the engines and systems are easily accessible, the layout does not require advanced skills and technologies for repair, and parts are easily accessible.

5.1.3 Takeoff / Landing Durability

In takeoff and landing, durability becomes a key factor in the overall design when the aircraft needs to be able to operate on austere airstrips. Primarily, for this design, decisions are based on engine location, since all other factors in the takeoff and landing of the concept designs are considered the same. For austere airstrips, it is important for the engines to be protected from debris and have significant ground clearance.

5.1.4 Stability and Controllability

Design considerations associated with stability and controllability include the complexity of avionics and control surfaces, based on reliability of current and proven technology. Traditional design approaches are considered to be neutral in this realm, while radical designs require more advanced technologies. With the use of advanced technologies, issues such as complexity and control surface saturation may have negative effects on the final decision.

5.1.5 Acquisition Costs

Acquisition costs were determined using a preliminary cost estimation method, as found in Roskam's *Aircraft Design: Volume VIII*.[11] Values of acquisition cost include the research, development, testing and engineering (RDT&E) phase of production, as well as the manufacturing phase. The RDT&E phase includes costs associated with airframe engineering and design, development support and testing, production of flight test models, and flight test operations. The manufacturing phase includes all costs associated with the production of the final design. The RFP requires evaluation for a production run of 100, 200, and 400 aircraft. Because RDT&E costs are only encountered once, producing a large number of one design results in the lowest acquisition cost per aircraft. Thus, using the lowest required value of 100 aircraft explores the worst-case-scenario for the decision matrix.

5.1.6 Lifetime Cost

Lifetime costs were determined using a preliminary cost estimation method, as found in Roskam's *Aircraft Design: Volume VIII*.[11] Values of lifetime cost are operational cost estimations using an estimated life of 30-years with 600 flight hours per year, as modeled using existing aircraft mission statistics from Roskam's book. These estimations include costs associated with fuel, oil and lubricants, direct program personnel (flight crew), indirect personnel (ground/maintenance crew), consumable materials, program cost of spares, program cost of depots, and miscellaneous operation costs.

5.1.7 Survivability

While any aircraft can be designed to be survivable using countermeasure systems, the platform itself may also have survivability advantages or disadvantages. For instance, an aircraft with top-mounted engines is less likely to lose an engine due to ground fire than one whose engines are mounted under the wings. Engine location may also play a role in heat and noise signature reduction, making the aircraft less observable by enemy ground forces. For the decision matrix, survivability characteristics do not include countermeasure systems, which can be applied to any of the designs.

5.2 Decision Matrix Rating System

To ensure the categories had a consequential effect on the final decision, each was weighted based on its relative importance to the overall design. The weightings, as a percentage, are shown in Table 2 below.

Table 2. Category weighting for decision matrix

Category	Weighting (%)
Marketability	8
Maintainability	12
Landing / Takeoff Durability	10
Stability & Controllability	15
Overall Cost	17
Lifetime Cost	20
Survivability	18

A relative rating system was established for the decision matrix, with values from -5 to 5, -5 being the lowest possible rating, 0 being neutral, and 5 being the highest.

Percentage comparisons were used for each of the cost categories, allowing for quantitative reasoning in the subsequent ratings. After completing cost analysis, a neutral rating was assigned to the concept with the lowest cost. Then, based on the percentage increase in cost for the other two concepts, proportional negative ratings were assigned based on a lowest possible rating of -5.

5.3 Concept Evaluations

Each concept was evaluated using the decision matrix, and then the concept with the highest overall score was chosen as the preferred design for further evaluation. Each evaluation was based on the characteristics and weighting previously described. The following evaluations show the ratings for each category, along with a

corresponding justification. For the justifications, the "+" signs indicate a positive aspect of the design, and the "-" signs indicate a negative aspect. These signs are qualitative, not quantitative, indications of the rating.

5.3.1 Concept 1

Table 3 shows the decision matrix evaluation of the modified conventional transport.

Table 3. Decision Matrix Evaluation for Concept 1

Criteria	Rating (-5 to +5)	Reasoning	Quantitative Data
Marketability	5	Traditional approach, already accepted(+)	
Maintainability	5	Easy engine access(+), readily accessible parts(+), standard layout(+)	
Landing/Takeoff Durability	-3	Engines exposed to debris(-)	
Stability / Controllability	0	Standard avionics, standard control surfaces.	
Acquisition Cost	0	Neutral	$30.7 Million per aircraft
Lifetime Cost	-1.25	Lower fuel efficiency(-), higher hourly cost(-), pro-rated from Concept 3	$16.6 Billion ($11.2 Thousand per hour)
Survivability (Without Countermeasures)	0	Engines exposed to ground fire (-), Engine out produces significant yaw(-)	
Total	**4.5**		

This evaluation shows that because the standard transport is a traditional approach, it excels in marketability and maintainability but suffers in durability and survivability. The easily accessible engines and standard parts allow for the engines to be easily maintained, but also allow for damage due to the ingestion of debris on austere airstrips and exposure to ground fire. The cost analysis resulted with this concept having the lowest acquisition cost due to low RDT&E cost and being tied for second in terms of lifetime cost. Following the cost analysis, Concept 1 was pro-rated for lifetime cost using the percentage comparison as previously described. Overall, Concept 1 received a rating of 4.5.

5.3.2 Concept 2

Table 4 shows the decision matrix evaluation of the modified transport with top-mounted engines and V-Tail.

Table 4. Decision Matrix Evaluation for Concept 2

Criteria	Rating (-5 to +5)	Reasoning	Ruling Quantities
Marketability	4	Traditional approach, already accepted(+), new tail / engine concepts(-)	
Maintainability	2	Hard to access engines(-), Readily accessible parts(+), non-traditional tail concept(-)	
Landing/Takeoff Durability	3	Engines shielded from debris(+)	
Stability / Controllability	1	Standard avionics, fewer control surfaces than traditional approach(+)	
Acquisition Cost	-0.5	Slightly higher cost from traditional approach(-), pro-rated from Concept 1	$34.8 Million per aircraft
Lifetime Cost	-1.25	Lower fuel efficiency(-), higher hourly cost(-), pro-rated from Concept 3	$16.6 Billion ($11.2 Thousand per hour)
Survivability (Without Countermeasures)	2	Lower heat signature from engine exhaust(+), centerline thrust(+)	
Total	**10.35**		

This evaluation shows that Concept 2 has much of the same characteristics as the traditional approach in Concept 1, but has modifications that increase its durability and survivability. Like Concept 1, it excels in marketability, but less so because of a fairly new tail design. Concept 2 suffers in maintainability primarily because its engines are difficult to access, being on top of the fuselage and mounted between the V-Tail sections. However, the engine placement also has advantages in durability and survivability. The rear fuselage and tail empennage shield the engines from ground fire. In addition, the engine intakes are protected from the ingestion of debris on austere airstrips, and the exhaust is cooled over the fuselage and hidden by the V-Tail. The cost analysis resulted with this concept scoring second for acquisition cost, pro-rated with Concept 1, and being tied for second with the lifetime cost, being pro-rated with Concept 3. Overall, Concept 1 received a rating of 10.35.

5.3.3 Concept 3

Table 5 shows the decision matrix evaluation of the blended wing body design.

Table 5. Decision Matrix Evaluation for Concept 3

Criteria	Rating (-5 to +5)	Reasoning	Ruling Quantities
Marketability	-1	Risk associated with new technology(-), not traditionally accepted(-), widely researched presently(+)	
Maintainability	-2	Less accessible engines(-), not readily accessible parts(-), new layout(-)	
Landing/Takeoff Durability	4	Engines highly shielded from debris(+),	
Stability / Controllability	-2	More complicated avionics(-), more control power necessary (-), multi-function control surfaces(+), possibility of control surface saturation(-)	
Acquisition Cost	-3.25	Increased funding for research and testing(-), expensive new technologies(-), pro-rated from Concept 1	$50.3 Million per aircraft
Lifetime Cost	0	Much better fuel efficiency than traditional approach(+), lower hourly cost(+)	$13.1 Billion ($8.8 Thousand per hour)
Survivability (Without Countermeasures)	4	Centerline thrust(+), naturally designed to deal with instability(+), reduced noise(+)	
Total	**-0.525**		

This evaluation shows that Concept 3 is very different from the previous two concepts. As such, it suffers in the categories of marketability, maintainability, and acquisition cost. The radically new configuration is not traditionally accepted, and it requires a significant amount of advanced technologies and testing. Although there is a lot of current research into the blended wing body design, the technology is simply not readily available at this time. A secondary effect of the lack of technology is the access to parts for repair. Because Concept 3 does not use standard actuators and flaps, parts are not easily accessible and maintenance becomes increasingly complicated. The complications associated with new technologies play a significant role in increasing the acquisition cost. Along with the price related to the use of new technologies, new configurations need extensive testing and analysis that a more traditional approach would not require, which means more time and money invested.

Perhaps one of the better qualities of this platform, however, is present in the areas of durability, survivability, and lifetime cost. Like Concept 2, the engines of Concept 3 are shielded from ground fire and debris,

and the body of the aircraft reduces the acoustic signature of the engine. In addition, the control surfaces of the blended wing body are designed such that they are multi-functional. Because this concept does not have a vertical or horizontal tail, the control surfaces on the aft section of the body are responsible for all maneuvers. However, this configuration may also lead to control surface saturation.

As previously described, the blended wing body is very efficient, so it is cheaper than the more traditional approaches in terms of lifetime cost. It is both aerodynamically efficient and fuel efficient. However, from simple calculations using the minimum required production run of 100 aircraft, it is apparent that in the worst-case-scenario, it would take 30 years for Concept 3 to become more cost-effective. In essence, because the technologies associated with this concept are so new, the acquisition cost far outweighs the efficiency of the design. Until the technology is readily available, this design will not be cost-effective. Overall, Concept 3 received a rating of -0.525.

5.3.3 Preferred Concept

Table 6 summarizes the numerical results of the decision matrix evaluation for all three concepts.

Table 6. Evaluation Results from Decision Matrix

	Concept 1	Concept 2	Concept 3
Criteria	**Rating (-5 to +5)**	**Rating (-5 to +5)**	**Rating (-5 to +5)**
Marketability	5	4	-1
Maintainability	5	2	-2
Landing/Takeoff Durability	-3	3	4
Stability / Controllability	0	1	-2
Acquisition Cost	0	-0.5	-3.25
Lifetime Cost	-1.25	-1.25	0
Survivability	0	2	4
Total:	**4.5**	**10.35**	**-0.525**

As is shown, the modified transport with top-mounted engines and V-Tail (Concept 2) had the highest overall rating, and was determined to be the preferred concept. From this, Concept 2 was evaluated to a greater detail, and Concepts 1 and 3 were no longer analyzed.

5.3.4 Progression of Preferred Concept

At this stage in the design process, many characteristics of the Casper were only preliminary estimations. Further analysis was conducted to finalize each aspect of the design. The most notable changes to the design were the wing, tail, and weapons configurations, as well as the housing of the engines. The following page contains a detailed drawing of the preferred concept, which will be clarified in the remainder of the report.

Compiled Data	Appendage	
	Wing	Dihedral Tail
Ref. Area (*sq ft*)	900	314
Aspect Ratio	9.38	4.5
Taper Ratio	0.3	0.5
Span (*ft*)	93.5	36.4
1/4 Chord Sweep (deg)	0	35
T/W Ratio	0.4	
TOGW (*lbs*)	89911	

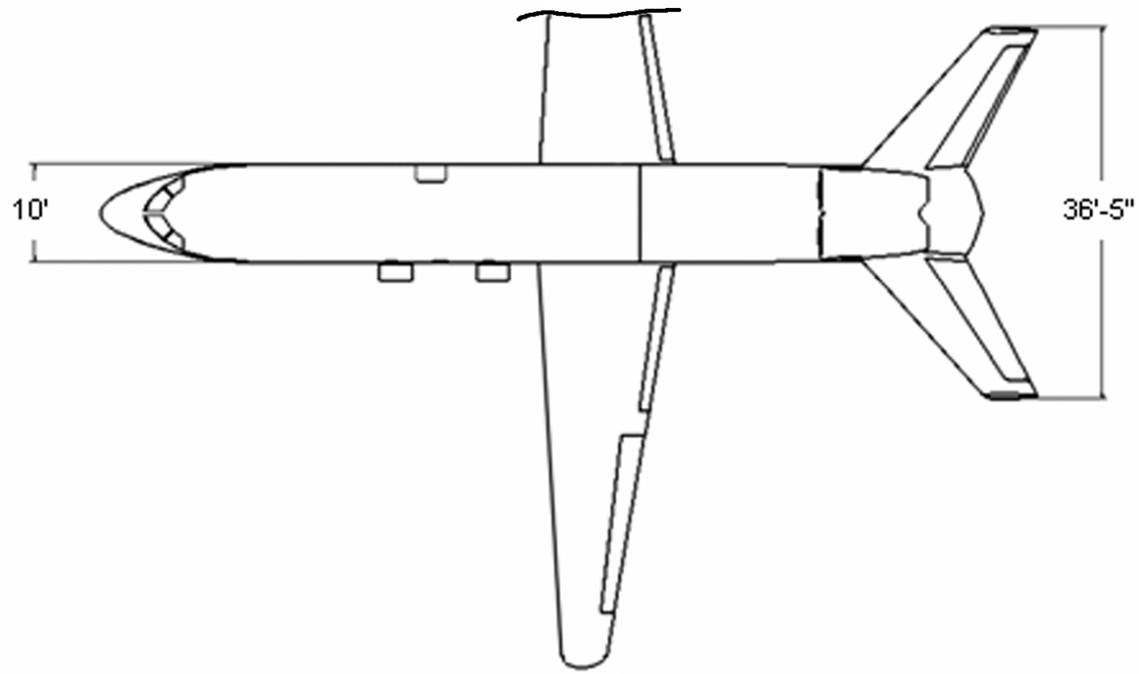

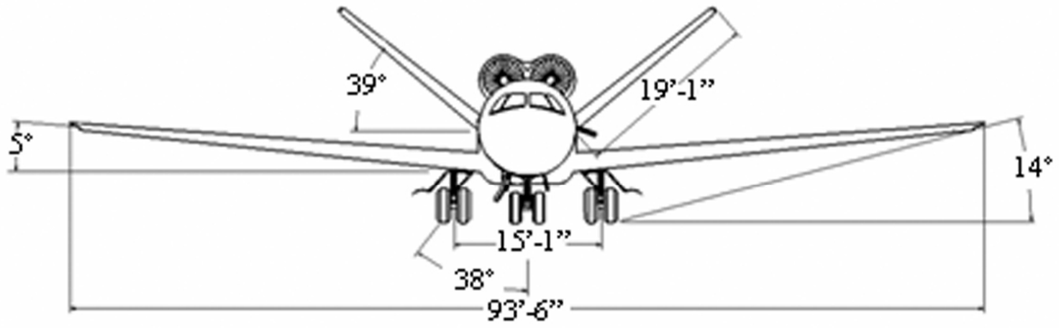

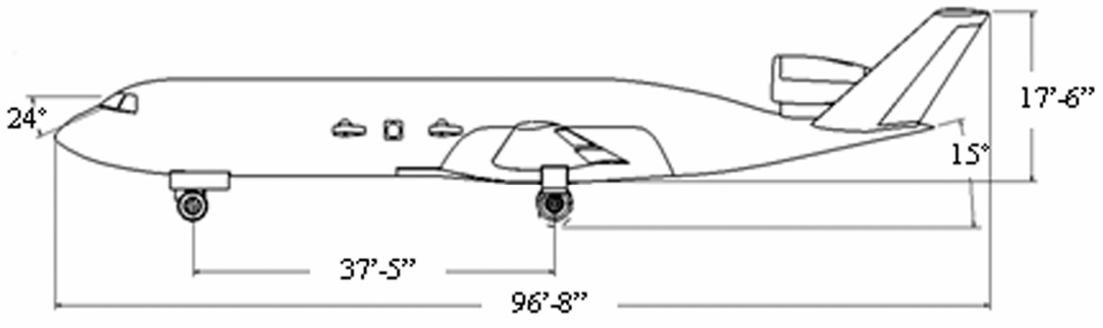

DRAWING TITLE: CASPER GENERAL ARRANGEMENT		
DESIGNED BY: TEAM CASPER		
DRAFTED BY: ANDREW HOPKINS		
SCALE: NTS	DATE: 5/5/05	DWG NO.

6. Mission Systems

The extensive nature of the RFP requires the investigation of mission systems. Among the systems investigated are weapons, countermeasures, and avionics. The role of each system is fundamental in meeting the RFP requirements.

6.1 Weapons

The RFP poses an interesting problem when defining the aircraft's payload and armament capabilities. The requirement is for sustained firepower that is effective and efficient at 10,000 *ft* against personnel, light armored vehicles, and buildings, while being cost effective. A versatile weapons system allows for planning, awareness, and adaptation during combat. Flexibility is essential to the effectiveness of the weapons systems since target packages will be assigned after takeoff. An investigation into presently deployed weapons systems was necessary to ensure the chosen systems met the requirements. Table 7 displays an array of weapons and their capabilities.

Table 7. Considered weapons systems[12]

	105mm Howitzer	40mm Bofors	GAU-12 25mm	Hydra 70 Rockets	AGM-114	JSOW	GBU-12
Weight of Weapon	4,980 lbs	4000 lbs	900 lbs	82 lbs	N/A	N/A	N/A
Weight of Munition	35 lbs - 46 lbs	4.75 lbs	1.83 lbs	35 lbs	110 lbs	1000 lbs -1500 lbs	800 lbs
Range	60,000 ft +	33,000 ft	12,000 ft	20,000 ft	30,000 ft	12 to 120 nm	8 nm
Targets	Mobile H/S, Fixed H/S	Mobile H/S, Fixed S	Mobile S	Mobile H/S, Fixed S	Mobile H/S, Fixed H/S	Mobile H/S, Fixed H/S	Fixed H/S
Rate of Fire	3 rnd/min	160 rnd/min	1800 rnd/min	N/A	N/A	N/A	N/A
Length	19.5 ft	8.2 ft	6.9 ft	8 ft	5.3 ft	13 ft	10.8 ft
Internal / External	Internal, Not Pressurized	Internal, Pressurized	Internal Pressurized	External	Both	Both	Both
Cost of Empty Weapon	$196,341	$223,000	$150,000	$1,500	N/A	N/A	N/A
Cost Per Shot	$230 - $360	$20 - $40	$6.50	$900	$164,485	$246,585 - $661,000	$19,000

Table 7 shows that the primary drivers in weapons selection are cost and the ability for sustained firepower. In order to ensure that all targets required by the RFP can be taken out, two turret-mounted 40 *mm* Bofors cannons and one GAU-12 25 *mm* gatling gun were selected for light armored vehicles and personnel. For fixed hard targets such as buildings, internal hard points will allow the platform to employ any and all types of bombs that fit within the geometry of the internal bay and do not exceed the total payload of the aircraft. The Howitzer cannon was omitted from consideration due to its size and weight, along with the high price per round. Also due to high cost, the Hydra-70 rockets, AGM-114, and Joint Stand-Off Weapons (JSOW) were omitted. While these weapons are effect

against all required targets, they put a limit on persistence and efficiency. Thus, a primary mission load-out will consist of 3 GBU-12's, 1500 rounds of the GAU-12, and 101 rounds for each Bofors cannon.

Advanced targeting systems will also be installed to increase precision and accuracy. A Synthetic Aperture Radar (SAR) system, manufactured by Sandia National Laboratories, will be used for targeting. This system uses all weather, day-and-night imaging sensors that provide a high resolution of both fixed and mobile targets.[13]

6.1.1 40 *mm* Bofors Cannons

The Bofors Cannon is to be used as the primary weapon aboard this gunship. It was originally designed as an anti-aircraft weapon, but was adapted for the AC-130 Gunship. Two 40 *mm* Bofors cannons, shown in Figure 11, are fully automated, and utilize 101-round magazines.

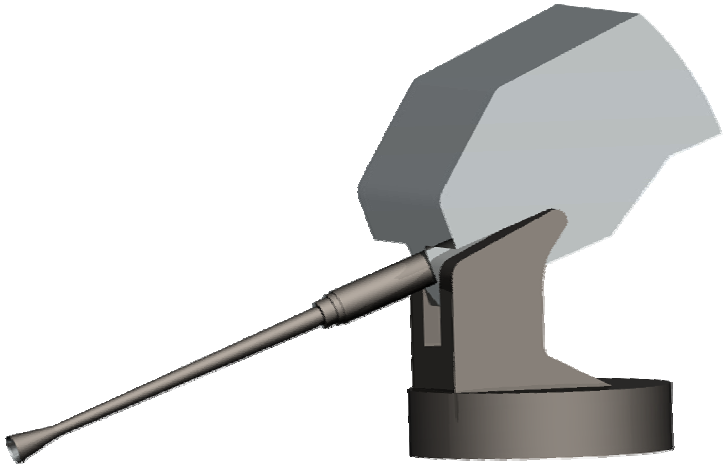

Figure 11. 40mm Bofors Cannon

These magazines have the ability to carry two types of rounds simultaneously, allowing the operator to select between rounds as necessary for varying target characteristics. The system has an overall weight, including the turret, of 4,000 *lbs*, overall length of 98.4 *in*, muzzle velocity of 2,890 *fps*, and a rate of fire of 160 *rounds/min*. Older systems have a barrel lifespan of 9,500 rounds, but more recent systems employ nitrogen cooling to increase this value.[7] The weight of the projectile is approximately 2 *lbs*, with a total round weight of 4.75 *lbs*.[14] The package includes the Bofors Optronic Fire-Control Instrument (BOFI) all-weather system, which utilizes a laser rangefinder, ballistic computer, image intensifier, and J-band pulse Doppler radar. This system makes the weapon both accurate and flexible. The all-inclusive cost of one cannon is approximately $223,000.[15] This cost is low compared to guided munitions and is a one time acquisition cost for the system.

Types of ammunition include armor-penetrating rounds, high-explosive rounds, and the 3P all-target rounds. The 3P rounds are pre-fragmented, programmable, proximity-fused rounds, which allow for increased flexibility. Programmability allows for a long fuse triggering distance, which is employed for air-burst attacks. This feature comes with a number of presets, including the multi-target, proximity, time-delay, impact, and armor-piercing modes. The time-delay and impact modes are specifically designed to destroy targets such as light-armored-vehicles or buildings, while the multi-target mode is used mostly against personnel.[12]

Ballistic dispersion was initially a drawback to using cannons. Current Bofors cannons have a dispersion of 0.4 to 0.5 *mil*.[16] This dispersion corresponds to a maximum miss distance of 15 *ft* at a 33,000 *ft* projectile range. This distance, although significant, is still within the blast radius of the 40 *mm* 3P all purpose rounds. Figure 12 shows the dispersion of a Bofors cannon aboard a ship in rough seas. The plot shows that 78% of rounds landed within 4 *m* of the target.

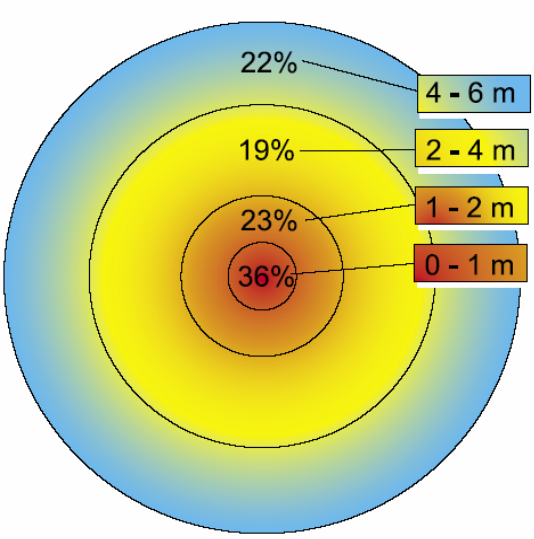

Figure 12. Dispersion of a 40mm cannon on ship in sea states of 4-5 at a 10,000 ft firing distance[17]

6.1.2 GAU-12 25*mm* Equalizer

A 25 *mm* gatling gun (Figure 13) will be used with a linkless feeding system, allowing it to be fully automated. An accompanying Lead Computing Optical Sight System (LCOSS) gun sight is hydraulically driven, nitrogen-cooled, and electrically fired. The weapon has been used aboard the AC-130U at altitudes of 10,500 *ft*.[18] This system targets mobile soft targets, such as light armored vehicles or installments and troops. The use of the GAU-12 allows the Casper to lay down a large amount of firepower with minimal weight and cost penalties.

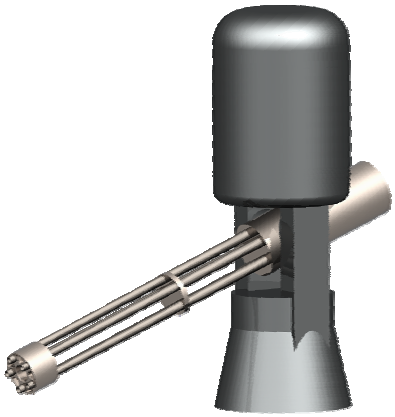

Figure 13. GAU-12 25mm Equalizer

This system will utilize an expansion of the attack sensor suite used on the AC-130U, which allows for a 360-degree field of vision. An APG-180 Strike Radar allows for the tracking of both fixed and moving targets through adverse weather.[19] With this system, the gatling gun is capable of engaging two targets simultaneously. The entire system weighs 900 *lbs* with an overall length of 83.2 *in.* For ammunition, PGU-25 high-explosive incendiary rounds are utilized, fired at 1,800 *rounds/min* with a muzzle velocity of 3,400 *ft/sec*. Each projectile weighs 0.406 lbs.[12] A typical load-out for the Casper will consist of 1,500 high-explosive rounds.

6.1.3 GBU-12 Laser Guided Bomb

The GBU-12, shown in Figure 14, is an 11 *ft* long, 800 *lb* bomb that utilizes a Semi-Active, Man-in-the-Loop, Laser Guidance System.[12]

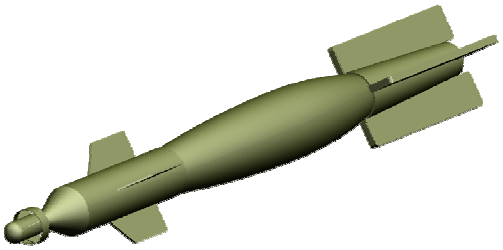

Figure 14. GBU-12 Laser Guided Bomb

Battle tested, the GBU-12 has a range of 8 *nm* and costs approximately $19,000 per unit. A typical load-out will carry three of these weapons mounted in the internal bomb bay.

These bombs will be used in response to the RFP requirement for targeting fixed hard targets, such as buildings. While the Bofors cannons are capable of neutralizing fixed hard targets, the use of laser guided bombs increases the reliability of the overall weapons system.

6.1.4 Weapons Configuration

Additional considerations for the weapons configuration are pressurization, mounting platforms, and an effective target area. Figure 15 illustrates how the guns will be configured. Large bins are installed to catch and store all of the empty, discharged shells, preventing the possibility of harm to friendly forces. The cannons and gatling gun will be mounted on the left side of the fuselage in a manner that allows the pilot to circle a given target area. This, in turn, allows for persistent firepower that would not be possible using a direct fly-over. Precision, along with the extended time-on-station, allows for isolated target selection and minimization of collateral damage.

Figure 15. Weapons configuration w/ pressurization hood

The weapons section of the fuselage on the Casper will remain un-pressurized because the chosen systems are fully automated. However, maintaining a seal from the environment remains important. Specifically, attention is paid to the two 40 *mm* Bofors cannons and the 25 *mm* GAU-12. A rubber hood (Figure 15), similar to the pressurization hood used on the AC-130U is used to provide a seal while allowing the cannons to be free to move. The GAU-12 is entirely contained within the aircraft utilizing an automated sliding door when not in operation.

Lateral and horizontal movement of the weapons will be limited to ± 5º. Additionally, the cannons will be mounted at an initial downward angle of 20° to optimize the target area.

The RFP states that all weapon deployment will occur at a 10,000 *ft* altitude. Based on the range of the weapons carried, two turning radii are specified to maximize effectiveness. For maximized effectiveness of the Bofors cannons, a maximum turning radius of 20,000 *ft* is selected. Performance calculations show that this radius with a flight velocity of 292 *ft/s* corresponds to a bank angle of 7.6° and load factor of 1.01, minimizing crew discomfort. This turning radius allows for effective firepower with the Bofors cannons and guided bombs. All required targets can be neutralized with these weapons systems, but for increased efficiency with targets such as personnel, a smaller turning radius must be specified. Because the GAU-12 gatling gun does not have the range to be fired at a turning radius of 20,000 ft, a new turning radius is calculated for efficient attack on mobile soft targets. This radius is calculated to be a maximum of 6,500 ft, corresponding to a bank angle of 22.2° and a load factor of 1.08. At this range, all weapons are effective, but the Casper is more susceptible to damage from AAA and MANPADS. Thus, this turning radius is used only after a majority of the targets have been neutralized.

For the turning radii specified, instantaneous and total target areas are calculated based on the range of motion of the guns and how they are mounted in the fuselage. Figure 16 shows the instantaneous and total target area for a turning radius of 20,000 *ft*.

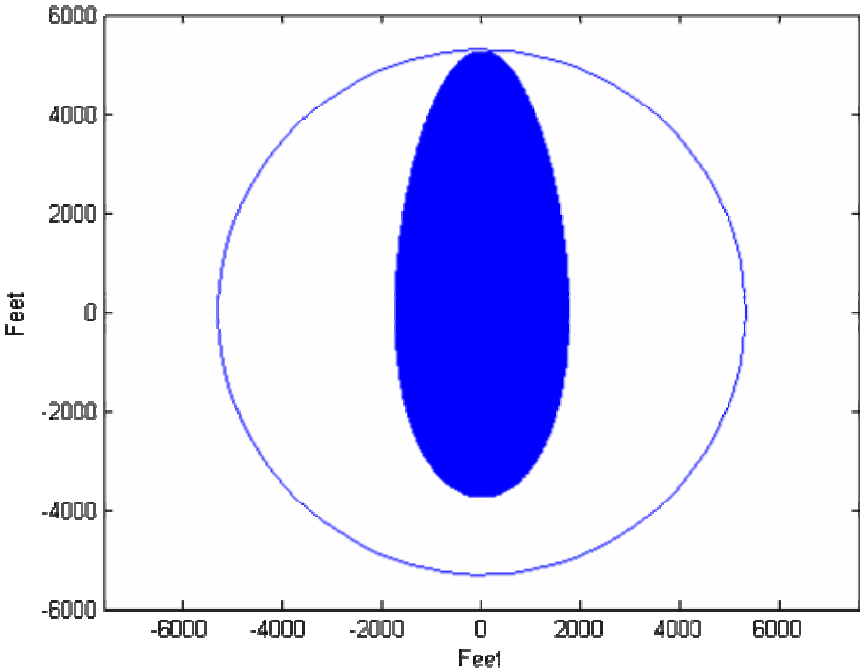

Figure 16. Instantaneous and total target area for 20,000 ft turn radius

The solid area illustrates the instantaneous target area, and the circle represents a rotation of the instantaneous area over one 360º turn. One turn takes roughly 7 minutes. In essence, at any point in time, a target in the solid region can be neutralized, and with one circular pass around a target area, anything within the outer line can be neutralized. The total target area is equal to 3.17 square miles.

Figure 17 shows the instantaneous and total target area for a turning radius of 6,500 *ft*.

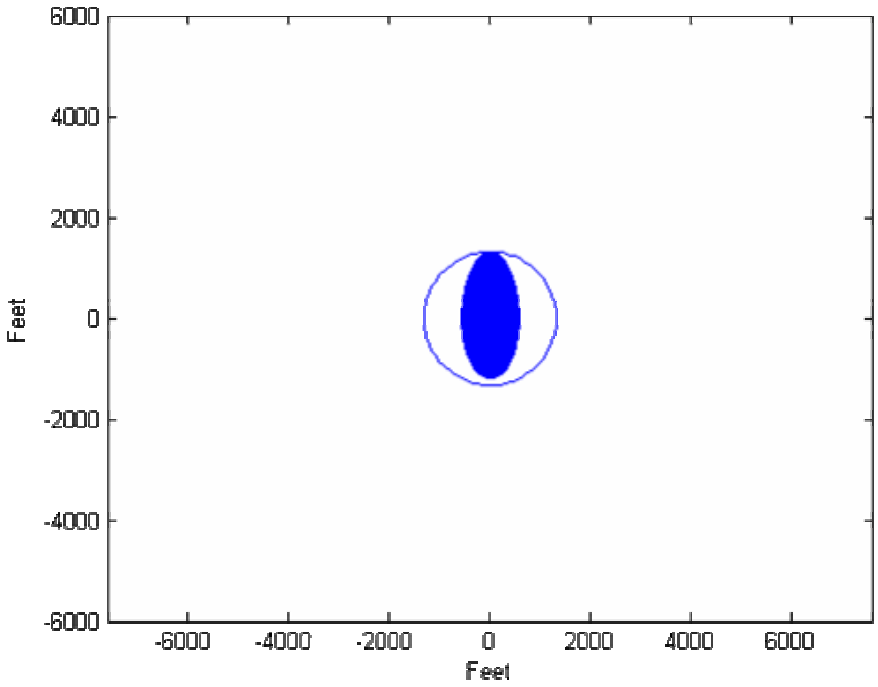

Figure 17. Instantaneous and total target area for 6,500 ft turn radius

The solid area illustrates the instantaneous target area, and the circle represents a rotation of the instantaneous area over one 360º turn. One turn takes roughly 2.5 minutes. In essence, at any point in time, a target in the solid region can be neutralized, and with one circular pass around a target area, anything within the outer line can be neutralized. The total target area is equal to 0.20 square miles.

6.1.5 Investigation of non-traditional weapons

The Casper is adaptable to many non-traditional weapons such as the advanced tactical laser and other non-lethal and directed energy weapons. These technologies include electromagnetic warfare, mechanical and kinetic, acoustic, and ancillary weapons. Current trends for these systems are not sufficient for meeting all the requirements set forth by the RFP.[20] For example, the tactical laser is expensive and does not currently allow for the rapid engagement of multiple targets. In addition, power requirements for such weapons hinder the ability to maintain

firepower over an extended period of time. As such, while the use of non-traditional weapons may be increasing in demand, the current and most efficient way to satisfy the RFP requirements is to utilize cheap and effective battle-tested weapons.

6.2 Survivability and Counter-Measure System

Anytime an aircraft, manned or unmanned, is sent into a combat environment, survivability becomes an issue. The RFP stipulates that all designs must have a less than 10% probability of an aircraft kill during any single engagement with AAA or MANPADS. This probability, symbolized $P_{k/e}$, can be calculated using the method described by Dr. Robert E. Ball in his text *The Fundamentals of Aircraft Combat Survivability Analysis and Design*.[21] According to Dr. Ball, $P_{k/e}$ can be calculated using the formula:

$$P_{k/e} = P_D P_L P_{KSS}$$

where P_D is the probability of being detected by the enemy, P_L is the probability of an enemy weapon launch, and P_{KSS} is the probability of an aircraft kill by a single shot.

Detailed information about the size, shape, and layout of the aircraft, the types and locations of vulnerable systems, and detailed data about detection systems and weapons types are all included in the calculations. The data needed to perform Dr. Ball's analysis is beyond the scope of the preliminary design; however, analyzing his approach provides a great deal of information. It shows that the probability of being detected by the enemy and the probability of being killed by a single shot are the two driving factors in determining how to control survivability in a design. Most importantly, technologies appropriate for each system type can be applied to reduce P_D, as well as influencing the miss distance to reduce P_{KSS}.

The AIAA has provided a simplified method for estimating the $P_{k/e}$ values for the advanced gunship. According to the AIAA Technical Committee for Survivability, it is assumed that any design has a $P_{k/e}$ value of 0.18 against AAA threats, and 0.45 against MANPADS threats if the aircraft is not equipped with any "vulnerability reducing technology."[22] Utilizing combinations of detailed vulnerability reducing technologies allows for a $P_{k/e}$ reduction to the required value of 0.1 for each threat. The technical committee provides six types of vulnerability reducing technologies, four of which are effective against both threat types. The remaining two are only effective against MANPADS. The first four technologies include engine fire detectors and suppressors, dry bay fire detectors and suppressors, fuel tank ullage systems, and highly separated redundancies. The MANPADS specific technologies are flare dispensers, and active infra-red countermeasure systems (IRCM). The engine fire detection and

suppression, dry bay fire detection and suppression, fuel tank ullage, and flare dispensing systems were all chosen to be implemented on the Casper. According to the technical committee, separated redundancies offer only a 5% reduction in $P_{k/e}$, which was not enough to justify their use. The active IRCM system was eliminated from consideration due to its listed $1.5 million cost.

6.2.1 Fire Detection & Suppression

Engine fire suppression systems are designed to alert the cockpit when there is an onboard fire occurring in an engine. The aircrew is then responsible for switching on the suppression system, which ideally extinguishes the fire. According to the technical committee, including such a system in the design offers a 20% reduction in the aircraft's $P_{k/e}$, and for our two engine design will cost us a weight penalty of 88.2 *lb* and a cost penalty of only $180,000.[22]

Dry Bay fire suppression systems detect and suppress fires located in the dry compartment spaces that are located close to the aircraft's fuel tanks. If an artillery fragment passes through the fuel tank and fuel leaks into the adjacent spaces, there is a high risk of fire, as they are not designed to hold highly flammable materials. According to the technical committee, including this system will reduce the aircraft's $P_{k/e}$ by 30%. Assuming 2,100 ft^3 of dry bay space, utilizing this system will include a weight penalty of 26.5*lb* and a cost of $124,000.[22]

6.2.2 Fuel Tank Ullage

Fuel tank ullage systems inject an inert gas (usually nitrogen) into the aircraft's fuel tanks as fuel is consumed. The inert gas occupies space that was previously occupied by liquid fuel, eliminating gas vapor inside the fuel tank. Thus, if a hot fragment passes through the tank, there is no gas vapor present to ignite and cause a fuel tank fire. Fuel tank ullage is listed as providing a $P_{k/e}$ reduction of 30%. Utilizing this system will cost a weight penalty of 13.2 *lb* and a cost penalty of $412,000.[22]

6.2.3 Flare Dispensers

Flare dispenser systems are only effective against MANPADS threats. They operate by ejecting a hot flare from the aircraft that is meant to confuse IR guided missiles. The flare is designed to mimic the heat signature of an aircraft engine and is often ejected such that it moves in a different direction than the aircraft. Even if the missile fails to lock onto the flare as its primary target, the presence of two targets moving in different directions is often enough to direct the missile away from its intended target. Flare dispenser systems are listed as providing a 50% $P_{k/e}$

reduction against MANPADS threats, and carries a weight penalty of 220.5 *lb* and a cost of $500,000.[22] The AN/AAR-47 Missile Approach Warning System will be used in conjunction with the flare dispensing system. This system automatically detects radiation associated with the rocket motor and initiates flare ejection.

6.2.4 Overall $P_{k/e}$ Reduction

Totaling the $P_{k/e}$ reductions for both AAA and MANPADS threats, and the overall cost of these systems, the results shown in Table 8 were found. It is important to note that these $P_{k/e}$ values can be achieved for any platform design. Additional survivability systems related to avionics can be found in section 6.3.

Table 8. Overall survivability estimates

AAA $P_{k/e}$	0.0756
MANPADS $P_{k/e}$	0.0945
Weight Penalty	345lbs
Cost Penalty	$1.216 million

6.3 Electronic Systems

All of the major systems in the Casper will be interconnected via a fly-by-light system. Figure 18 shows the general systems arrangement, and Foldout 3, on page 41, shows the layout of the major electronic systems. The following sections contain detailed descriptions of each component.

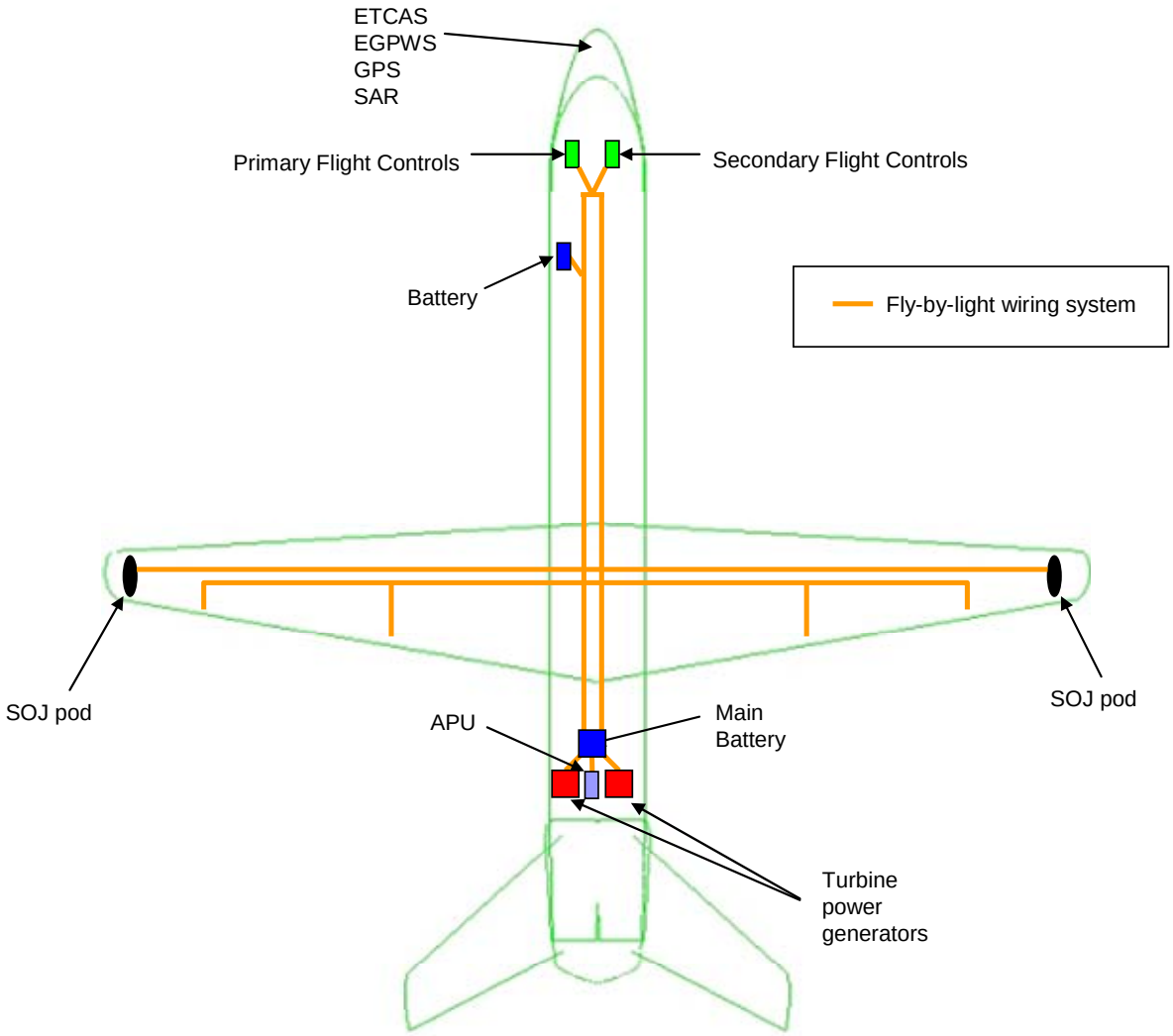

Figure 18. General systems layout

6.3.1 Cockpit

The cockpits of the Airbus A380 and Boeing 777 were studied when designing the layout for the Casper. These aircraft both employ the latest technologies in integrated avionics. The cockpit of the Casper is a compilation of the best features from these two existing aircraft. Figure 19 shows the Casper's cockpit, illustrating the seating

arrangement for the pilot and co-pilot. All the necessary items fit within the aircraft's dimensions while allowing the pilots to comfortably move around.

Figure 19. Three-dimensional cut-away of cockpit layout

The primary avionics are controlled by Honeywell's Versatile Integrated Avionics 2000 (VIA) system, currently used on the C-5. This system is made up of six Arinc D-size Liquid Crystal Displays (LCD) laid out as seen in Figure 19. The VIA 2000 is used to integrate the various cockpit systems, such as the flight control computer, autopilot and auto-throttle controls, and the thrust management computer.[23] The major benefit of this system is that it requires fewer separate systems which allows for more efficient storage. The system also has good maintainability and high dispatch reliability.

6.3.2 Fly-by-Light

The Fly-by-Light system uses fiber-optic cables instead of copper wires. These cables offer a reduction in both weight and volume over the traditional fly-by-wire design while offering high bandwidth capabilities. The fly-by-light system has reduced vulnerability to both to electromagnetic interference and an electromagnetic impulse.[24] In addition, the cables are not prone to any short-circuiting or sparking. The system is low maintenance and is easily upgradeable. The Casper is equipped with both a primary and backup fly-by-light system.

6.3.3 Cockpit Systems

An Enhanced Ground Proximity Warning System (EGPWS) is utilized, providing visual and aural alerts for obstacle avoidance while increasing alert time. An Enhanced Traffic Alert/Collision Avoidance System (ETCAS) provides the capability to coordinate flight formations while maintaining a high level of situational awareness and safety for the pilots. This system performs interrogation surveillance to a range of 40 nautical miles with azimuth coverage of 360 degrees, and up to 12,700 *ft* above and below the aircraft.[25] A Global Positioning System (GPS) is used for inertial reference. The Global Navigation Satellite Sensor Unit (GNSSU), a 12-channel receiver, continuously tracks all GPS satellites in view, allowing for continuous coverage.[26] These cockpit systems are primarily provided by Honeywell.

6.3.4 Weapons Console

A general view of the weapons console is shown in Figure 20. This station will be used for all weapons deployment and targeting. Three crew stations will be located at the weapons console, each with a large, multi-function LCD monitor and a corresponding keyboard and joystick.

Figure 20. Weapons console

The aforementioned SAR system will be used for reconnaissance, surveillance, and targeting. This system uses all weather, day-and-night imaging sensors that provide a high resolution. It can recognize distinct terrain features in addition to mobile objects such as cars and trucks.[13]

6.3.5 Hydraulics

The Casper uses electro-hydrostatic actuators. This hydraulic system uses fiber optic cables instead of conventional hydraulic lines running through the aircraft. Not only are these actuators cheaper, lighter, and require less maintenance, but are also safer and more reliable.[27] The use of an electro-hydrostatic system, as opposed to

traditional hydraulic lines, allows for a faster control response. A hydraulic reservoir is located inside each actuator and is connected only by a power and fiber optic cable.

6.3.6 Power Systems

Power is supplied by turbine power generators connected to each engine. The aircraft is started by a main battery and Auxiliary Power Unit (APU) in the aft section of the fuselage next to these generators. The primary power system utilizes engine driven generators while a secondary system consists of batteries and the APU. The secondary system batteries are located near the cockpit, providing power and increasing survivability in the case of engine failure. All systems will be shielded from both lightning strikes and electromagnetic interference, in addition to being serviceable, accessible, and redundant.

6.3.7 Survivability systems

Avionics play a major role in increasing survivability. The Raytheon APG-63 V2 radar is equipped with X band Active Electronically Scanned Arrays (AESA). This system can see small cruise missiles or airframes with stealth shaping at 50 nautical miles. It can track multiple targets automatically and simultaneously and is currently on the F-15, F-18, F-22, and F-35. The system also sends target location updates to expelled weapons during flight, increasing kill probability.[28] While it will not be used for locating targets on the ground, this system is important for the enhancement of battlefield awareness and can be used in conjunction with other network centric warfare techniques to aid friendly forces.

Electronic warfare is being considered for this aircraft. One component of this is a computer network attack device. This device can hijack enemy transmissions, insert specially designed algorithms, and then send the altered data stream back to the enemy network. The Stand-Off Jamming system (SOJ), currently on the B-52, is a simple design comprised of one pod placed on each wing with only one power line connecting each pod. It can sharply focus a signal from an individual target with enough power to be disruptive at long ranges.[29] This system is manufactured by BAE systems and is easily adaptable to a wide range of aircraft sizes.

6.3.8 Deicing

The formation of ice on the wing during flight causes degradation of aerodynamic performance. Ice removal is controlled by the Electro-Mechanical Expulsion Deicing System (EMEDS). The anti-icing element of the

system heats the leading edge of the wing, preventing ice from forming.[30] The system uses much less energy than other products that provide equivalent protection, thereby decreasing the operating cost.

To break up and remove ice behind the leading edge, an actuator changes shape from a flat oval to a circle when electrical energy is applied. This change causes the actuator to impact the inside of the leading edge surface, which responds with a small but rapid flex movement that expels the accumulated ice from the surface of the aircraft's erosion shield. EMEDS has been shown to remove ice to within 0.030 inches thickness. The system is resistant to deterioration from both sun exposure and extended exposure to moisture. While systems with rubber leading edge surfaces require periodic replacement, EMEDS' metal leading edge surface enables it to last through the aircraft's life cycle.[30]

6.3.9 Fuel system

All fuel will be stored internally. In addition, the Casper will be capable of mid-air refueling, as required by the RFP. The remainder of this section shows the detailed design of the fuel system.

6.3.9.1 Fuel Storage

Bladder tanks will be located in the wing structure, allowing for all fuel to be stored internally. These thick rubber bags are widely used for military aircraft because of their self-sealing properties.[3] In the event of a bullet passing through the rubber tanks, the material seals the puncture, preventing extensive fuel loss and reducing the probability of fire damage. Figure 21 illustrates the fuel system layout, showing fuel lines and internal tanks.

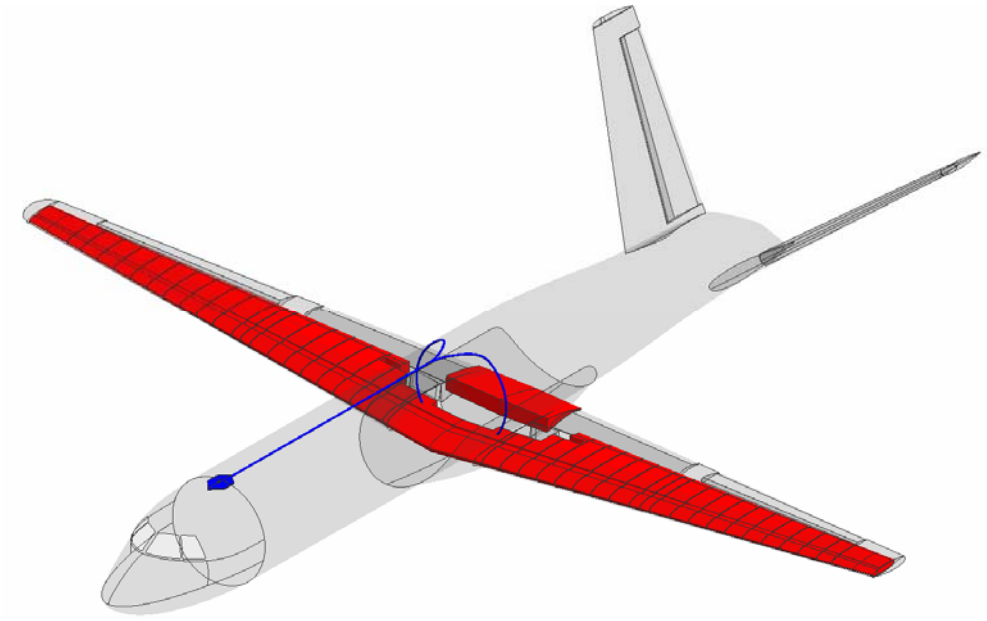

Figure 21. Fuel system layout (bladder tanks are depicted in red and fuel lines for aerial refueling in blue)

6.3.9.2 Mid-Air Refueling

The Casper will be capable of aerial refueling via the Air Force boom-and-receiver method. In this method, the receiving aircraft flies up to a standard position below and behind the tanker, maintaining level flight at constant speed. A boom operator in the tanker lowers a rigid, telescoping boom to the receiving port of the aircraft. The boom has a small, v-shaped wing near its end, which allows the operator to accurately control its position.[31]

The Casper is equipped with a receiver along the center line of the fuselage, as shown in Figure 21. When the boom is inserted, valves are opened that allow the fuel to be transferred. Once fueling is complete, the valves are automatically closed, and the boom is retracted. The advantage of this system over flexible drogue methods, utilized by the Navy, is a higher rate of fuel flow. Figure 22 illustrates the boom-and-receiver method for the Casper.

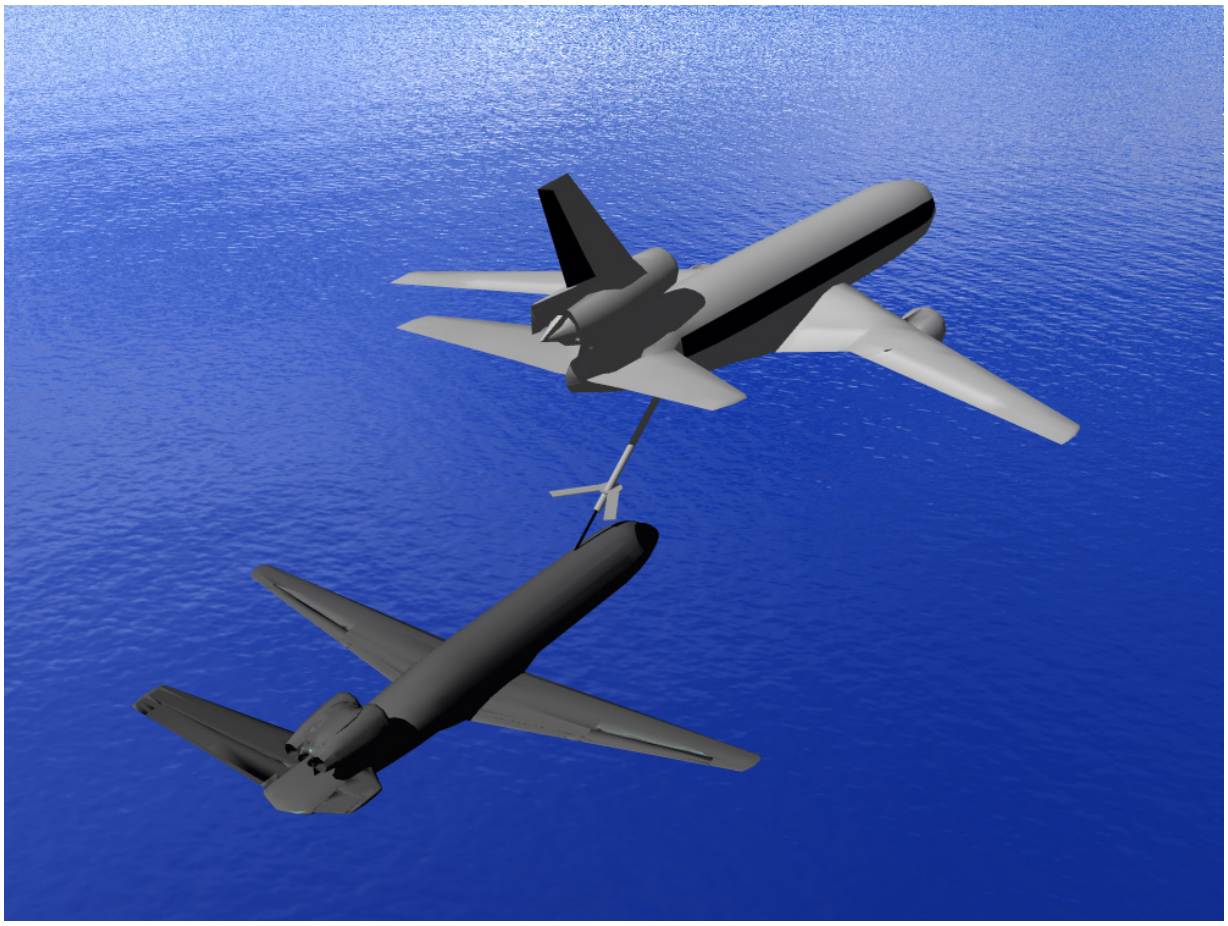

Figure 22. The Casper in a midair refueling

6.3.10 Additional Systems

There will also be pressurization, pneumatic, air conditioning, and oxygen systems onboard. Their effects on the CG location of the aircraft are included in the weights and balances section of the report (Section 8).

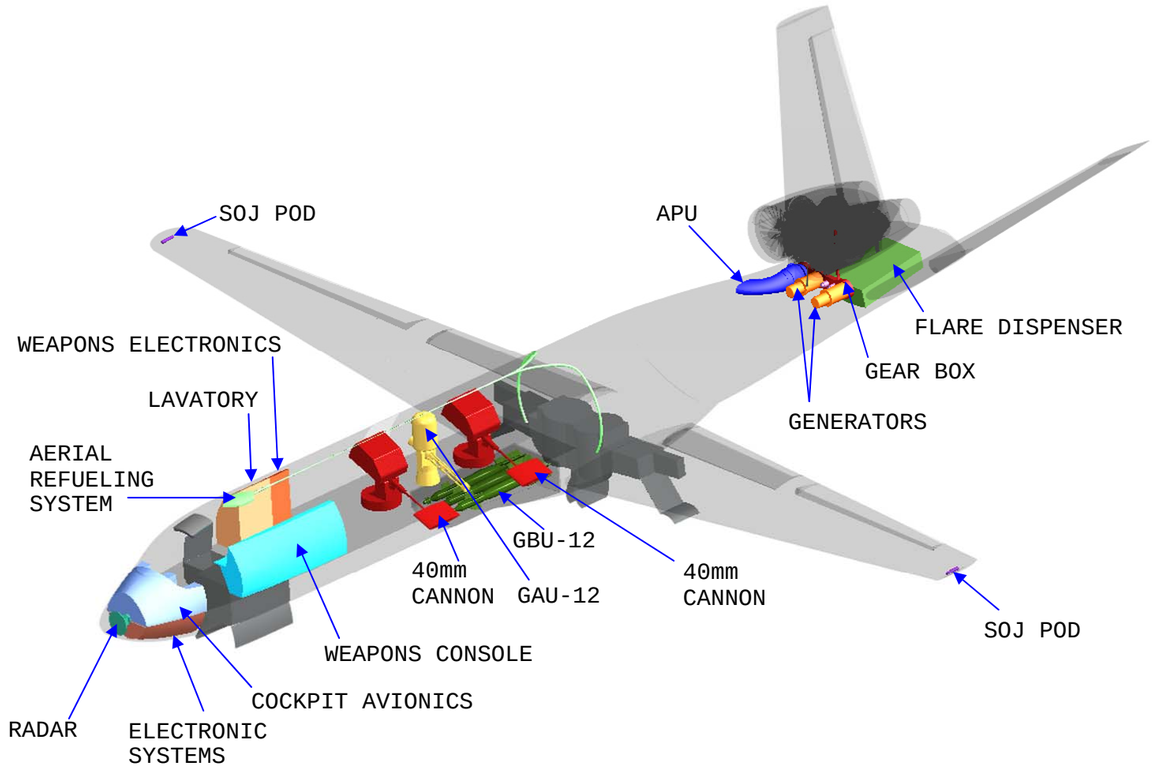

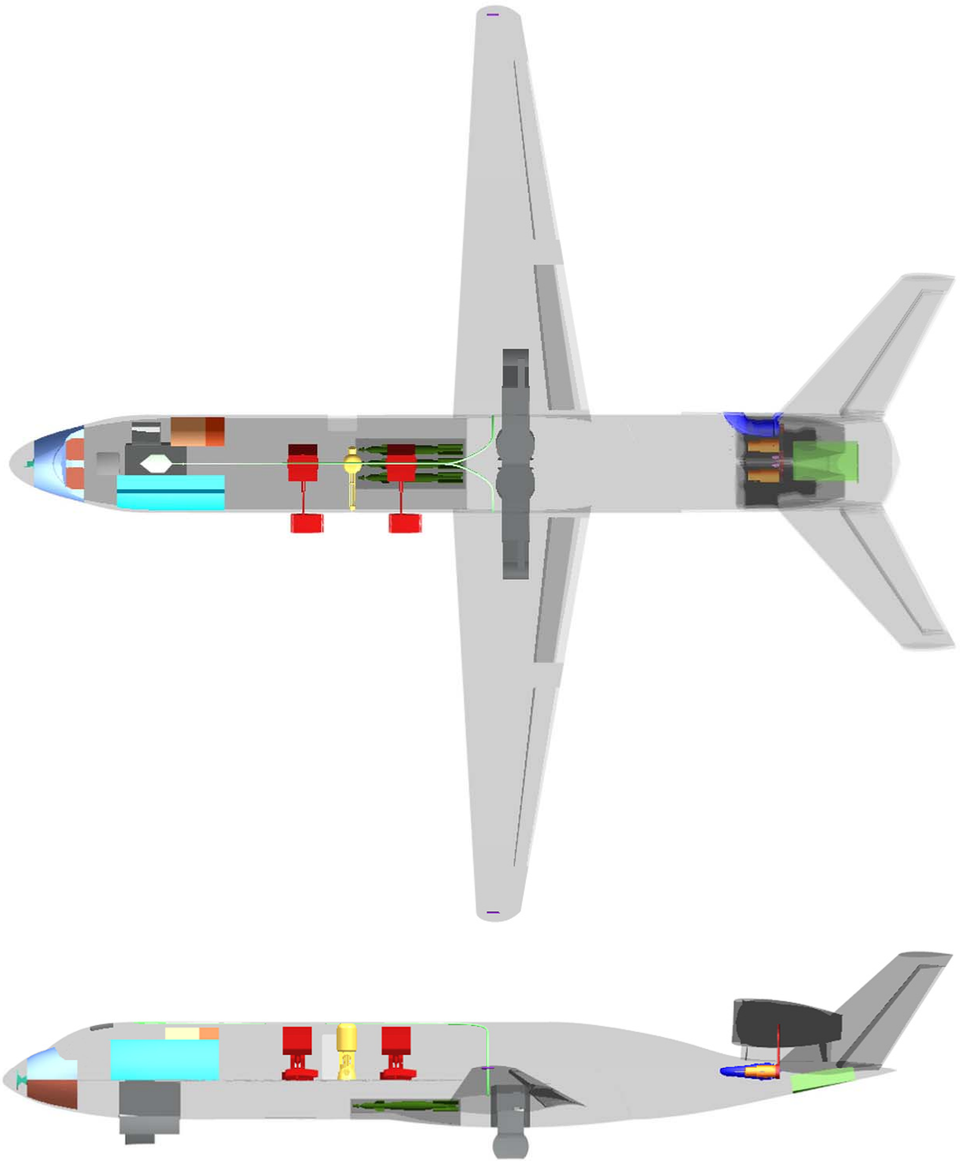

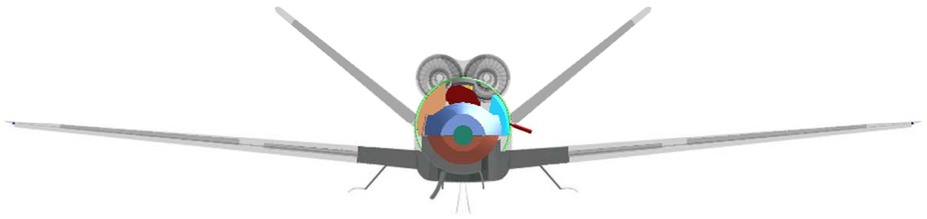

DRAWING TITLE: CASPER SYSTEMS LAYOUT		
DESIGNED BY: TEAM CASPER		
DRAFTED BY: ANDREW HOPKINS		
SCALE: NTS	DATE: 5/5/05	DWG NO.

7. Materials and Structures

The structural design of the Casper is shown in Foldout 4 on page 44. The remainder of this section will describe the necessary materials and structural analysis for the separate components.

7.1 Materials

The following factors were considered when selecting materials for the Casper: strength, weight, cost, safety, practicality, and survivability. The Casper will utilize traditional materials whenever possible, which have proven to be reliable, have standardized production methods, and give the best balance of all the deciding factors. Table 9 shows the properties of the materials that were analyzed. Selections for materials were made based on density (ρ), ultimate tensile strength, maximum allowable temperature, Young's specific modulus (E/ρ), shear specific modulus (G/ρ), and cost. Figure 23 shows the material layout of the Casper based on the color scheme of Table 9.

Table 9. Materials used (color coded for aircraft location illustration)[32]

MATERIAL	ρ (lb/in³)	Max Temp (°F)	Tensile Strength (ksi)	E (10^6 psi)	G (10^6 psi)	E/ρ (10^6)	G/ρ (10^6)	COST ($/lb)
Aluminum-7075-T6	0.101	250	83	10.3	3.9	102	38.61	4
Titanium-Ti-6A1-4V	0.16	750	131	16	6.2	100	38.75	25-59
Graphite / Epoxy (±45°)	0.056	350		2.34	5.52	41.78	98.57	90-100

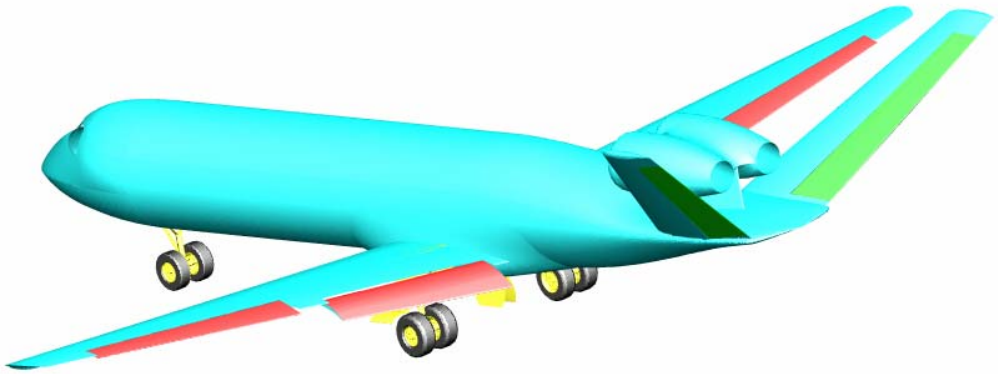

Figure 23. Color-coded layout of primary materials used

Aluminum will be used for the majority of our aircraft because of its proven resiliency, reliability, and practicality. It will be used for most of the aircraft structure, including the engine nacelles, bulkheads, and wing spars and ribs. We have chosen to use the alloy Aluminum-7075 which is commonly found on many aircraft. Aluminum is an extremely resilient material and will hold together even after being dented or punctured. Moreover, it has a great balance of strength, weight, and cost. It is readily available and its manufacturing processes have been standardized within the aerospace industry. It is a relatively cheep alloy, and its strength is sufficient enough to be used on the majority of the aircraft. Steel is far too heavy, and composites are too expensive. The gains in weight savings and strength would not outweigh the exponentially greater cost. Magnesium was considered due to its extremely light weight, however, it is flammable, and military specifications advise against the use of magnesium.[32]

For some parts of our aircraft, aluminum is not a viable option. These areas include places of high stress and high temperature. The landing gear, wing connections, and engine connections are the areas of the gunship that will experience the greatest stress and will require the high strength of a titanium alloy. Titanium weighs about one and a half times as much as aluminum but also costs a great deal more. However the strength to weight ratio is superior to most other materials. We will use Titanium (Ti-6A1-4V) for these high stress areas.

The wing and tail control surfaces of our aircraft will also experience high stress. Furthermore, it is important that they also be lightweight. For these reasons, composite materials will be used for the wing control surfaces. In addition to being lightweight, however, composites are harder to obtain and more difficult to inspect and repair. We will be utilizing a graphite/epoxy material for our control surfaces. This gives us a material that weighs about half as much as aluminum alloys, but also has a specific modulus that is three times that of aluminum.

The cockpit windshield will be made out of Lexan polycarbonate sheet, which is a very strong plastic. It can be scratched but will not break. It is a durable, reliable plastic that allows for visibility, while protecting the crew.[33]

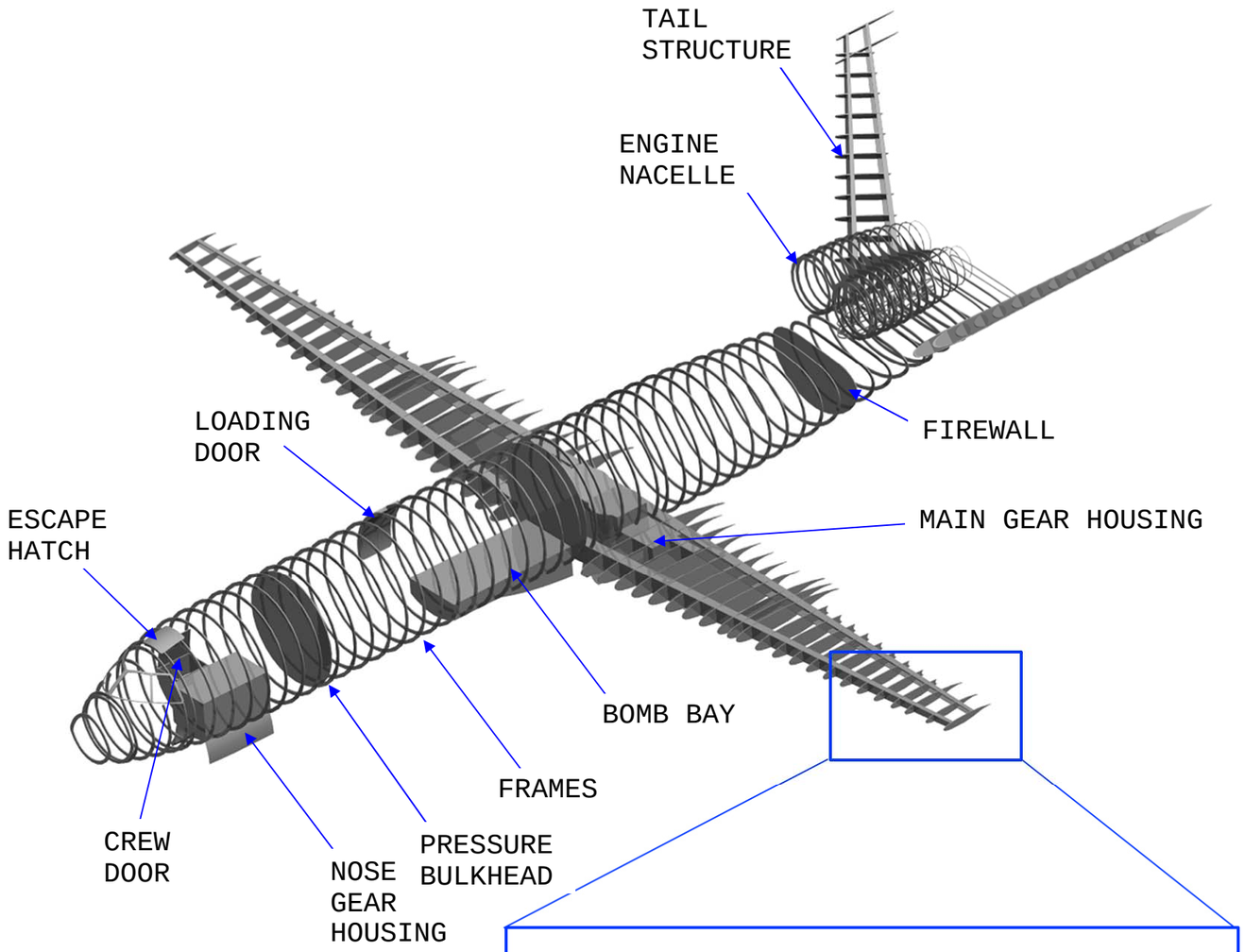

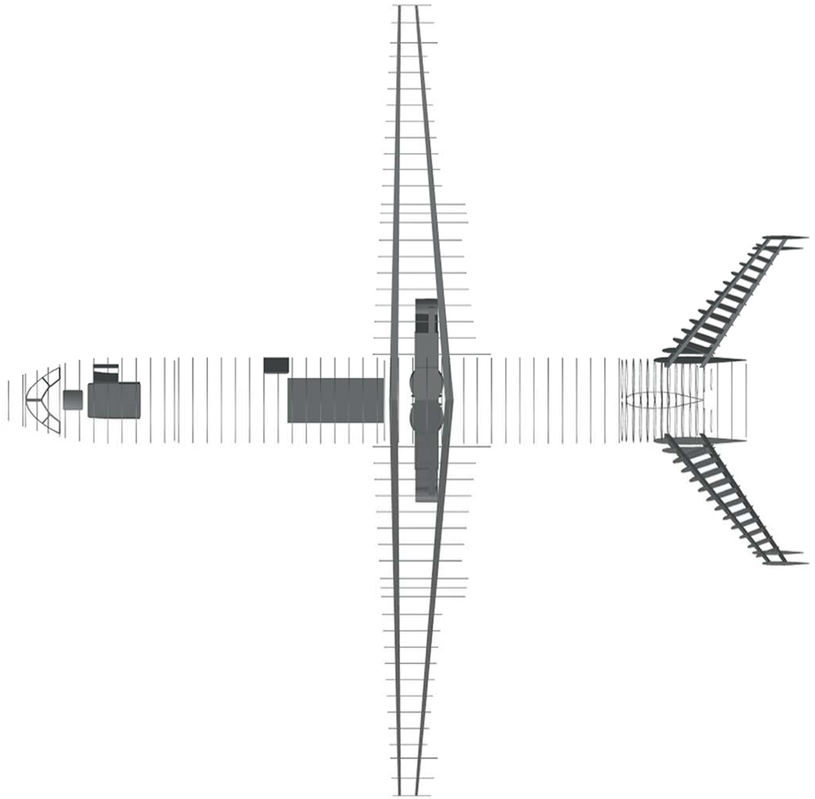

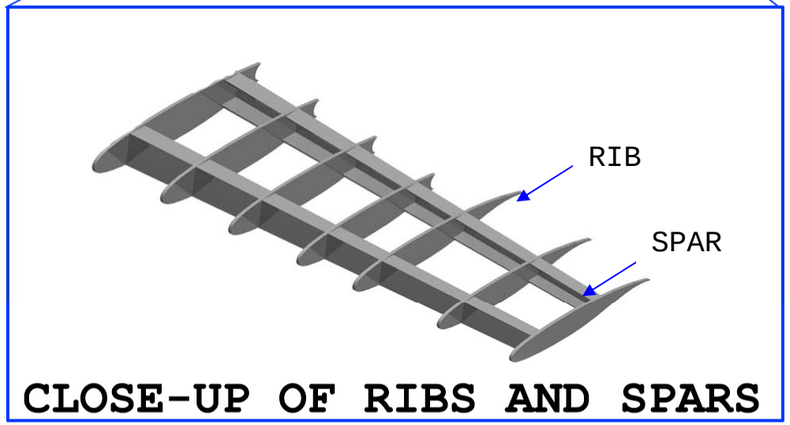

CLOSE-UP OF RIBS AND SPARS

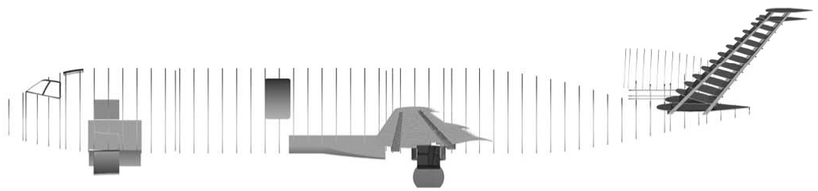

DRAWING TITLE: **CASPER STRUCTURAL DESIGN**

DESIGNED BY: TEAM CASPER		
DRAFTED BY: ANDREW HOPKINS		
SCALE: NTS	DATE: 5/5/05	DWG NO.

7.2 V-n Diagram

The V-n diagram of the Casper is shown in Figure 24 below. This diagram represents the aircraft's limit load factor as a function of airspeed and provides the structural flight envelope for the design. The analysis uses sea level equivalent airspeed so that the results can easily be applied to any altitude. The positive and negative maneuvering lines, which are represented using blue dashes, are based on a C_{nmax} of 2.08 and a C_{nmin} of -1.21. The dive speed is assumed to be 1.5 times the cruise speed at 30,000 *ft*, which converts to 367 *keas*. The positive limit maneuvering load factor was found to be 2.34 based on the gross weight of the aircraft; however, a minimum positive limit of 3.5 is required by the RFP. The negative design limit load factor was assumed to be -1 up to the cruise speed and then to vary linearly to zero at the dive speed. The gust lines, which are shown in red, are based on standard gust velocities of 66 *ft/s* for max gust, 50 *ft/s* for cruise gust, and 25 *ft/s* for dive gust. These gust lines do not limit the maneuvering diagram. The flight envelope, taking into account all constraints, can be seen outlined in black.

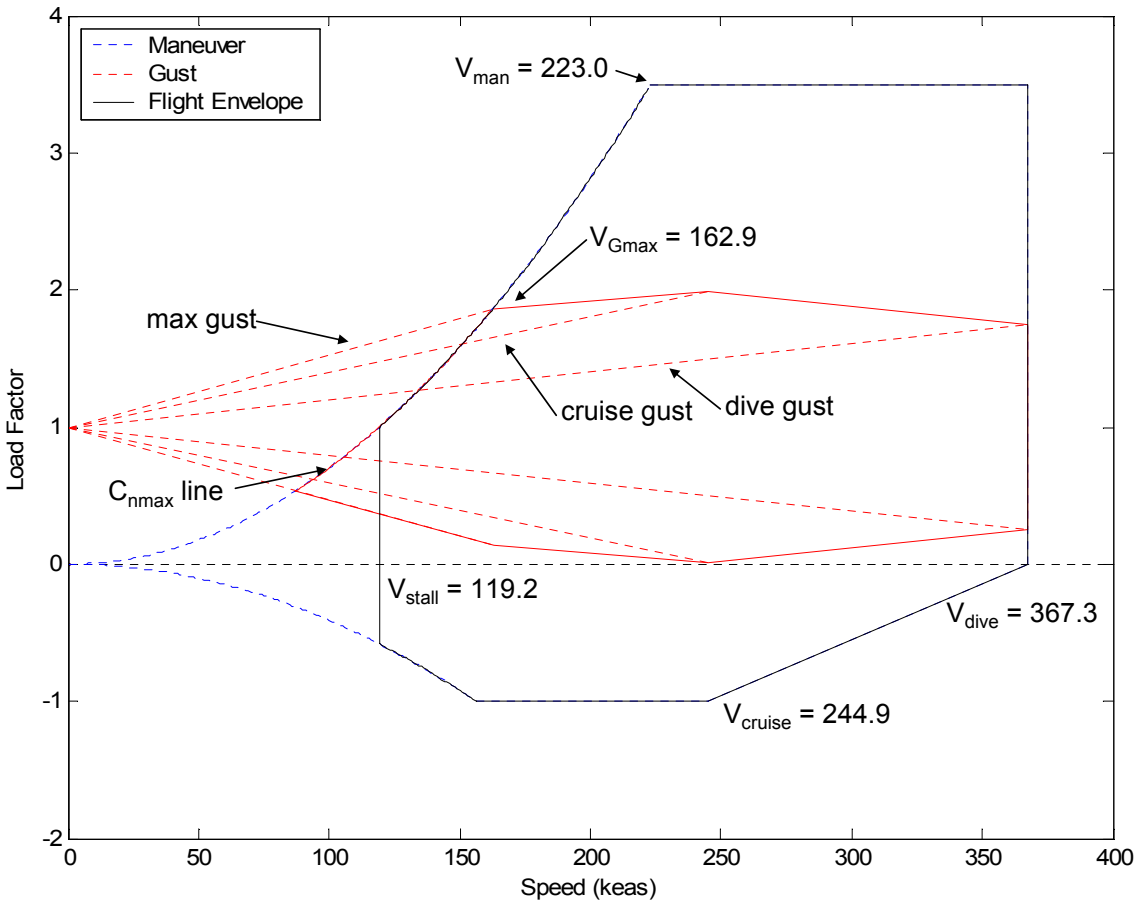

Figure 24. V-n Diagram showing load factor as a function of airspeed

7.2 Wing Structural Layout

The main wing structure, as shown in Figure 25, is composed of two spars, 46 ribs, and the wing skin. Stringers are also incorporated into the wing structure; however they are not visible in Figure 25. The spars are placed at 15 and 65 percent of the chord to allow room for the control surfaces and actuators as well as to maximize the usable area within the wing cross-section which saves weight. The rib positions were laid out by first placing a rib on either side of the ailerons and flaps, and then filling the gaps in evenly, leaving no more than 24 *in.* between each rib. The 24 *in.* minimum was chosen because it is the standard for transport aircraft.[34]

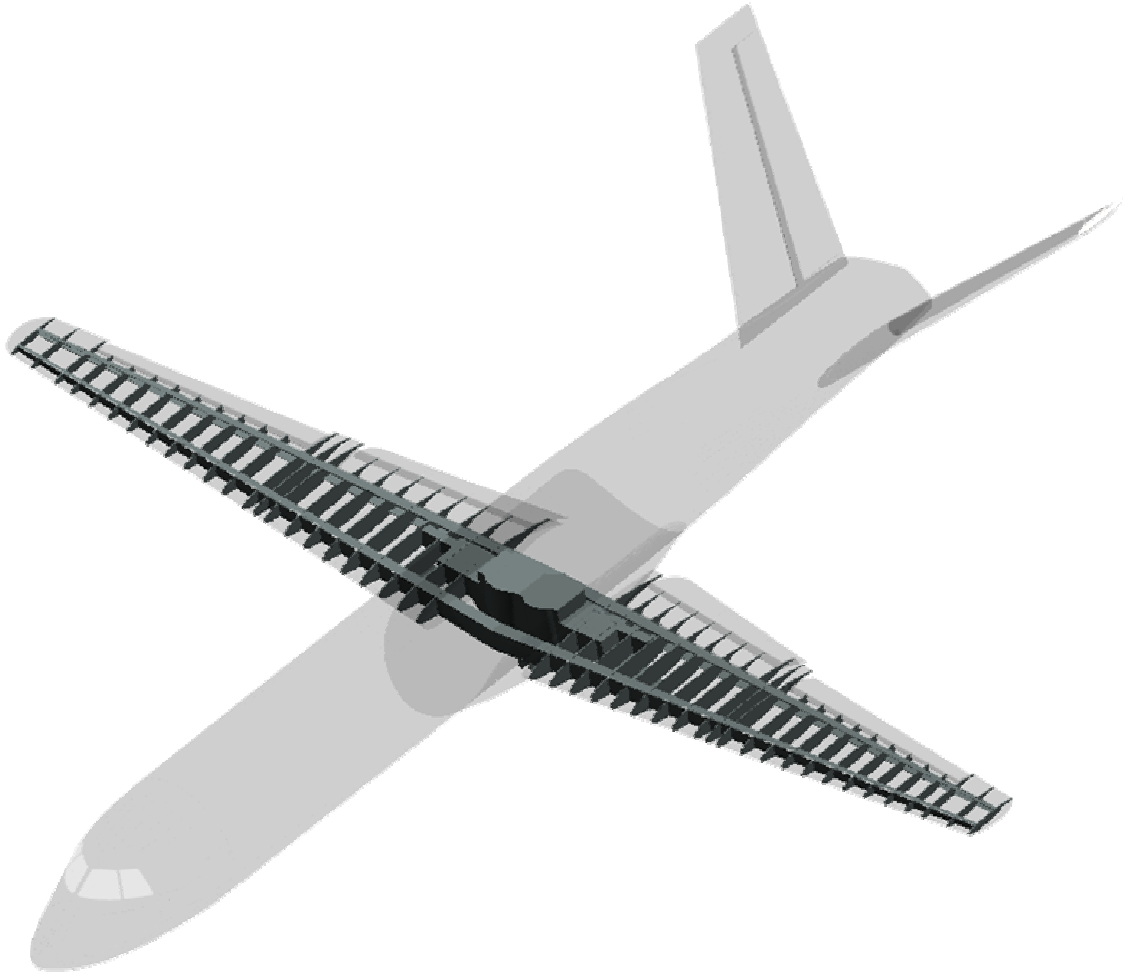

Figure 25. Wing structural layout

7.3 Wing Structural Analysis

The structural analysis of the wing assumes an elliptical lift distribution with a total transverse load equal to 3.5 times the Casper's gross take-off weight. This scenario models a load factor of 3.5, which is the highest load

factor expected in service. The resulting shear and bending moment along the wing can be seen in Figure 26 and Figure 27.

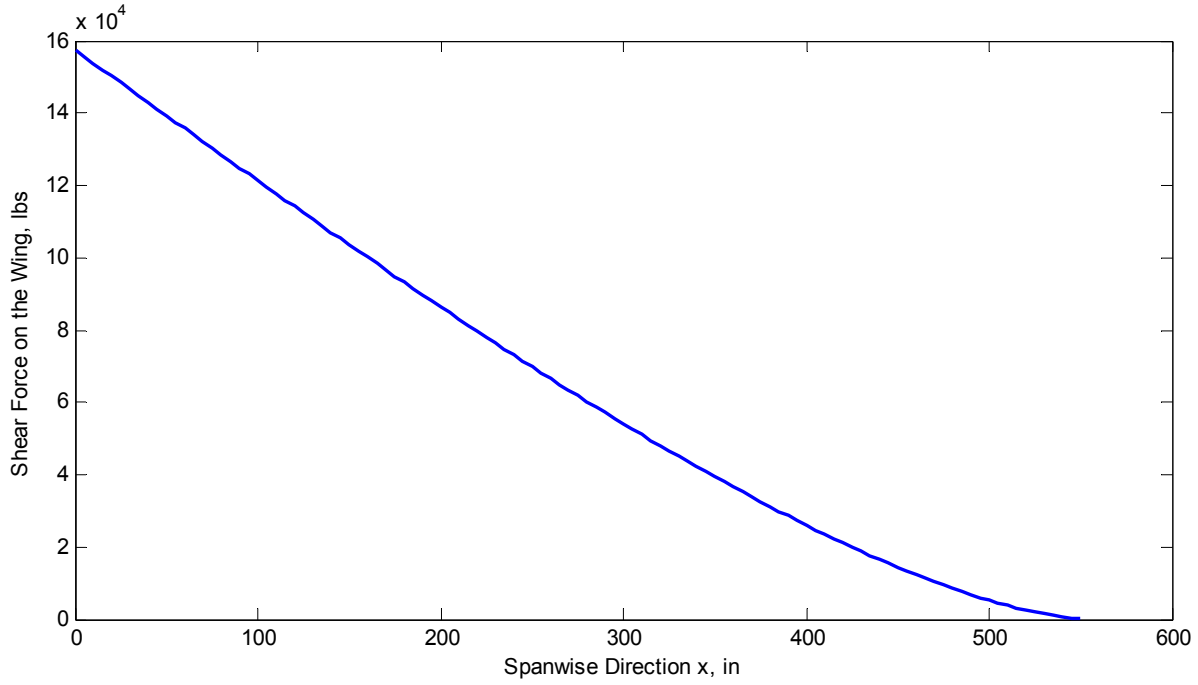

Figure 26. Shear Force over the semi-span of the wing due to an elliptical lift distribution, n = 3.5

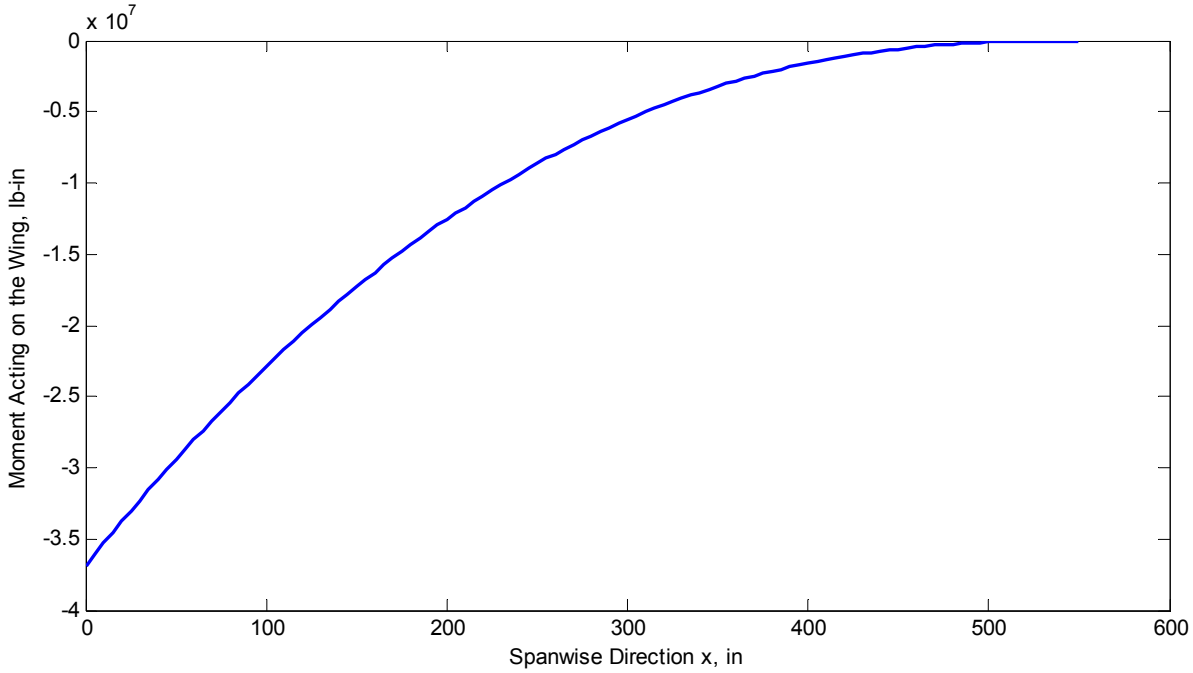

Figure 27. Bending moment across the semi-span of the wing due to an elliptical lift distribution, n = 3.5

The wing structure was modeled as a cantilever wing-box, shown in Figure 28. The area of the flange, A_f, the thickness of the web, t_w, and flange, t_f, determine the structural integrity of the wing box in tension, compression, and torsion. In practice, the wing-box is a trapezoid consisting of two C-beam spars and the wing skin; however, for the ease of calculation it is assumed to be rectangular with point areas representing the beam flanges. The height of the box, b_w, is taken to be average spar height in a given cross-section.

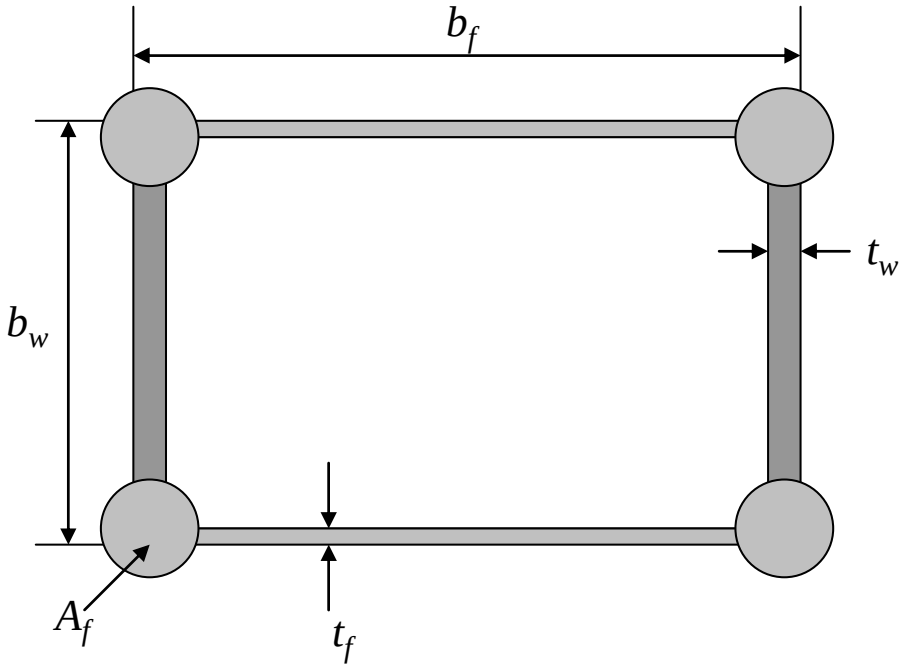

Figure 28. Theoretical representation of wing box

The maximum allowable stress of the wing box is defined as the ultimate strength of the material divided by the factor of safety, *FS* (1.5 as stated in the RFP). The wing box is constructed of Aluminum 7075-T6 which has an ultimate strength of 83 *ksi* in tension and 48 *ksi* in shear.[32] This makes the maximum allowable stress 55.3 and 32.0 *ksi* respectively.

The thickness of the web and flange are limited by the shearing stress due to torsion and bending and by the minimum manufactured thickness of aluminum. For the Casper, the minimum thickness based on these parameters is taken to be 1/8 of an inch for each component. Using the location of the maximum bending moment to be the wing root, the minimum moment of inertia of the wing box was found to be 6540 in^4. A constraint diagram, as seen in Figure 29 was used to determine the area of the flange. The thickness of the flange does not appear in this analysis

because the skin thickness is constant over the entire aircraft to save cost in manufacturing. The constraint diagram yields a flange area of 10.89 in^2.

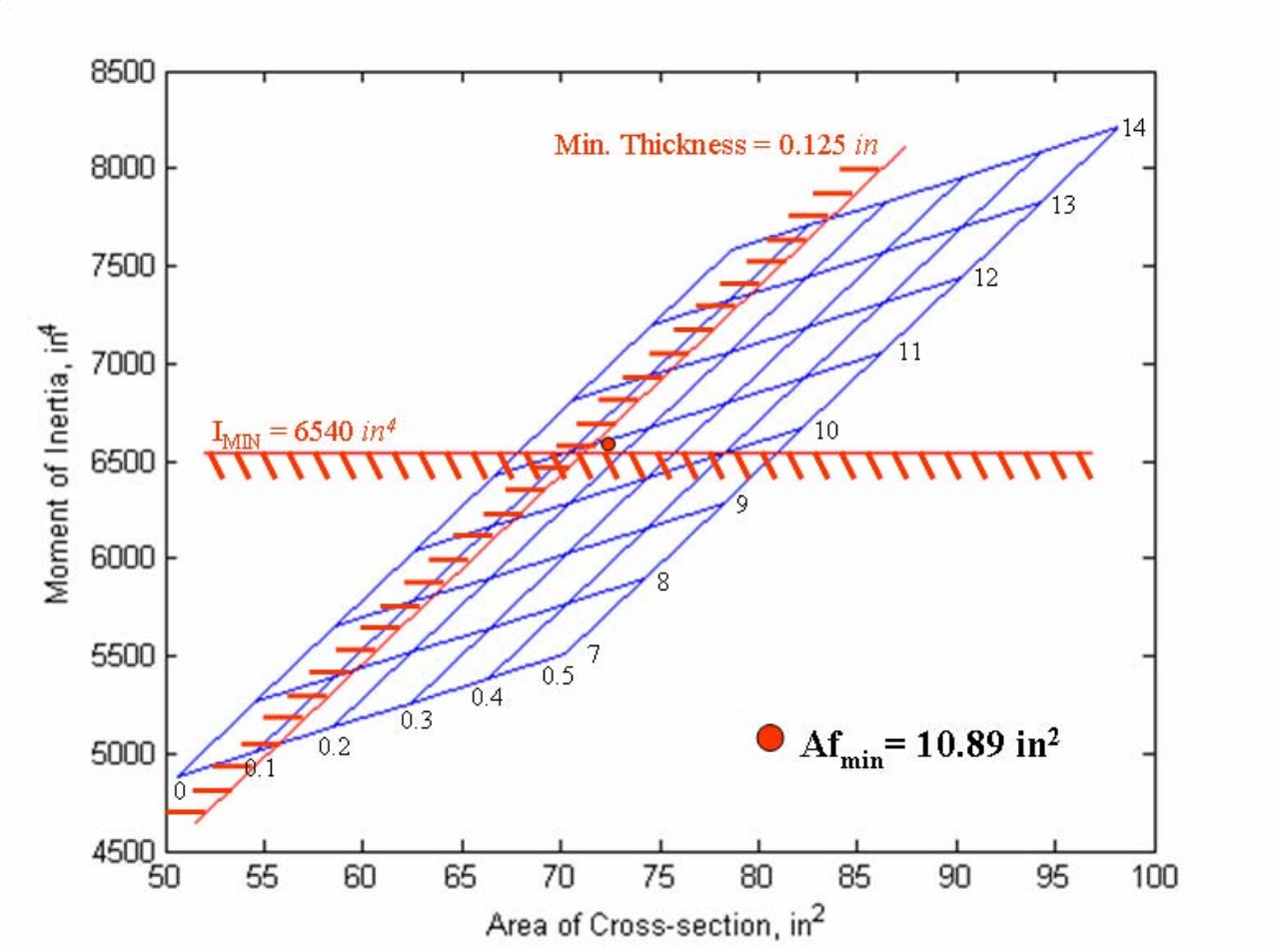

Figure 29. Wing Box Constraint Diagram: shows the optimum area of the flange to be 10.89 in^2

Due to the taper ratio of the wing, the wing box is smaller at the tip than at the root and therefore has a lower moment of inertia. The area of the flanges decreases quadratically due to the linear taper of the wing, requiring the inertia values to be compared at all locations across the span to ensure that the stress requirements are satisfied. This comparison, shown in Figure 30, reveals that the preliminary analysis at the root of the wing was sufficient.

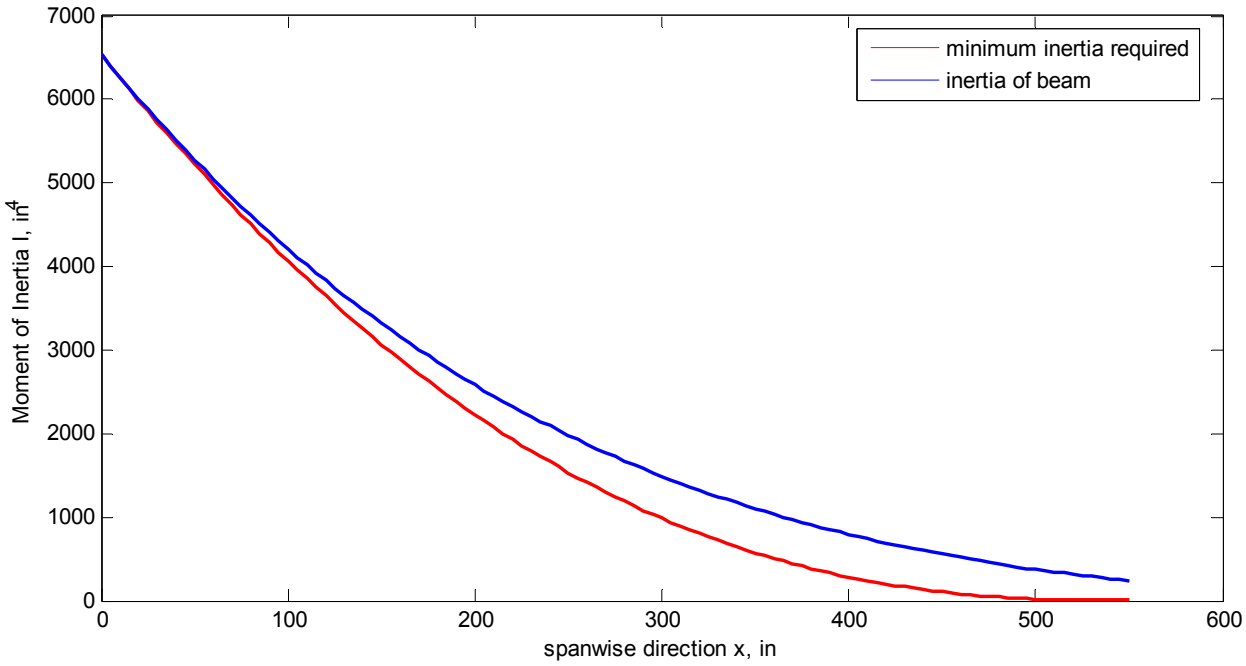

Figure 30. Diagram showing the inertia of the wing box is always greater than the required minimum moment of inertia across the span of the wing.

7.4 Fuselage Design

The main fuselage structure is composed of frames, stringers, and pressure bulkheads. The frames are placed 20 *in.* apart and are 3.4 *in.* deep. Additional frames are added at locations that carry large loads such as at the attachment of the landing gear, wing spars, and tail spars. The stringers are placed 10 inches apart around the circumference of the fuselage. For clarity, the stringers are not shown in Foldout 4. Pressure bulkheads are located near the nose of the aircraft and in front of the weapons bay to enclose the area where the crew will be operating. To make the Casper more adaptable for future missions, another pressure bulkhead can be added to the rear of the aircraft for optional total pressurization. A firewall is present at all times at the rear of the fuselage to protect the internal space from the APU.

7.5 Landing Gear

A tricycle landing gear arrangement is used for the Casper. For both the main gear and nose gear, a dual wheel configuration is used. For the main gear, there are two struts located 15° aft of the C.G. location and 38º off the centerline. The configuration of the main gear is modeled after that of the Boeing 737-300, while the nose gear configuration is modeled after the aft-retracting gear of the Fokker F-28. The dual wheel tricycle configuration

allows the CG to be ahead of the main landing gear, improves forward visibility on the ground, has good steering characteristics, and allows for a level floor while on the ground.[27]

Large tires with small wheel rim diameters allows for a smoother landing on uneven ground. For design purposes, it is assumed that the total main gear load is equal to 90% of the total aircraft weight, and the total nose gear load is equal to 10% of the total aircraft weight. To account for the conditions associated with austere airstrips, low pressure Type III tires are used for the design of the Casper. For the main gear, the Casper uses Type III 15.50-20 tires with a maximum width of 16.00" and a maximum diameter of 45.25". These maximum values give an allowance of 7.0" between the landing gear tires in the stowed configuration. The nose gear uses two Type III 7.50-14 tires with a maximum width of 7.65" and a maximum diameter of 27.75". Both the main gear and nose gear tires are pressurized to 90 *psi*. The main gear wheels have a diameter of 20.0" and are made of forged aluminum alloy, while the nose gear wheels have a diameter of 14.0". Coupling the wheels onto one shock absorber balances the shock forces in the gears, rather than the fuselage. All tires and wheels used are manufactured by BF Goodrich.

To absorb the high stresses associated with landing, oleo-pneumatic shock absorbers are utilized. This type of shock absorber has excellent energy dissipation with good rebound control. Oleo-pneumatic shocks have an efficiency of up to 90%, compared to the 50% for steel spring, 60% for rubber, and 75-90% for oil/liquid shock absorbers. For the main gear, the diameter of the shock absorbers is 6", with a stroke of 9".

The main landing gear is wing-mounted and retracts into a modified underbelly of the fuselage, as shown in Figure 31. The maximum time for retraction or extension of the gear is 30 seconds.

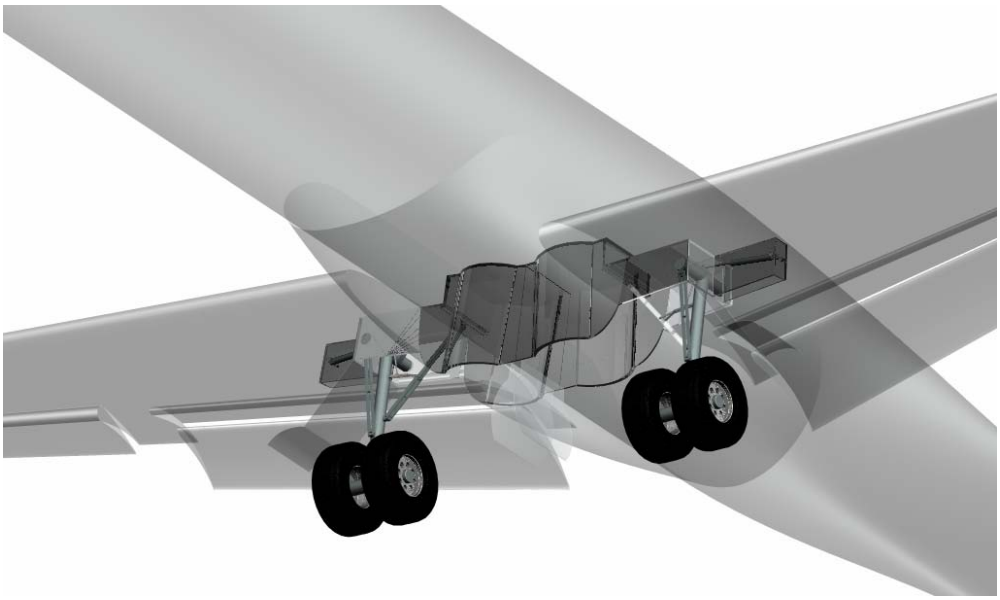

Figure 31. Main landing gear extended

7.5.1 Gear Retraction

Figure 32 shows the retraction and specifications of the nose landing gear.

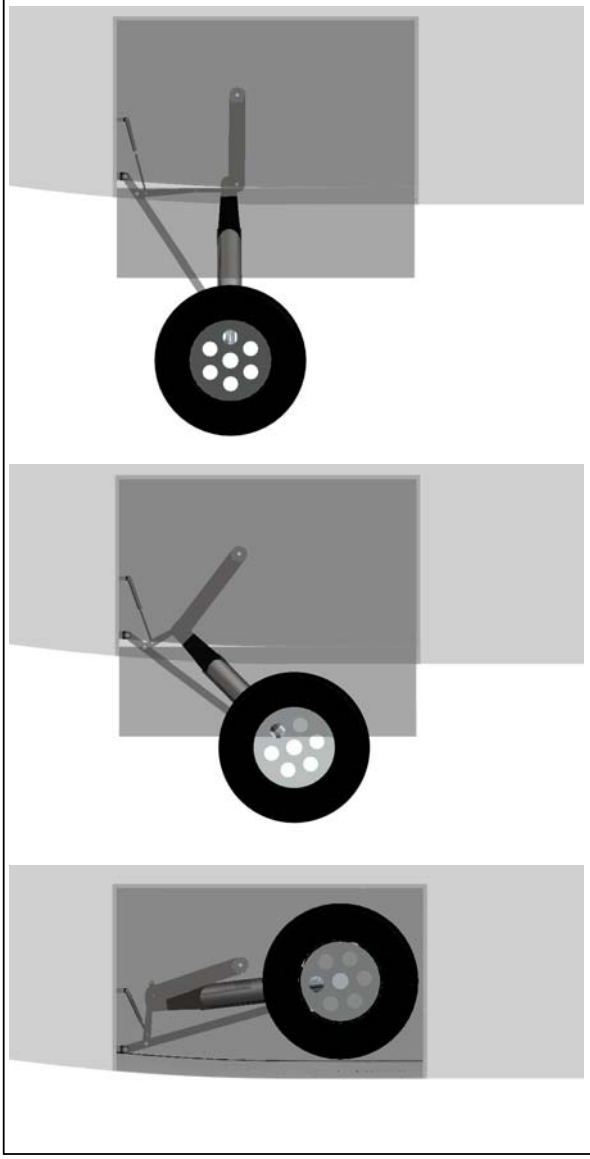

NOSE LANDING GEAR RETRACTION AND SPECIFICATIONS

RETRACTION:
TYPE: AFT-RETRACTING
CONFIGURATION: DUAL
RETRACTION TIME: 30 sec

TIRES:
CLASS: TYPE III 7.50-14
MAX. WIDTH: 7.65”
MAX. DIAMETER: 27.75”

WHEELS:
MATERIAL: FORGED Al ALLOY
DIAMETER: 14.0”

STRUTS & SHOCKS:
TYPE: OLEO-PNEUMATIC
MATERIAL: Ti-6A1-4V

Figure 32. Retraction and specifications of the nose landing gear

Figure 33 shows the retraction and specifications of the main landing gear.

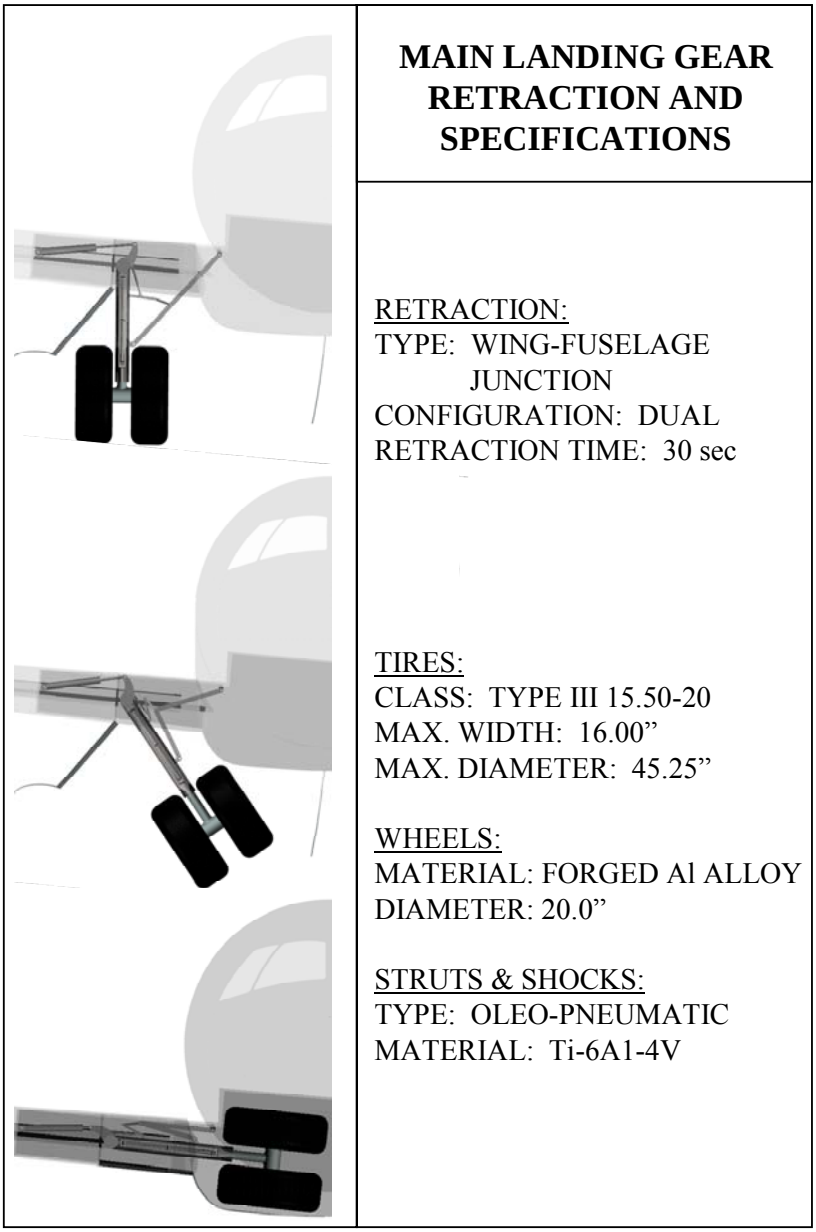

Figure 33. Retraction and specifications of the main landing gear

8. Weights and Balance

An estimate of the initial weight of the Casper was determined to be 90,000 *lbs* using a method based on weight fractions and mission specifications. Using this estimate, component weights can be determined using of a combination of methods described by Raymer[3] and Roskam.[35] A breakdown of the component weights can be seen in Table 10, along with component x-CG location measured from the nose of the aircraft. With a final TOGW of 89,911 *lbs*, less than 1% off of the original estimate.

Table 10. Weight breakdown

Weight Group		Weight Average pounds	Fusleage Station inches
Wing Group		8268	50.61
Empennage Group		1804	88.51
Fuselage Group		5658	43.17
Nacelle Group		2296	78.71
Landing Gear Group		2725	
	Nose Gear	818	8.00
	Main Gear	1908	53.00
Structures Total Weight		20751	48.34
Engines		9440	78.71
Fuel System		30	73.46
Propulsion Systems		4327	78.71
Engine Cooling		460	76.71
Power Plant Total		14257	78.64
Avionics		1538	10.00
APU		248	25.00
Instruments		564	8.00
Oxygen System		54	25.00
Surface Controls		225	
	Ailerons	105	54.61
	Ruderrvators	120	92.51
Hydraulic/Pneumatic System		243	64.80
Electrical System		792	22.50
Air Conditioning System		439	25.00
Pressurization System		225	15.50
Anti-Icing System		156	50.61
Furnishings		5577	15.00
Paint		405	43.17
Lavatory		100	20.00
Aircraft Systems Total		10566	17.65
Unuasble Fuel/Oil		280	50.61
Oil		50	58.11
Useable Fuel		28000	50.61
Fuel Total		28330	50.62
Crew		1000	20.00
Fixed Weight	Bofors Cannon 1	4000	33.00
	Bofors Cannon 2	4000	23.00
	GAU-12	1000	28.00
Dispensible Weight	Bofors Rounds 1	557	38.00
	Bofors Rounds 2	557	27.00
	GAU-12 Rounds	3294	28.00
	GBU's	1600	39.00
Payload(Design)		15007	29.51
Takeoff Gross Weight		89911	48.74

The CG of the Casper is located 48.74 *ft* from the nose of the aircraft with the TOGW of the primary mission. Due to the loss of fuel and payload, the CG location moves during flight. A diagram of the CG travel during the design mission can be seen in Figure 34. Using the Athena Vortex Lattice code, created by MIT, forward and aft limits to the CG travel were calculated to be 7.6% and 54.4% of the mean aerodynamic chord, respectively. To ensure that a reasonable static margin is maintained, forward and aft limits of the CG were placed at 5% and 40% of the mean aerodynamic chord, respectively. The CG location stays within these bounds during the entire flight. A similar diagram for the ferry mission can be seen in Figure 35. Again, the CG location stays within the set bounds.

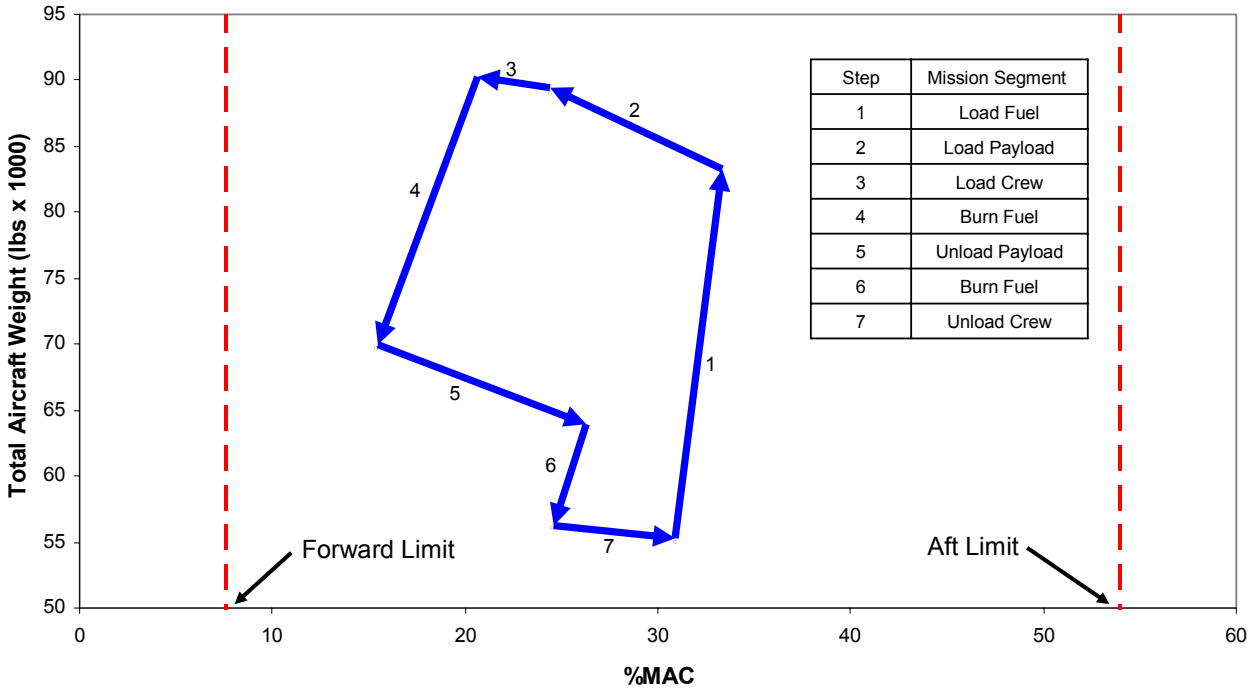

Figure 34. CG travel for the design mission

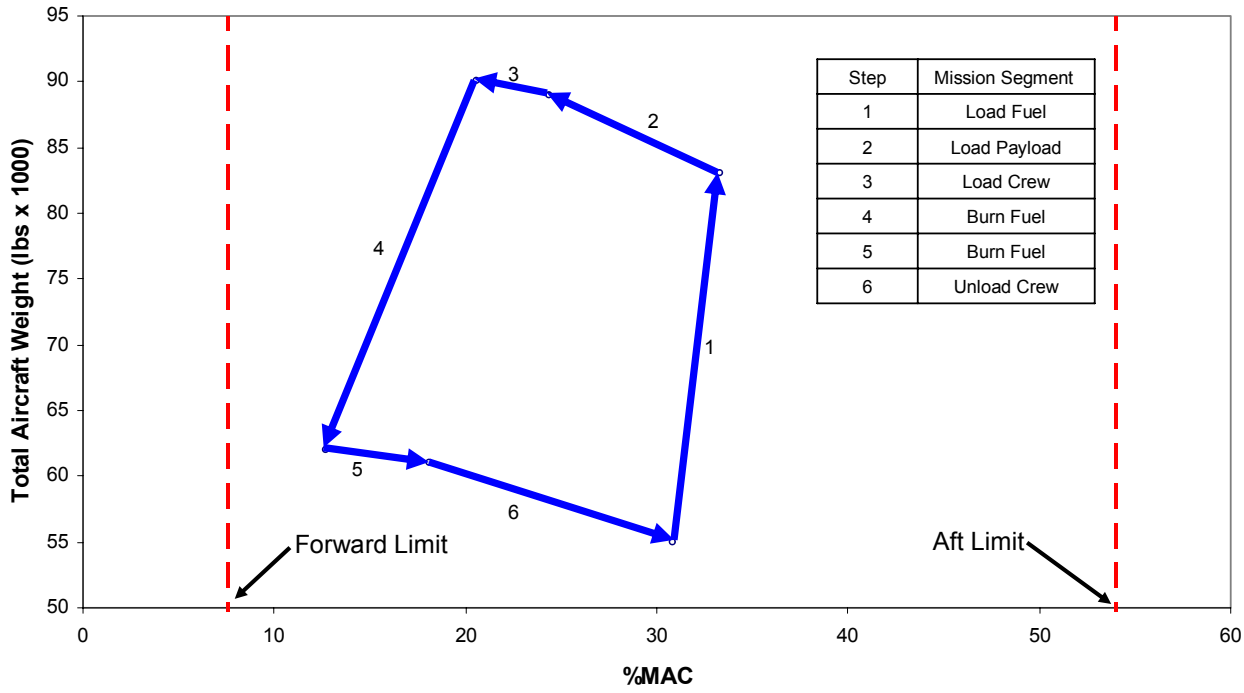

Figure 35. CG travel for the ferry mission

9. Aerodynamics

The airfoil section and the geometry of the wing and tail were selected to meet the takeoff, landing and cruise requirements specified by the RFP. Minimizing both the drag and the structural weight of the lifting surfaces was also taken into consideration. The airfoils were selected to reduce the drag at transonic speeds. The flaps are designed to enable the Casper to take off and land on austere airstrips. The aerodynamic analysis utilized a combination of computer software, such as AVL and X-FOIL, analytical methods, and available experimental data.

9.1. Airfoil Selection

Since the Casper cruises near the transonic flow regime ($M \approx 0.7$), NASA supercritical airfoils were selected for the wing and the V-Tail to delay the transonic drag rise. The wing uses a NASA SC(2)-0714 airfoil (Figure 36), which has a design lift coefficient of 0.7 and a maximum thickness ratio of 0.14[1]. The V-Tail uses the symmetrical NASA SC(2)-0012 airfoil (Figure 37) with a maximum thickness ratio of 0.12.[2]

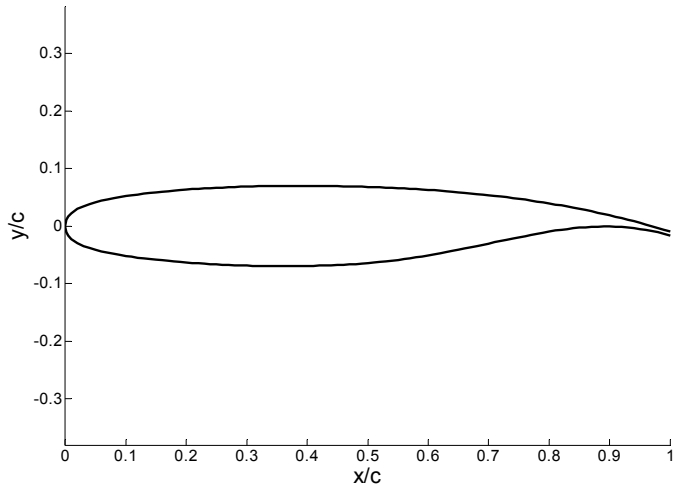

Figure 36. NASA SC(2)-0714 airfoil used for wing

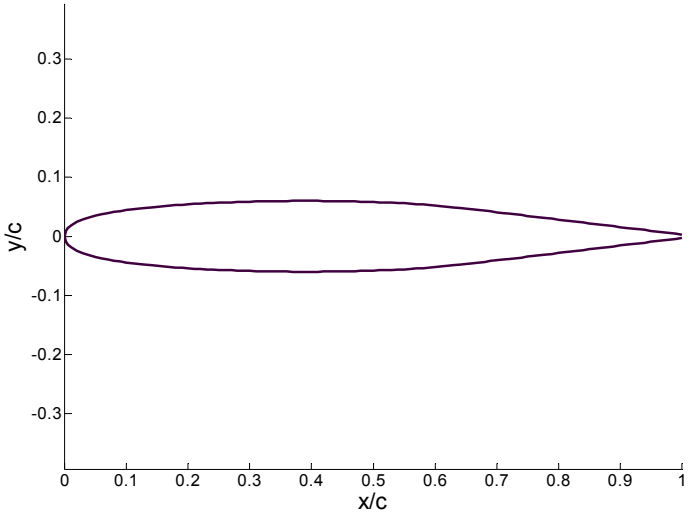

Figure 37. NASA SC(2)-0012 airfoil for V-Tail

The critical Mach number of a 3D wing can be calculated using the following equation, which is plotted in Figure 38.

$$M_{crit_{3D}} = \frac{M_{crit_{2D}}}{(\cos\Lambda_{1/4})^{0.5}} = \frac{A_F - 0.1C_{L_{cr}} - (t/c)}{(\cos\Lambda_{1/4})^{0.5}}$$

where A_f is the technology factor, $C_{L_{CR}}$ is the cruise lift coefficient, $M_{crit_{2D}}$ is the 2-D critical Mach number, $\Lambda_{1/4}$ is the quarter-chord sweep, and *t/c* is the thickness ratio. The values of A_f and $C_{L_{CR}}$ are estimated to be 0.9

and 0.58 respectively. Using this method, Figure 38 illustrates the relationship between the thickness ratio and critical Mach number for a 3-D airfoil versus quarter-chord sweep.

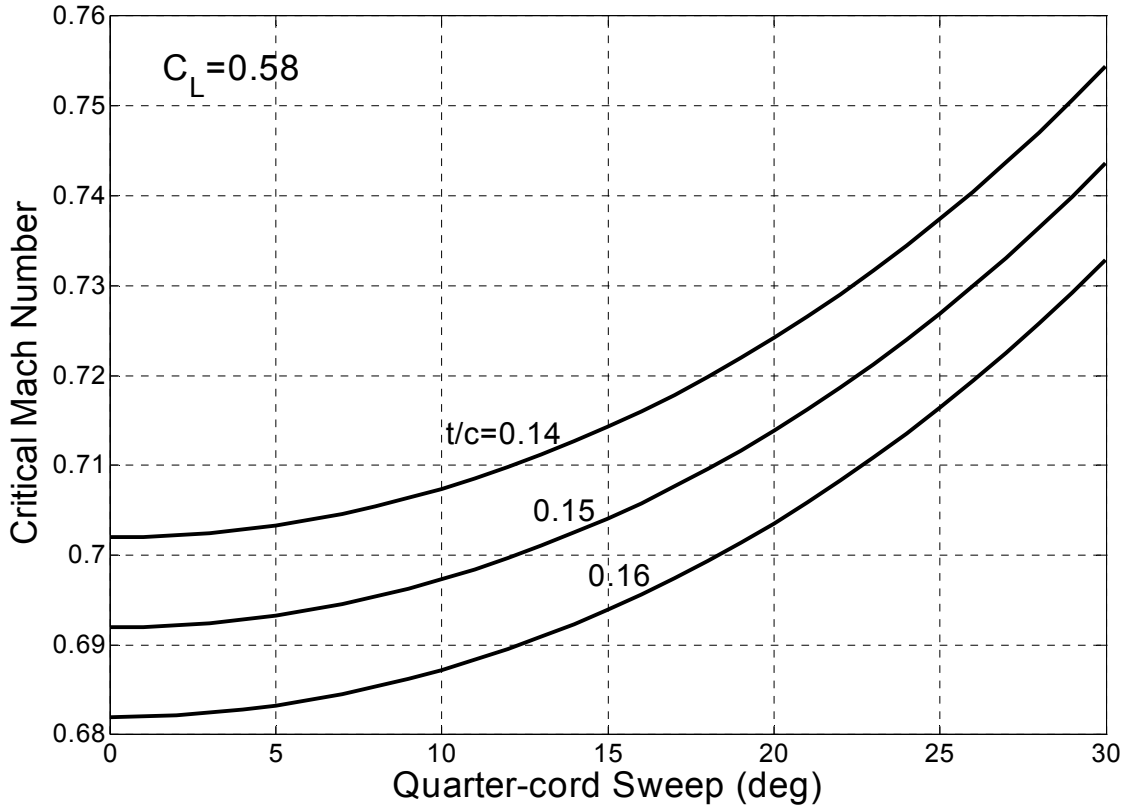

Figure 38. Critical Mach number vs. quarter-chord sweep

Figure 37 shows that a thickness ratio equal to or less than 0.14 should allow the critical Mach number of the wing and V-Tail to be above the cruise Mach number of 0.7.

9.2. Wing Geometry

The Casper's wing employs an un-swept trapezoidal planform shape with a high aspect ratio and a moderate taper ratio. The aspect ratio is estimated to be 9.38 from statistical data for tactical transports. A taper ratio of 0.3 is chosen based on statistical data and a compromise between wing structural weight and near-elliptical lift distribution. A twist of $\varepsilon_t = -3^o$ (washout) was chosen to improve control at high angles of attack during takeoff and landing, and a dihedral of $\Gamma_w = 5^o$ was chosen to improve stability during cruise. An incidence angle of

$i_w = -0.5^o$ was chosen to ensure that the fuselage is level while cruising. To reduce the induced drag of the wing, a Hoerner wingtip was chosen, as shown in Figure 39.[3]

Figure 39. Hoerner wingtip used to reduce drag

Hoerner wingtips are commonly used as low-drag wingtips. A summary of the wing geometric parameters is presented in Table 11.

Table 11. Detailed Wing Geometry

S	900 ft^2
AR	9.38
λ	0.3
$\Lambda_{1/4}$	0
ε_t	-3° (Washout)
Γ_w	5°
i_w	-0.5

9.3. Prediction of Airplane Lift

The airplane lift is approximated as the sum of the lift generated by the wing and the V-Tail. The subsonic 2D lift curve for the wing airfoil was estimated using XFOIL and corrected using experimental data. The transonic lift curve for the wing airfoil was obtained from experimental data at M = 0.7.[36] The subsonic 2D lift curve for the dihedral airfoil was estimated using X-FOIL and verified against that predicted using the DATCOM method. The transonic 2D lift curve for the V-Tail airfoil was obtained from experimental data at M = 0.7.[37] The clean lift curve for the 3D aircraft was estimated using the DATCOM method. The trim calculations were performed using AVL, which assumed the change in airplane lift varies linearly with ruddervator deflection. The DATCOM method was used to compute the trimmed lift curve for the airplane.[38] The sizing and lift calculation for the flaps was done using a combination of DATACOM method and X-FOIL.

9.3.1 Takeoff, Landing and loitering

To meet the 5000 *ft* takeoff and landing requirement stated in the RFP, the Casper utilizes a Fowler flap sized to be 30% of the wing chord and extend to 34% of the wingspan. The maximum flap deflection is 30°, with an achievable $\Delta C_{L_{Max}}$ of 0.71. The Fowler flaps are illustrated in Figure 40.

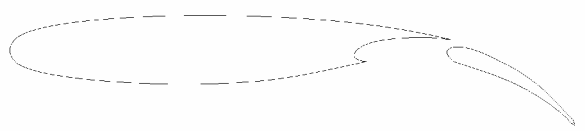

Figure 40. Wing with fowler flaps deflected

Viscous flow calculations are performed using XFOIL to estimate the lift coefficients of the two supercritical airfoil sections at a takeoff speed equivalent to $M = 0.18$. Although the Casper loiters at $M = 0.35$, no separate lift curve is computed for loitering because the difference in Mach number is minimal. An experimentally determined value of $C_{L_{MAX}} = 2.1$ is used.[39] For the V-Tail, NASA SC (2)-0012 airfoil, the maximum lift coefficient is determined and verified against XFOIL results.[38] Figure 41 shows the trimmed lift curve of the entire airplane at subsonic speeds. When the flaps are not deployed, the trimmed maximum lift coefficient is $C_{L_{\max}} = 1.78$ at $\alpha_{stall} = 18^o$. When the flaps are deployed, the trimmed maximum lift coefficient is $C_{L_{\max}} = 2.66$ at $\alpha_{stall} = 15^o$. At a loitering C_L of 1.05, the angle of attack of the aircraft is about 4°.

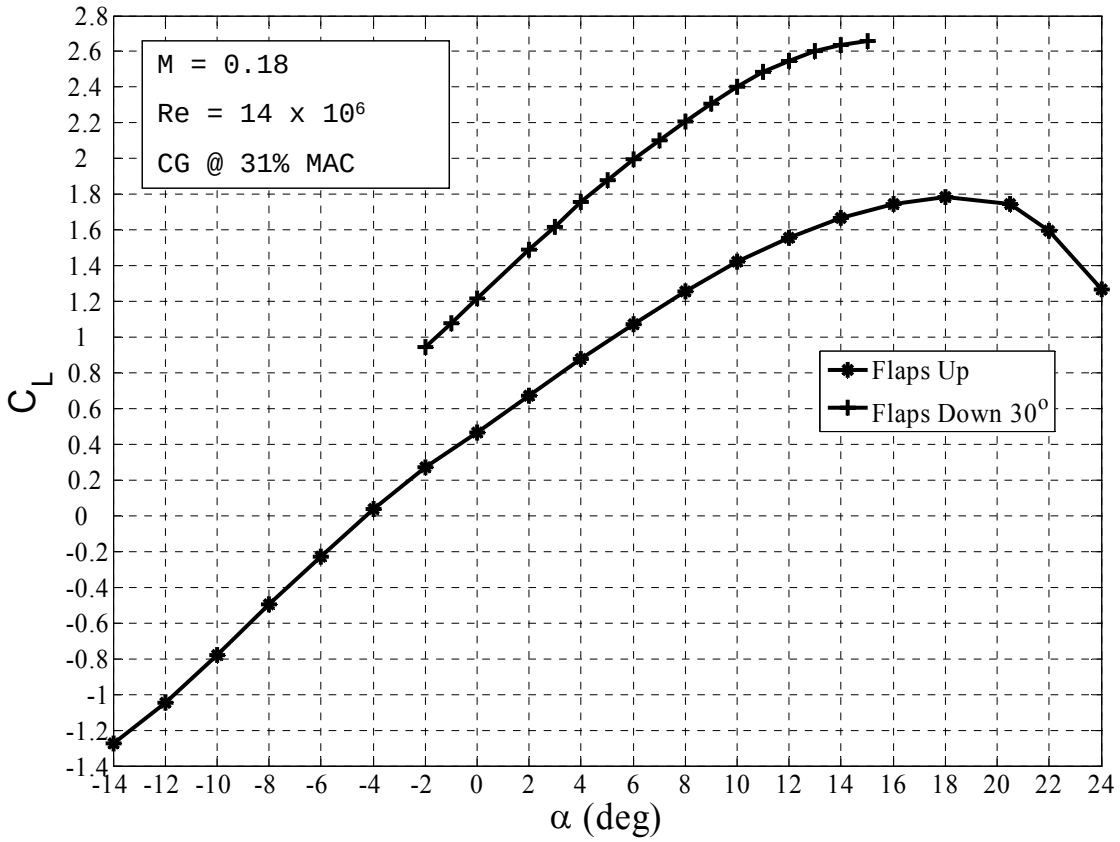

Figure 41. Trimmed subsonic airplane lift curves

9.3.2. Cruise

Figure 42 shows the trimmed airplane lift curve at Mach 0.7. The lift curve is constructed using the airfoil lift data for angles of attack ranging from -4° to 4°. First order least-square fits are done on the data, and the data are extrapolated to -5 and 5 degree angles of attack. The lift coefficient at cruise conditions is about 0.53, which correspond to an angle of attack of 0.25°.

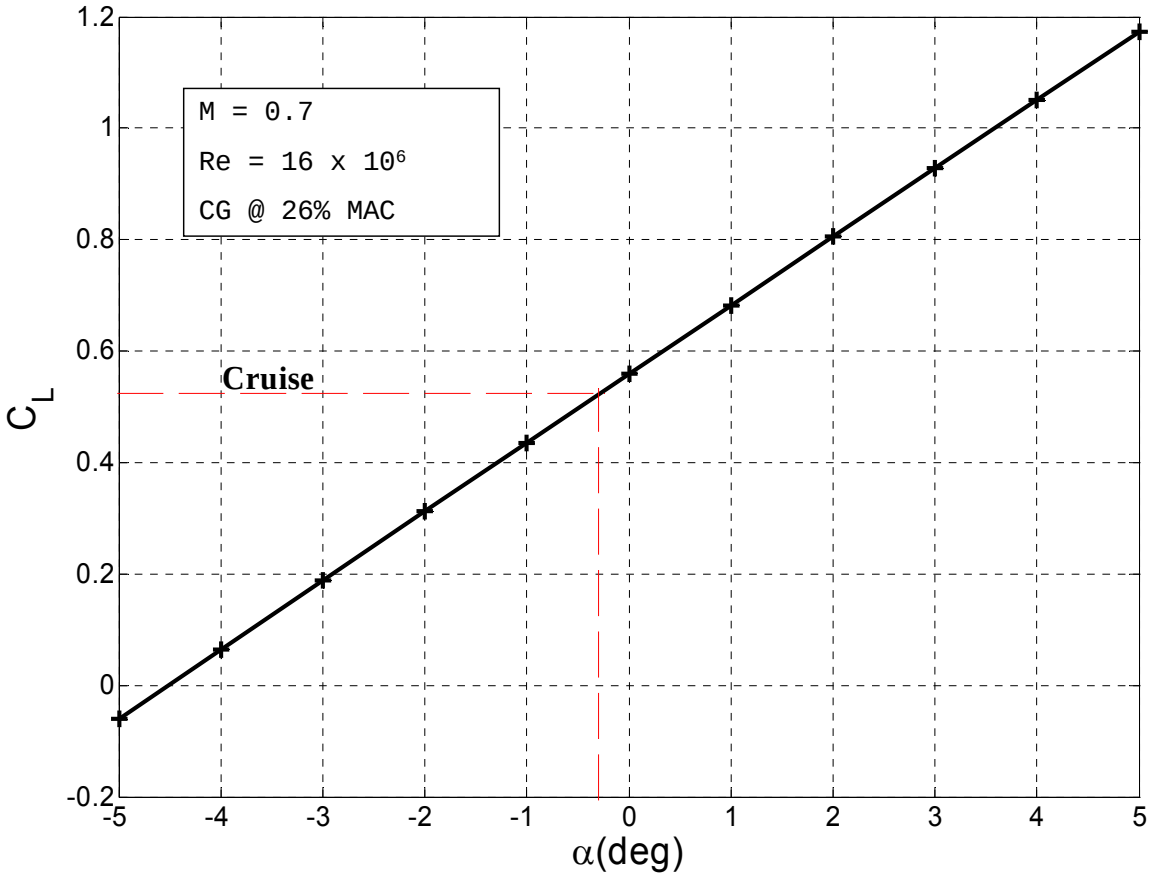

Figure 42. Trimmed Airplane Lift Curve at Cruise Mach number of 0.7

9.4 Prediction of Airplane Drag Polar

The aircraft drag polars at high-lift and cruise conditions were estimated using a combination of the DATCOM method and experimental data. Fairings were used to reduce the drag caused by the cannon barrels and external sensors. For the cannon barrels, the fairings were small rectangular wings with NASA SC(2)-0012 airfoils (Figure 15). A ball bearing design is used to keep the fairings aligned with the flow at different angles of attack. This drag reduction technique was experimentally shown to reduce the drag caused by the 40mm cannon barrels by approximately 55%.[40]

9.4.1 Takeoff, landing and loitering

The drag polars at takeoff, landing and loitering conditions are estimated using the methods presented in Reference 38 and Reference 41. The total airplane drag is equal to the sum of the parasite drag and the drag due to lift of each component of the aircraft, including miscellaneous drag for additional components. Most of the interference drag was already taken into account in the calculation of the drag of each component. Additional interference drag is ignored in our calculations. A miscellaneous drag of 0.0007 is added to take into account any protuberances on the airplane such as a targeting pod and antennas. Table 12 shows the parasite drag buildup of the Casper at takeoff and landing conditions.

Table 12. Drag coefficient breakdown for takeoff and landing

Component	C_{D_0}
Wing	0.00728
V-Tail	0.00311
Fuselage	0.00782
Nacelle	0.00181
Pylon	0.00039
Flaps(30^o)	0.05650
Landing Gears	0.01100
Cannon Barrel Fairings	0.00024
Miscellaneous	0.00070
Total	**0.0889**

Figure 43 shows the airplane drag polar at takeoff, landing (with full flap deflection) and loitering conditions.

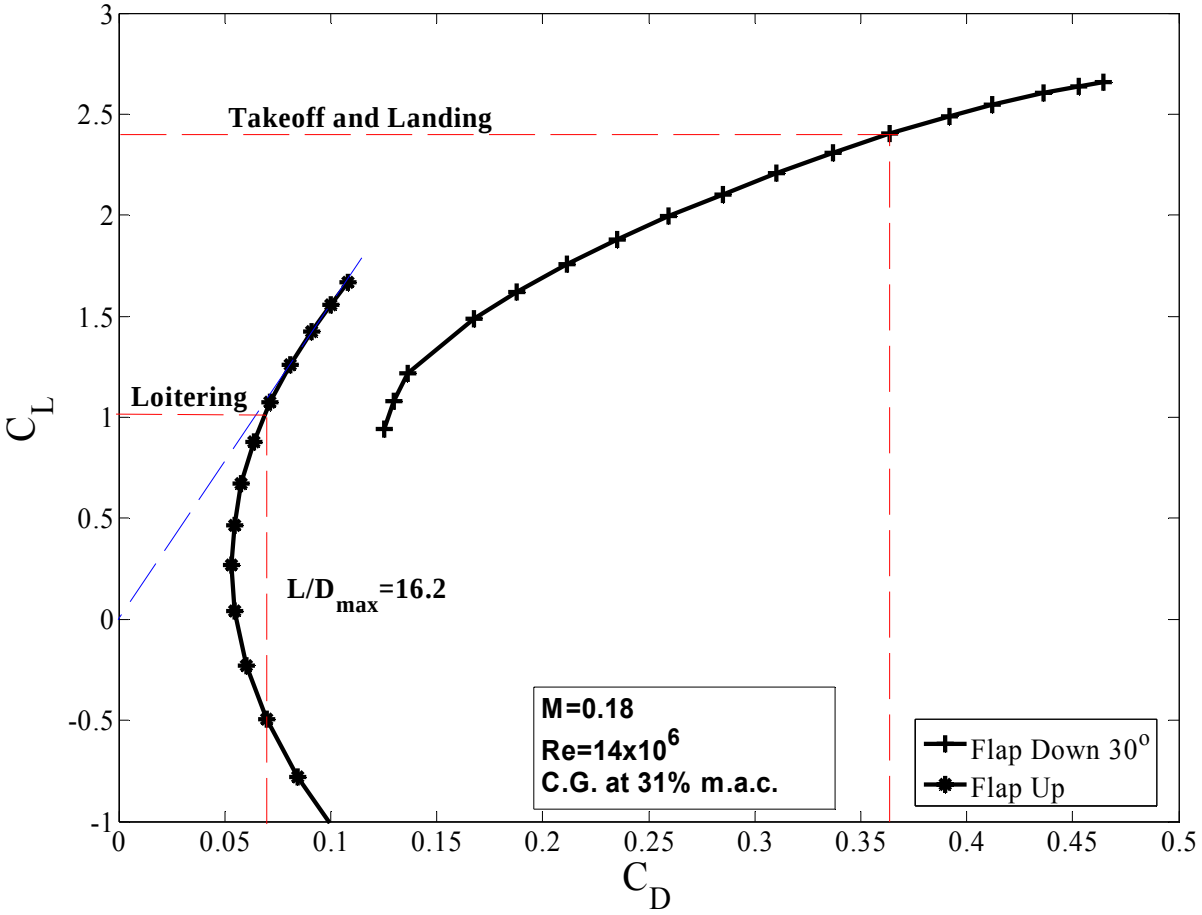

Figure 43. Trimmed airplane drag polar at takeoff, landing and loitering conditions

9.4.2 Cruise

Since the Casper cruises near the transonic flow regime, methods presented in Ref. 5 and Ref. 9 were used to estimate the drag of each component, excluding the wing, the tail, and the fairings for the cannon barrels. The drag of the wing, V-Tail, and the barrel fairings was estimated using the experimental drag polar of the two supercritical airfoils, presented in Reference 37 and Ref. 39. A polynomial fit of the experimental airfoil drag polars was performed to generate the airplane drag polar. Table 13 lists all the components included in the drag polar estimation, and the analytically estimated parasite drag for the fuselage, nacelles, and pylons.

A miscellaneous drag of 0.001 is added to account for any additional drag that is not considered in our calculations. Figure 44 shows the drag polar of the aircraft at cruise conditions. Table 14 shows the L/D values at different stages of the mission.

Table 13. Cruise parasite drag by component

Component	C_{D_0}
Wing	0.00909
Dihedral Tail	0.00824
Fuselage	0.00629
Nacelles	0.0016
Pylons	0.00035
Cannon Barrel Fairings	0.000303
Miscellaneous	0.001
Total	**0.0269**

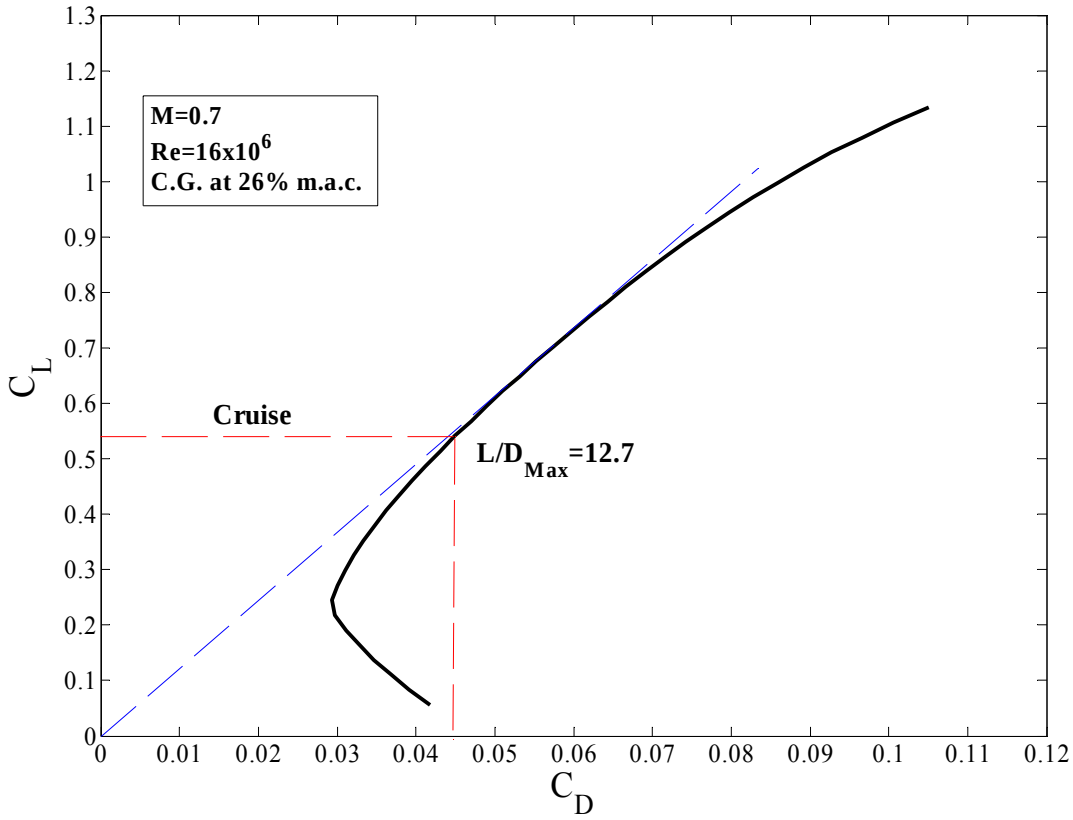

Figure 44. Trimmed drag polar at cruise conditions

Table 14. Lift to drag ratio for different mission segments

	Altitude(ft.)	Mach #	C_L	L/D
Takeoff and Landing	Sea Level	0.2	2.6	7.9
Cruise: Ingress and Ferry	34,000	0.69	0.54	11.8
Cruise: Egress	42,000	0.69	0.54	11.8
Loitering	20,000	0.35	1.05	14.3

10. Stability and Control

Using the Athena Vortex Lattice (AVL) code, stability and control analysis for the Casper was performed at takeoff/landing, loitering, and attack conditions. In addition, DATCOM methods presented in *Airplane Design: Part VII* by Roskam were utilized to check the validity of the stability and control derivatives output by AVL.[42] The dynamic stability characteristics of the Casper at each of the flight conditions were also calculated using AVL.

10.1 Wing Placement, Tail Design and Sizing

The placement of the wing was decided based on a trial-and-error method, which ensured the aircraft was stable and controllable at all flight conditions. The V-Tail design was selected for survivability considerations, especially against MANPADS threats. Specifically, the V-Tail helps to block visibility of the engine exhaust and the engine combustion air nozzle, thus reducing the Casper's IR signature. The initial sizing of the tail was based on the tail-volume method presented in *Aircraft Design* by Raymer for a jet-transport aircraft (c_{HT}=1.00, c_{VT}=0.09).[3] The horizontal and vertical areas were obtained using this method and were equated to be the horizontal and vertical projections of the V-Tail. After the initial sizing, the tail size was refined through AVL trim calculations. Tail planform characteristics were based on historical data presented by Raymer. A summary of the V-Tail planform is shown in Table 15.

Table 15. V-Tail planform characteristics

S_Γ	314ft^2
Γ_t	38.9º
AR	4.5
Λ	35 º
λ	0.5
Airfoil	NASA SC(2) 0012

10.2 Control Surfaces

The initial control surface sizing was based on historical guidelines and data for similar aircraft as presented in *Airplane Design: Part VII* by Roskam[42] and *Aircraft Design* by Raymer.[3] After initial sizing, trim calculations were performed in AVL to refine the sizing. The ailerons extend from 50% to 90% of the half-span length, and compose the aft 30% of the wing chord. The ailerons are capable of a +/-25 degree deflection. Such large control surfaces for an aircraft of this size were chosen to counteract any rolling moments that resulted from the operation of the V-tail, and to help Casper meet military roll performance requirements.

The V-Tail configuration requires the tail control surfaces, or "ruddervators" to control both pitch and yaw for the aircraft. Due to their dual-function nature, the ruddervators are relatively large. The ruddervators cover from 10% to 90% of the tail span, and 50% of the tail chord length. Ruddervators also have a maximum deflection of ±25º. These control surfaces require a computerized flight control system, as each individual ruddervator must move independently of its counterpart.

10.3 Control Deflections for Trim and Takeoff

Trimming the aircraft at the mission required 1g cruise condition requires a -4.02º deflection of the ruddervators ([-] deflection yields nose up moment). This will cause Casper to cruise at an angle of attack for the entire aircraft of about 0.26º, which should be quite comfortable for the aircrew.

The one engine out condition yields a yaw moment of about 42,000 *ft-lbs*. Trim requires a 1.51º deflection of the ruddervators, one [+] deflection and one [-] deflection. Deflecting the ruddervators in this manner causes a roll moment of roughly 9670 *ft-lbs*. To counteract this moment, the large ailerons require only 0.328º of deflection. The resulting bank angle is less than two degrees.

To achieve our desired takeoff coefficient of lift with a flap deflection of 30º and a takeoff velocity of 200 *ft/s*, will require a ruddervator deflection of -17.5º. This will cause the aircraft to rotate about 12º at takeoff, which is less than the design limit of 15º. All required deflections for trim and takeoff are within our deflection limits.

10.4 Stability and Control Derivatives

Stability and Control derivatives were determined using the AVL program written by Harold Youngren at MIT in 1988.[43] Since that time the program has gone several revisions with the last update coming on 28 August 2004. AVL is a vortex-lattice method utilizing program. The paneling scheme for the Casper, as input into AVL, is illustrated in Figure 45 below.

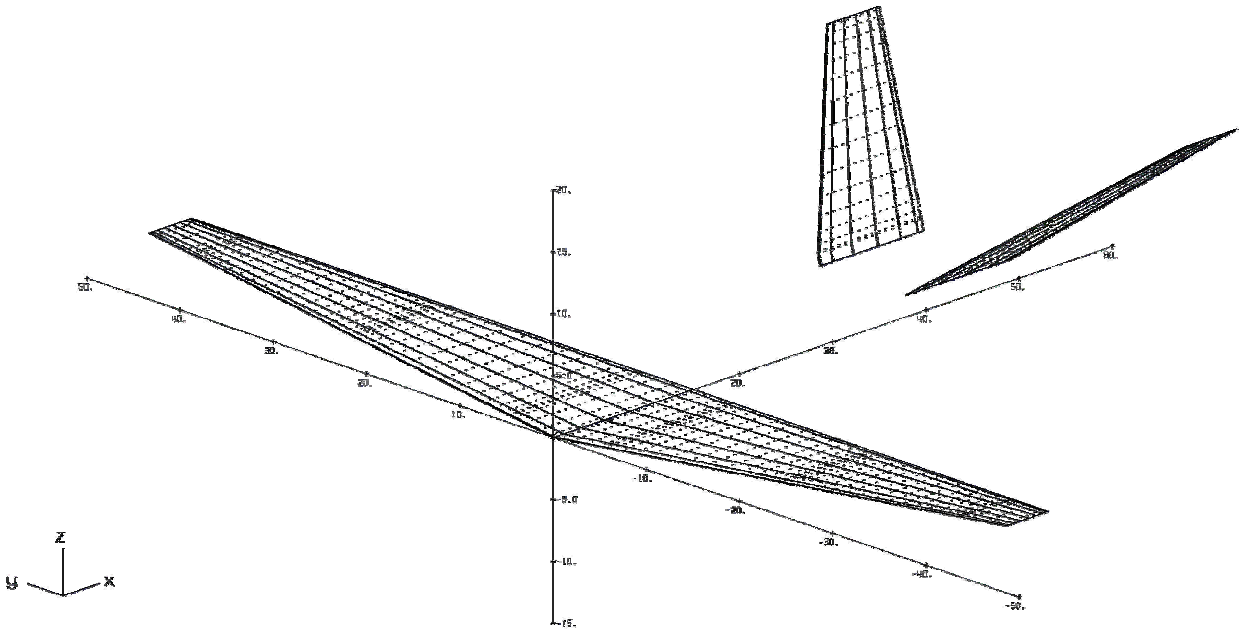

Figure 45. Paneling scheme for AVL code showing wings and V-Tail

The aircraft was evaluated at cruise, takeoff/landing, and two attack modes. The primary attack mode, utilizing the 40 *mm* cannon is executed with the aircraft in a 7.4º bank at a turning radius of 20,000 *ft*. The secondary attack mode is executed in a 22º bank at a turning radius of 6,500 feet, and utilizes the smaller caliber weapon. Results are seen in Table 16.

Table 16. Stability and control derivatives

	Cruise	Takeoff/Landing	Primary Attack	Secondary Attack
$C_{L\alpha}$	5.85	5.20	5.76	5.73
$C_{m\alpha}$	-1.656	-2.07	-1.77	-1.79
C_m/C_L	-0.283	-0.398	-0.307	0.312
C_{Lq}	10.87	10.49	10.77	10.75
C_{mq}	-17.57	-18.98	-17.95	-18.00
$C_{L\delta rv}$	0.0087	0.0087	0.0087	0.0087
$C_{m\delta rv}$	-0.031	-0.031	-0.031	-0.031
$C_{n\delta rv}$	0.0028	0.0028	0.0028	0.0028
$C_{l\delta rv}$	0.0015	0.0015	0.0015	0.0015
$C_{l\delta a}$	0.0069	0.0069	0.0069	0.0069
$C_{n\delta a}$	0.0004	0.0004	0.0004	0.0004
$C_{Y\beta}$	-0.356	-0.326	-0.326	-0.324
$C_{n\beta}$	0.133	0.141	0.128	0.127
$C_{l\beta}$	-0.156	-0.229	-0.167	-0.168
C_{Yr}	0.339	0.378	0.356	0.357
C_{nr}	-0.138	-0.176	-0.144	-0.144
C_{lr}	0.224	0.506	0.303	0.317
C_{lp}	-0.560	-0.492	-0.54	-0.536
C_{np}	0.00025	-0.166	-0.041	-0.048

10.5 Dynamic Response

The dynamic response properties of Casper are evaluated at all three categories set forth in MIL-F-8785C. Class A flight categories include combat maneuvering and weapons release, Class B categories include cruise, and Class C categories include takeoff and landing. Results can be seen in Table 17, Table 18, and Table 19 below. All frequency data is in units of Hz, and all time data is in units of seconds. As is shown, Casper meets MIL-F-8785C requirements for Short Period, Phugoid, Spiral, and Rolling Convergence modes. The aircraft struggles to meet the Dutch Roll requirement, and thus a yaw-damping system is required.

Table 17. Class A dynamic response properties

Class A Categories	Minimum Req't	Maximum Req't	Primary Attack	Secondary Attack
ζ_{SP}	0.35	1.3	0.36	0.36
ω_{SP}	0.28	3.6	1.43	1.43
ζ_{Ph}	0.04	-	0.047	0.054
ω_{Ph}	-	-	0.069	0.072
ζ_{DR}	0.19	-	0.02	0.02
ω_{DR}	0.4	-	0.69	0.69
τ_r	-	1.4	1.3	1.4
T_{2A}	12	-	154.4	37.0

Table 18. Class B dynamic response properties

Class B Categories	Minimum Req't	Maximum Req't	Cruise
ζ_{SP}	0.3	2.0	0.32
ω_{SP}	0.085	3.6	2.4
ζ_{Ph}	0.04	-	0.22
ω_{Ph}	-	-	0.018
ζ_{DR}	0.08	-	0.061
ω_{DR}	1.0	-	1.08
τ_r	-	1.4	1.08
T_{2A}	20	-	1544

Table 19. Class C dynamic response properties

Class C Categories	Minimum Req't	Maximum Req't	Takeoff	Landing
ζ_{SP}	0.35	1.3	0.35	0.35
ω_{SP}	0.28	3.6	0.97	0.97
ζ_{Ph}	0.04	-	0.23	0.23
ω_{Ph}	-	-	0.095	0.095
ζ_{DR}	0.19	-	0.02	0.02
ω_{DR}	0.4	-	0.1	0.1
τ_r	-	1.4	1.3	1.4
T_{2A}	12	-	142	142

10.6 Roll Performance

The Casper Advanced Gunship most suitably falls into the MIL-F-8785C aircraft classification system as a Class II "Medium weight, low-to-medium maneuverability, heavy attack" aircraft. Today's AC-130 gunship falls within this Class as well. The most constraining time to roll requirement put forth in the document for a Class II aircraft requires a bank angle change of 45º to be accomplished in 1.4 *sec*. Due to Casper's close air support mission profile and the capability to attack targets with bombs, it is conceivable that the aircraft will operate within the Category A flight phase known as ground attack (GA). Aircraft that operate within this flight phase are evaluated as Class IV aircraft. The MIL-F-8785C Flight Phase GA roll requirement is that a bank angle change of 90º must be accomplished within 1.7 *sec*. Roll performance data for Casper is shown in Figure 46 below. This figure plots Casper's roll performance against the GA roll performance requirement. It can clearly be seen that Casper easily beats the roll performance requirements. The high rate of roll the aircraft is capable of is largely contributed to the large value of $Cl_{\delta a}$ which is in turn contributed to the large size of the ailerons.

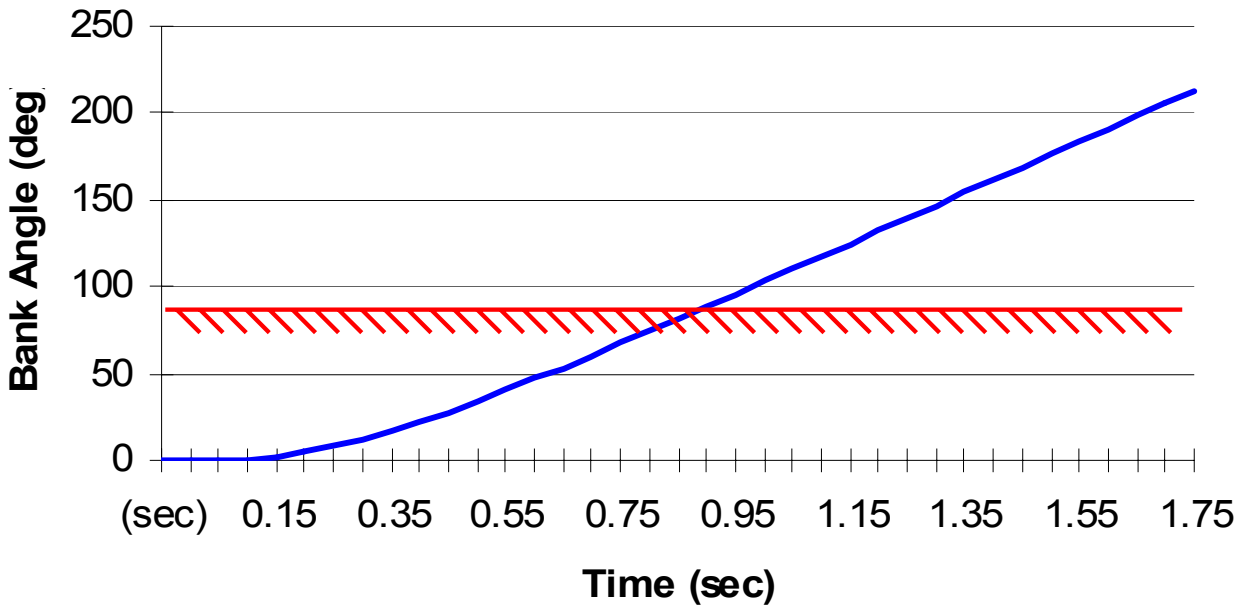

Figure 46. Roll performance vs. flight phase GA requirement

10.7 System Considerations

A Fly-by-Light control system was utilized in our advanced gunship design. This system is advantageous due to weight savings and an increased survivability level for the aircraft. A Fly-by-Light system is also advantageous for the reason that our aircraft will require a computerized Stability Augmentation System in the form of a yaw-damper. Yaw-dampers are a common system on aircraft today, especially on aircraft that operate at

altitudes above 40,000 ft. While our aircraft is not designed to typically operate at such altitudes, a yaw-damping device is included to help Casper meet MIL-F-8785C requirements for Dutch Roll as described in Section 10.5.

11. Propulsion

The Casper utilizes two turbofan engines, scaled from the provided AIAA engine deck.[44] In investigating different engines, it was determined that the AIAA engine deck was sufficient for meeting the needs of the Casper. As previously mentioned in the initial sizing, with a TOGW of roughly 90,000 *lbs* and a takeoff thrust-to-weight ratio of 0.4, the required static thrust is 36,000 *lbs*. Each engine, therefore, is scaled to provide 18,000 *lbs* of thrust.

11.1 Nacelle Design

The Casper's engines are located slightly in front of the V-Tail and are housed together in one nacelle, as is shown in Figure 47. Separation of the engine inlets ensures that if one engine fails, the turbulent flow generated by the failed engine does not cause the remaining engine to stall, but is rather diverted around the remaining engine's inlet. Armor plating will be utilized to separate the engines and prevent the loss of both when one is damaged.

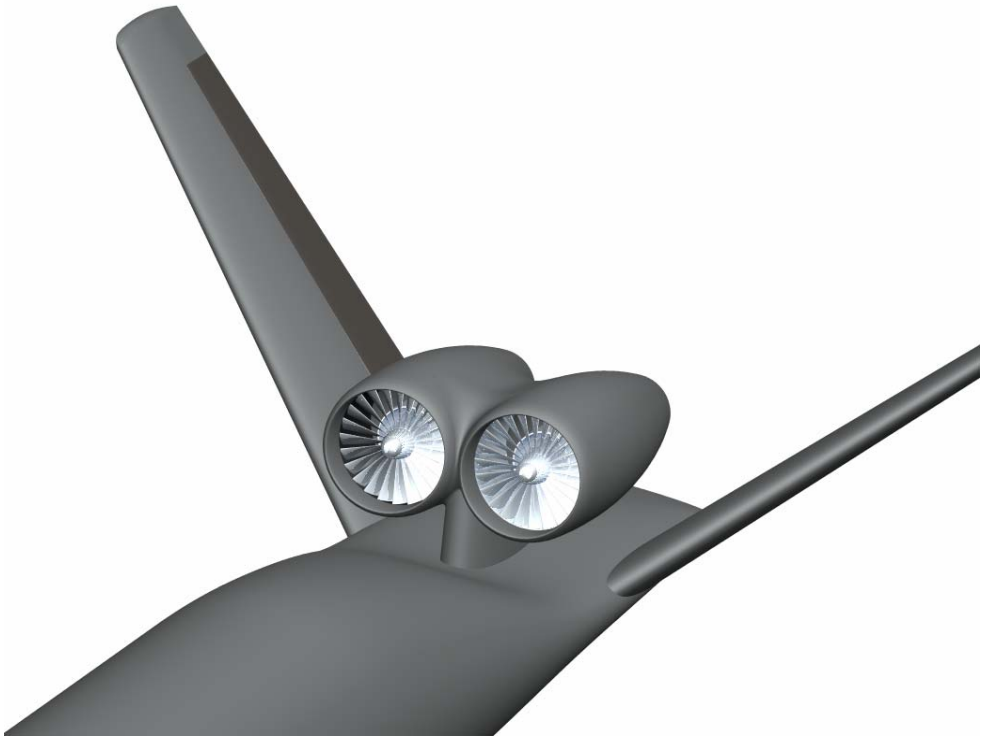

Figure 47. Nacelle design with both engines in a single housing

An area inlet ratio of 0.917 was chosen based on methods described in Raymer's *Aircraft Design*. Pressure losses into the engine were neglected because they are too low to have an effect on the performance for a subsonic engine.[3] The exhaust nozzle is sized similarly to the inlet and was determined to have an area equal to 70% of the inlet area. Particular emphasis was placed on the engine location to ensure that the exhaust will not interfere with the deflected tail control surfaces.

11.2 Engine Removal

With the engines located between the surfaces of the V-Tail, all servicing must be done from the top of the aircraft. Should the engines need to be removed for servicing or replacement, a crane would be required to remove the engines. Figure 48 shows how the nacelle can be opened to allow for the engines to be removed.

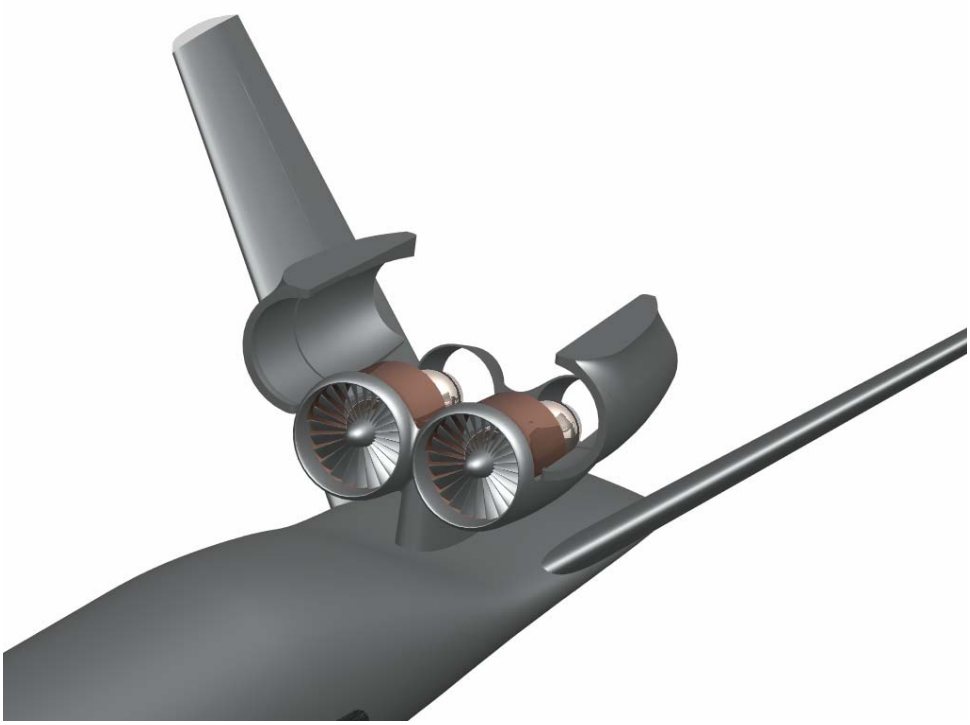

Figure 48. Demonstration of engine removal from nacelle

12. Performance

Aircraft performance calculations were carried out using a combination of methods described in *Airplane Design: Part VII* by Roskam[42] and *Aircraft Performance Notes* by Dr. Frederick Lutze.[45] Iterative techniques and programs written in MATLAB were used for a majority of the performance calculations. These methods were used for the analysis of both missions based on the performance requirements and constraints given in the RFP. Table 20 summarizes these requirements for the design and ferry missions.

Table 20. RFP Performance Requirements

Mission Segment	Design Mission	Ferry Mission
Takeoff & Landing BFL	≤ 5000 *ft*	≤ 5000 *ft*
Cruise Speed	≥ 400 *knots*	≥ 400 *knots*
Cruise Altitude	≥ 30000 *ft*	≥ 30000 *ft*
Block Range	500 *nm* x 2	2700 *nm*
Loiter Time	4 *hrs*	N/A
Landing Distance	≤ 5000 *ft*	≤ 5000 *ft*

12.1 Takeoff and Landing Performance

Several takeoff and landing requirements constrain the design of the Casper. For takeoff, the RFP states that the design must have a balanced field length (BFL) of less than or equal to 5000 ft. For landing, the design must be able to land in less than 5000 *ft* with 40% internal fuel, maximum payload, and one engine inoperative on a wet runway. Using the MIL-C-005011B standard, a 50 *ft* obstacle must be cleared for both takeoff and landing with a speed of $1.2V_{stall}$. In addition, the RFP states that the design must be able to operate on austere airstrips, and both requirements were stated to be evaluated at sea level conditions. Because the RFP states that the ferry mission includes maximum TOGW, there is no difference in calculations for the design and ferry missions.

For takeoff performance, the takeoff distance and balanced field length are calculated for various ground surface types to ensure that the austere airstrip requirement is met. Figure 49 illustrates the military requirements used in the takeoff analysis, where S_{TOG} is the ground run distance, S_{TO} is the total takeoff distance to clear a 50 *ft* obstacle, V_{LOF} is the liftoff speed, V_{STO} is the stall speed at takeoff, and V_S is the stall speed at sea level.

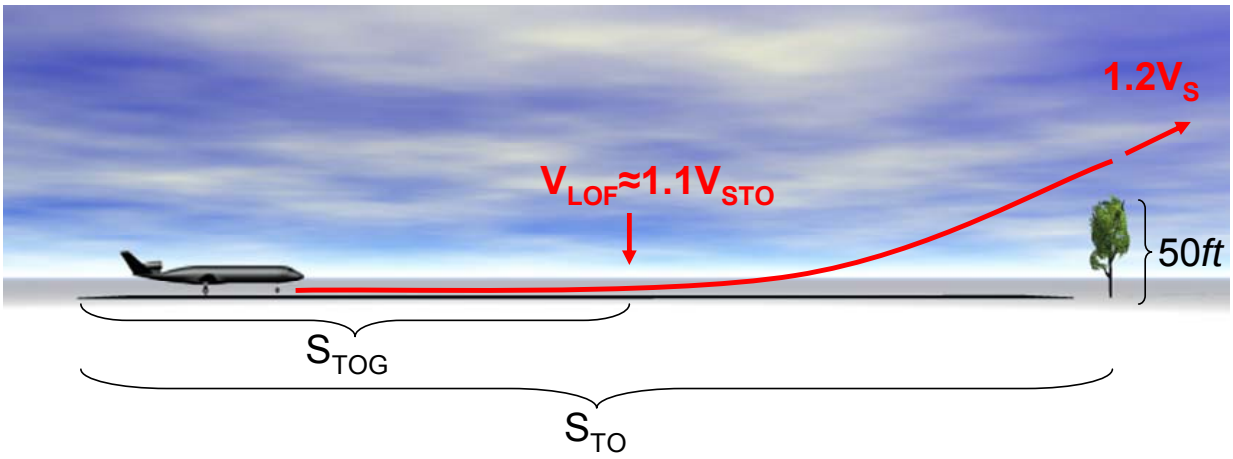

Figure 49. Military requirements for takeoff analysis

Table 21 shows the takeoff distance, balanced field length, and lift coefficient needed to takeoff in less than 5000 *ft* for different surfaces at sea level.

Table 21. Takeoff length and balanced field length for various ground surface types

Ground Surface Type	Friction Coefficient	S_{TO} (ft)	BFL (ft)	Cl_{MAX}
Concrete/Asphalt	0.02	3301	4927	2.1
Hard turf	0.04	3305	4901	2.2
Short grass	0.05	3386	4990	2.2
Long grass	0.1	3451	4989	2.5
Soft ground	0.2	N/A	N/A	N/A

With a maximum lift coefficient of 2.6 with flaps fully deflected, the Casper can takeoff on all ground surface types, excluding soft ground. For austere airstrips, the hard turf friction coefficient is an acceptable approximation, and the results of Table 21 show that this requirement is met.

The analysis for landing performance was similar to that for takeoff. As previously mentioned, the landing requirement includes clearing a 50 *ft* vertical obstacle, carrying 40% internal fuel, having one engine inoperative, and landing on a wet runway. Figure 50 illustrates the distances calculated in the analysis of landing performance.

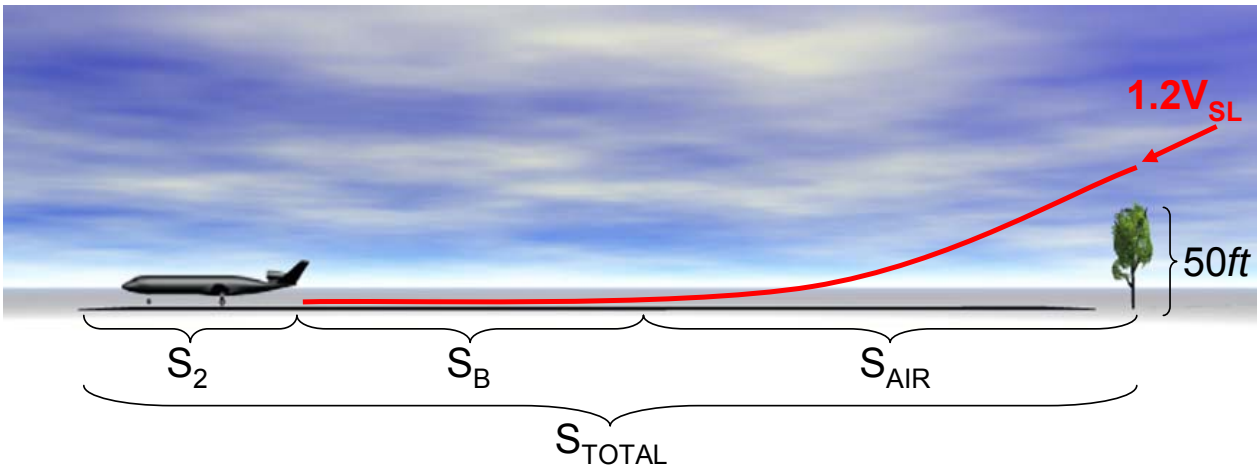

Figure 50. Military requirements for landing analysis

S_{AIR} is the distance from clearing the obstacle to touchdown. S_B is the ground run distance before applying breaks, equivalent to the distance at which the landing velocity is 80% of the touchdown velocity. S_2 is the ground run distance after applying standard breaks. S_{TOTAL} is the total landing distance. Table 22 shows the landing field length for the missions.

Table 22. Breakdown of landing field length for various ground surface types

Ground Surface Type	Friction Coefficient	S_{AIR} (ft)	S_B (ft)	S_2 (ft)	S_{TOTAL} (ft)
Wet Concrete/Asphalt	0.01	1294	2498	1030	4822
Concrete/Asphalt	0.02	1294	2438	1030	4762
Hard turf	0.04	1294	2329	1030	4653
Short grass	0.05	1294	2279	1030	4603
Long grass	0.1	1294	2236	1030	4560

The results of Table 22 show that in the worst case scenario of landing on wet concrete or asphalt, the total landing distance is less than 5000 ft. The data also shows that there is no need for reverse thrust on landing in order to meet the RFP requirement.

12.2 Rate of Climb, Ceilings and Time to Climb

Because there is no change in operating weight for the ferry mission, the calculations for climbing performance are identical to the design mission. Using the performance methods aforementioned, calculations are made for best climb rate, climb rate at the best velocity gradient, time to climb, and climb angle, including calculations of the absolute, service, and cruise ceilings. The hodograph diagram in Figure 51 graphically shows the

maximum rate of climb at sea level, forward velocity to achieve the maximum rate of climb, and best velocity gradient. Table 23 summarizes the climbing performance at sea level for both missions.

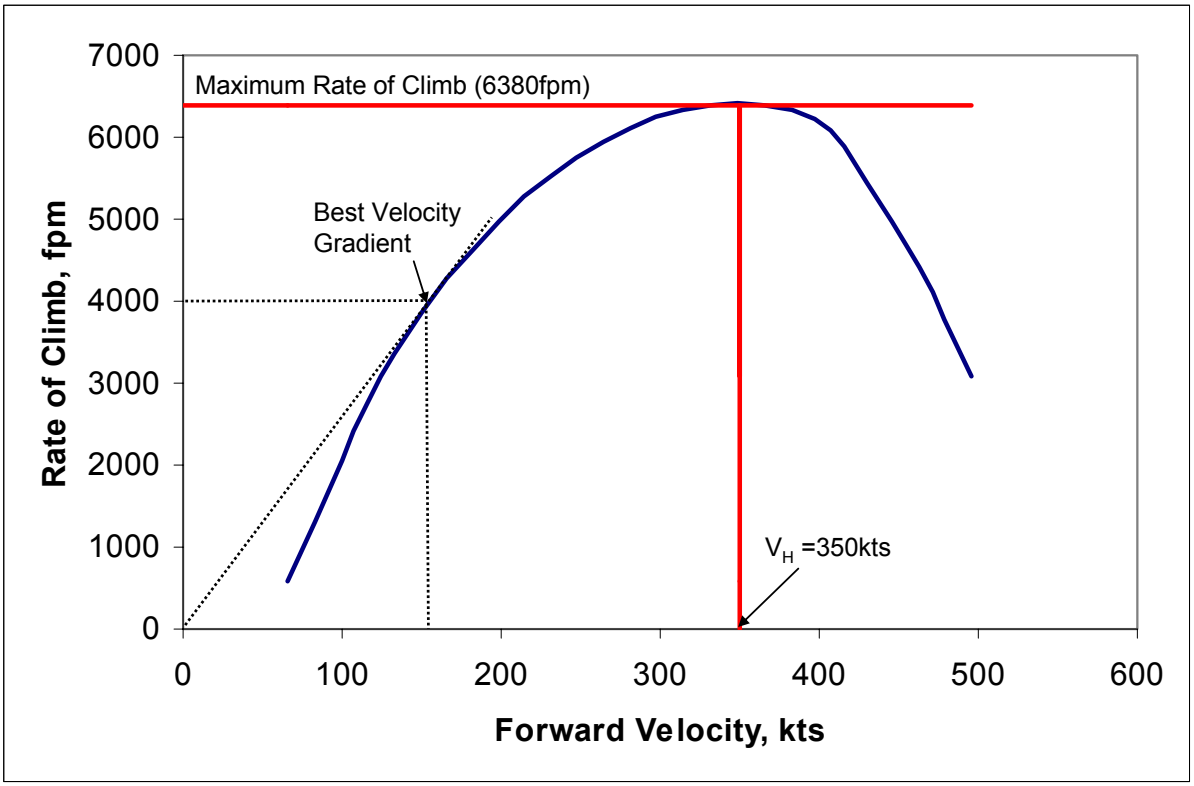

Figure 51. Hodogram diagram showing rate of climb at sea level

Table 23. Summary of climbing performance at sea level

Best Rate of Climb			**Best Velocity Gradient**		
Rate of Climb	FWD Velocity	Angle	Rate of Climb	FWD Velocity	Angle
(ft/min)	(knots)	(degrees)	(ft/min)	(knots)	(degrees)
6380	350	10.20	4000	160	13.87

Figure 51 and Table 23 show that the best rate of climb is 6380 *ft/min*, corresponding to a forward velocity of 350 *knots* and a climb angle of 10.20º. The rate of climb for the best velocity gradient is 4000 *ft/min*, corresponding to a forward velocity of 160 *knots* and a climb angle of 13.87º.

Using the military standard, the absolute ceiling is defined as the altitude at which the climb rate is 0 *fpm*, the service ceiling at a climb rate of 100 *fpm*, and the cruise ceiling at a climb rate of 300 *fpm*. Figure 52 shows the relationship for altitude versus maximum rate of climb for the design parameters. Because the aircraft weight on the return leg of the primary mission does not include the entire payload, two sets of ceiling values are calculated. For the first leg of the mission, the ceiling calculations assume the full weight of the aircraft, payload, and fuel. On the

return leg, new values are calculated for an aircraft weight equal to the empty weight plus the remaining internal fuel after weapons deployment. For the first leg of the primary mission, numerical values for the absolute, service, and cruise ceiling are calculated using the data illustrated in Figure 52, and the results are summarized in Table 24. For the return leg of the primary mission, numerical values for the absolute, service, and cruise ceiling are calculated using the data illustrated in Figure 53, and the results are summarized in Table 25.

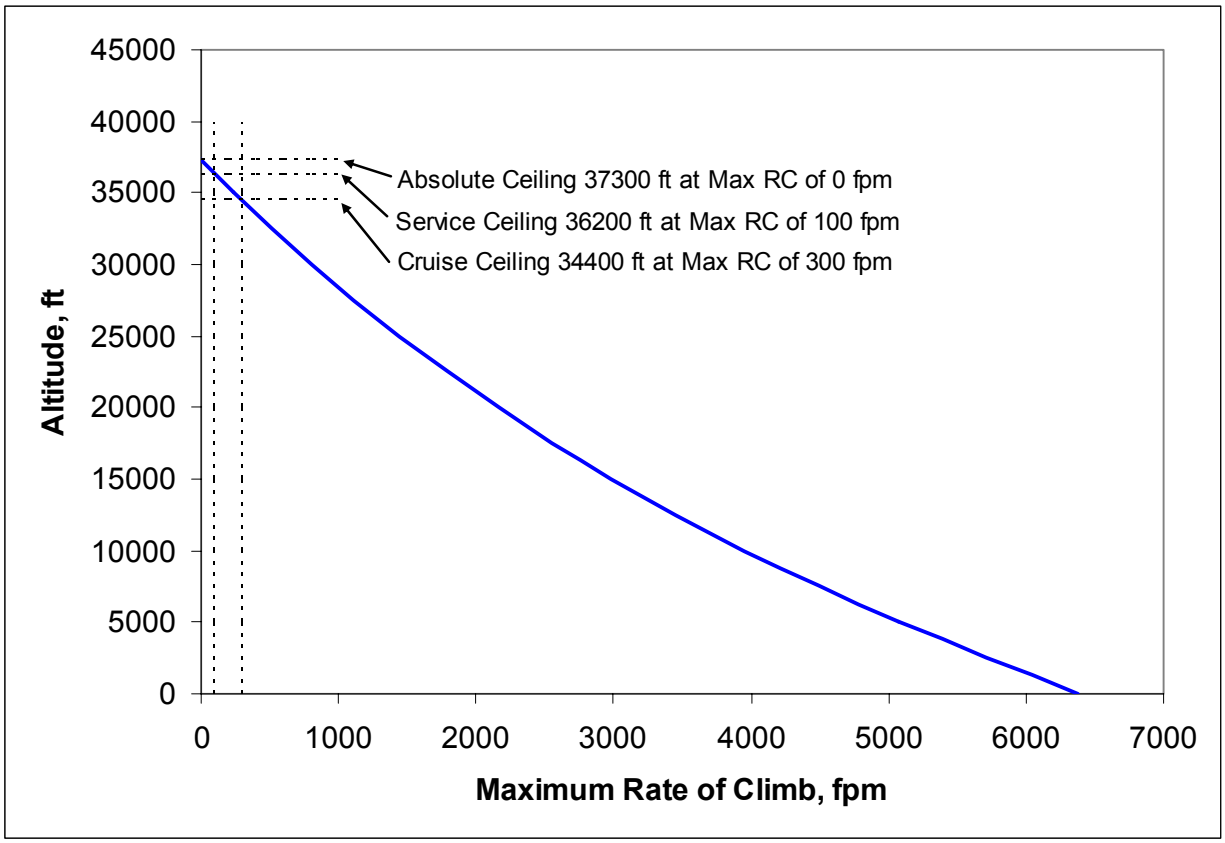

Figure 52. Absolute, Service, and Cruise Ceiling for first leg of primary mission

Table 24. Absolute, Service, and Cruise Ceiling for first leg of primary mission

	Rate of Climb (fpm)	Ceiling (ft)
Absolute	0	37300
Service	100	36200
Cruise	300	34400

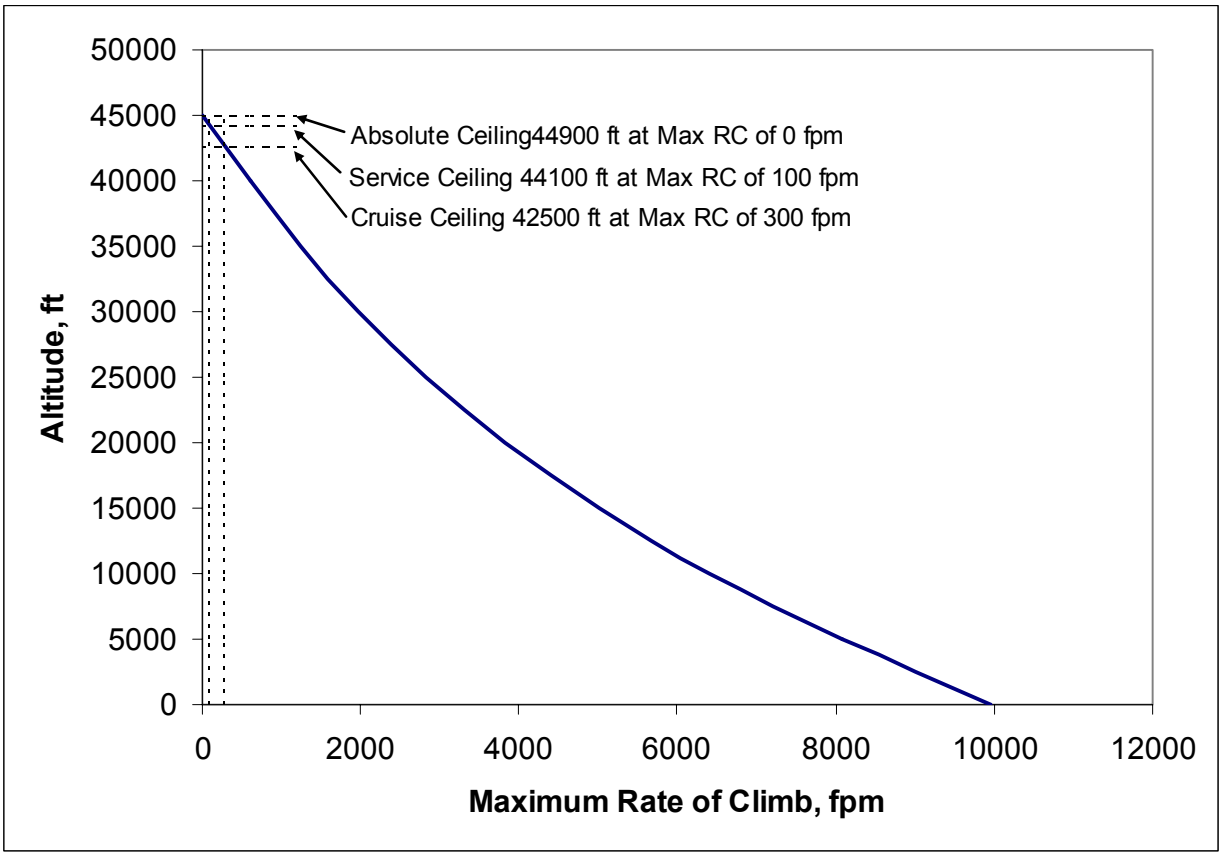

Figure 53. Absolute, Service, and Cruise Ceiling for return leg of primary mission

Table 25. Absolute, Service, and Cruise Ceiling for return leg of primary mission

	Rate of Climb (fpm)	Ceiling (ft)
Absolute	0	44900
Service	100	44100
Cruise	300	42500

The RFP establishes that the minimum cruise ceiling for this design is 30,000 *ft*. Table 24 and Table 25 show that the Casper meets this requirement.

Using a linear approximation for maximum rate of climb versus altitude, it is possible to estimate the time to climb to cruise altitude for each leg of the mission. Using this approximation, the time to climb to 34,000 *ft* from sea level is determined to be 19.1 *min*, and the time to climb to 42,000 *ft* from 10,000 *ft* is determined to be 17.7 *min*.

12.3 Cruise/Range Performance and Level Flight Envelope

The contributing factors for evaluating cruise performance are the altitude and velocity for best range. A minimum cruise speed of 400 *knots* is specified by the RFP. The airfoil used in the wing design of the Casper is stated to have a drag divergence Mach number of 0.726. All mission performance calculations are made with an optimum cruise Mach number of 0.7, equivalent to a cruise speed of 406 *knots* at an altitude of 34,000 *ft*. Performance calculations show that the maximum range for the primary mission is less than the 2,700 *nm* requirement for the ferry mission. For this reason, the ferry mission requirements are used to make payload-range calculations. Figure 54 illustrates the relationship between payload and maximum range for the ferry mission, including all stages of the mission.

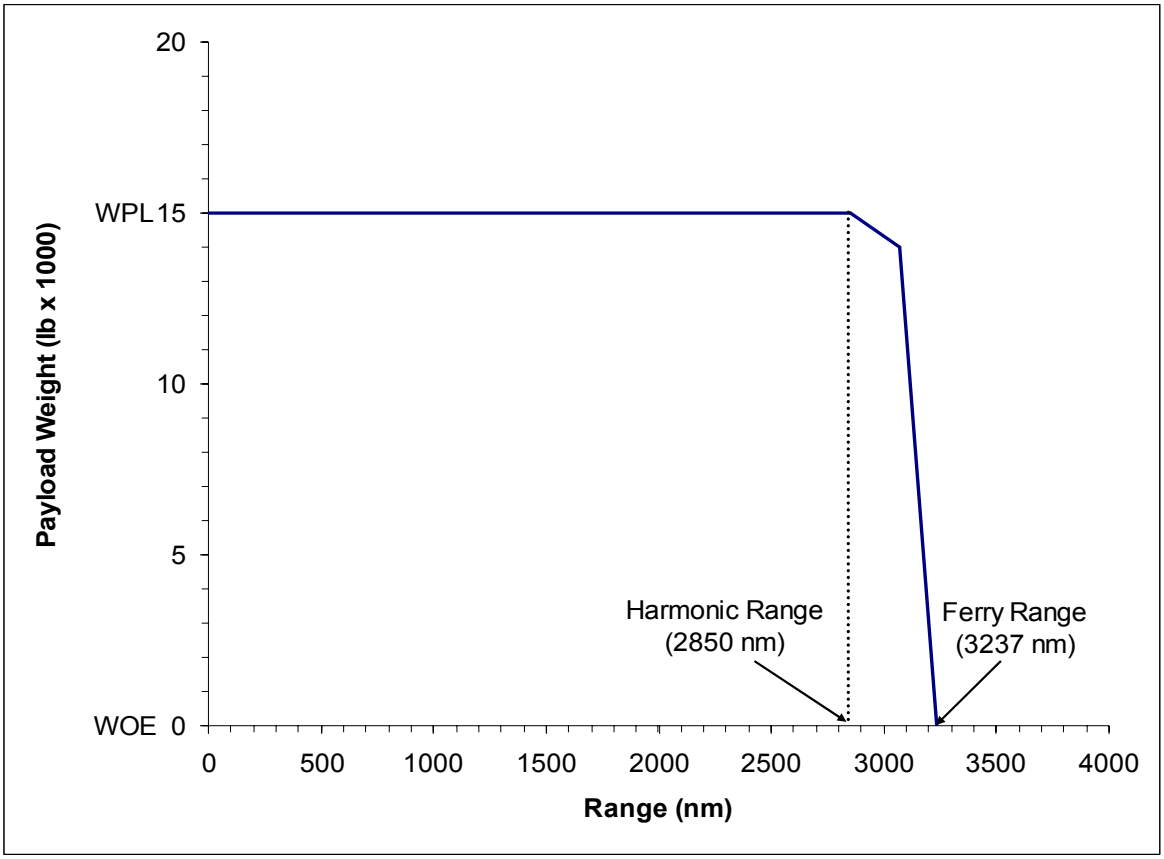

Figure 54. Payload-Range Diagram

The harmonic (design) range is the design range for the RFP requirements. Figure 54 shows that the Casper can fly with a full payload of 15,000 *lbs* for a range of 2,850 *nm*. The ferry range of 3237 *nm* is the maximum range of the design platform with no payload. All range calculations allow for 5.0% reserve fuel for the ferry mission, which equates to 6.2% reserve fuel for the design mission for the same amount of initial fuel weight.

Figure 55 shows the 1-g operational flight envelope for the design. The stall locus shows the stall Mach number at all operational altitudes. The drag divergence Mach number was determined based on airfoil data, as previously described. The maximum Mach number constraint is created by setting the thrust required for level flight equal to the maximum thrust available at that altitude. Using this data, the maximum obtainable Mach number is determined to be 0.9, corresponding to a speed of approximately 550 *knots* at 20,000 *ft*.

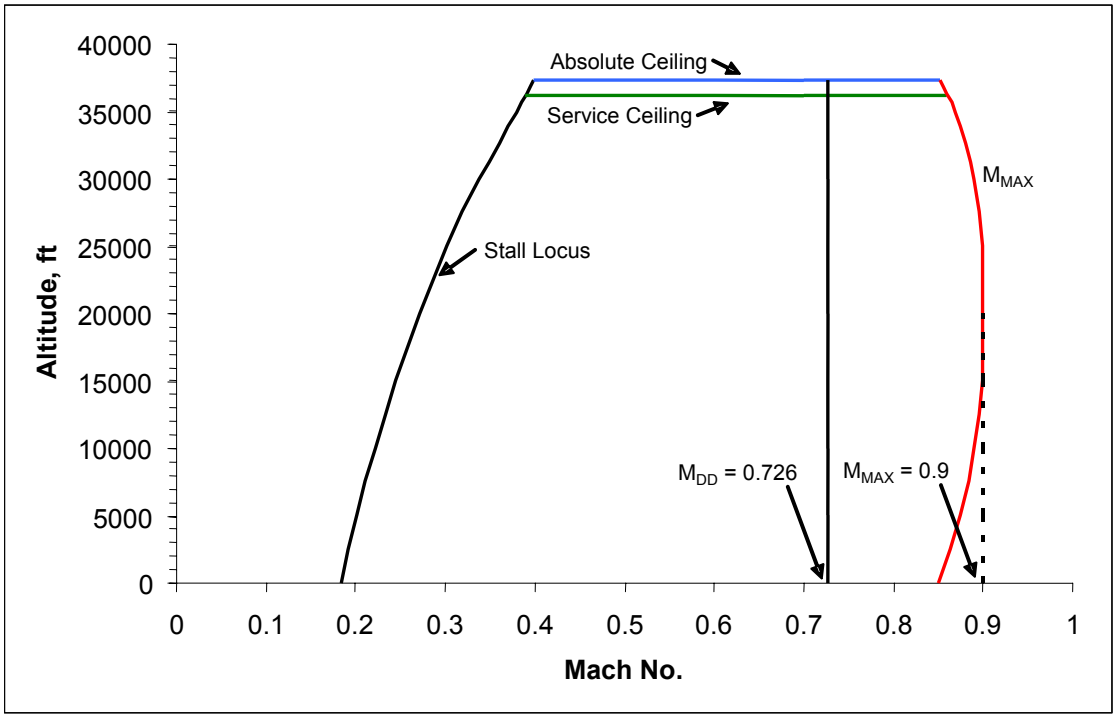

Figure 55. 1-g level flight envelope at maximum weight

12.4 Endurance and Loiter

For the mission requirements set forth in the RFP, the design platform must loiter for 4 *hrs* at 20,000 *ft* and an additional 30 *min* hold at sea level. To allow for sustained fire over a target, a 30 *min* loiter during weapons deployment is estimated for performance calculations. Table 26 summarizes the loiter performance for the phases described, including the altitude, time required, distance traveled, and fuel required. For the ferry mission, the same 30 *min* loiter applies. The aircraft speed required to maintain the loitering conditions of Table 26 at 20,000 ft is equal to Mach 0.34. At 10,000 ft, the required speed is Mach 0.57.

Table 26. Loiter/Endurance Data for Primary Mission

Phase	Altitude (ft)	Time (min)	Distance (nm)	Fuel Required (lb)
Loiter	20000	240	857	11176
Expend Payload	10000	30	86	1386
Landing Hold	0	30	66	1286

12.5 Maneuvering

The RFP states that a 1.5*g* maneuver must be maintained at 20,000 *ft*. Table 27 summarizes the maneuvering performance at the loitering speed at 20,000 *ft*. The speed at which the maneuver is performed is equal to Mach 0.34, equivalent to approximately 208 *knots*.

Table 27. 1.5*g* Maneuvering Performance at 20,000 *ft* and V=208 *knots*

Pull-up Pitch Rate	2.63 *deg/sec*
Level Turn Pitch Rate	4.38 *deg/sec*
Turn Rate	5.87 *deg/sec*
Turn Radius	3422 *ft*
T (required)	8542 *lb*
T (available)	11566 *lb*

The values presented in Table 27 are easily obtained with the design of the Casper. In order to pull a 1.5*g* maneuver at loitering altitude, both the pitch rates and the turn rate are less than 6 *deg/sec*. In addition, excess thrust is available for maneuvering at the speed indicated.

12.6 Performance Summary

A summary of performance calculations for respective mission phases is displayed in Table 28. The displayed data shows that the Casper meets each of the aforementioned mission and performance requirements set forth in the RFP. In addition to the performance calculations, elapsed times are calculated for the entirety of both the design and ferry mission. For the design mission, the sum of the mission segments requires a total time of 513.0 *min*, or approximately 8.5 *hrs*. For the ferry mission, the sum of the mission segments requires a total time of 467.2 *min*, or approximately 7.8 *hrs*.

Table 28. Performance Summary

TAKEOFF				
Ground Surface Type	**Friction Coefficient**	**S_{TO} (*ft*)**	**BFL (*ft*)**	**Cl_{MAX}**
Concrete or asphalt	0.02	3301	4927	2.1
Hard turf	0.04	3305	4901	2.2
Short grass	0.05	3386	4990	2.2
Long grass	0.1	3451	4989	2.5

LANDING		
Ground Surface Type	**Friction Coefficient**	**$S_{LANDING}$ (*ft*)**
Wet Concrete/Asphalt	0.01	4822
Concrete/Asphalt	0.02	4762
Hard turf	0.04	4653
Short grass	0.05	4603
Long grass	0.1	4560

CLIMBING		
Best Rate of Climb		
Rate of Climb	FWD Velocity	Angle
(*ft/min*)	(*knots*)	(*degrees*)
6380	350	10.2
Best Velocity Gradient		
Rate of Climb	FWD Velocity	Angle
(*ft/min*)	(*knots*)	(*degrees*)
4000	160	13.87

Ceilings			
	Rate of Climb (*fpm*)	Ceiling [Ingress] (*ft*)	Ceiling [Egress] (*ft*)
Absolute	0	37300	44900
Service	100	36200	44100
Cruise	300	34400	42500

CRUISE/RANGE	
Cruise Mach Number	0.7
Harmonic Range (*nm*)	2850
Ferry [Empty] Range (*nm*)	3237

ENDURANCE/LOITER				
Phase	**Altitude (*ft*)**	**Time (*min*)**	**Distance (*nm*)**	**Fuel Required (*lb*)**
Loiter	20000	240	857	11193
Expend Payload	10000	30	65	1038
Landing Hold	0	30	66	638

MANEUVERING	
Pull-up Pitch Rate	2.63 *deg/sec*
Level Turn Pitch Rate	4.38 *deg/sec*
Turn Rate	5.87 *deg/sec*
Turn Radius	3422 *ft*
Thrust (required)	8542 *lb*
Thrust (available)	11566 *lb*

13. Cost Estimation

The Casper's cost was estimated using the DAPCA IV method, as found in Roskam's *Aircraft Design: Volume VIII*.[11] This weight-based cost analysis takes into account the complexity of the structure, materials used and the size of production runs. The result is an estimate of the research and development, acquisition, and operating costs. The RFP requires analysis for production runs of 100, 200 and 400 aircraft.

13.1 Research and Development

Research and development is a fixed cost in the production of an aircraft. This is primarily a function of the complexity of the structure, weight of the structure, and the amount of testing required. A simple design will lead to a lower total R&D and acquisition cost. The Casper's R&D cost was estimated to be $1.01 billion using the DAPCA IV method. The breakdown of the R&D cost can be seen in Figure 56.

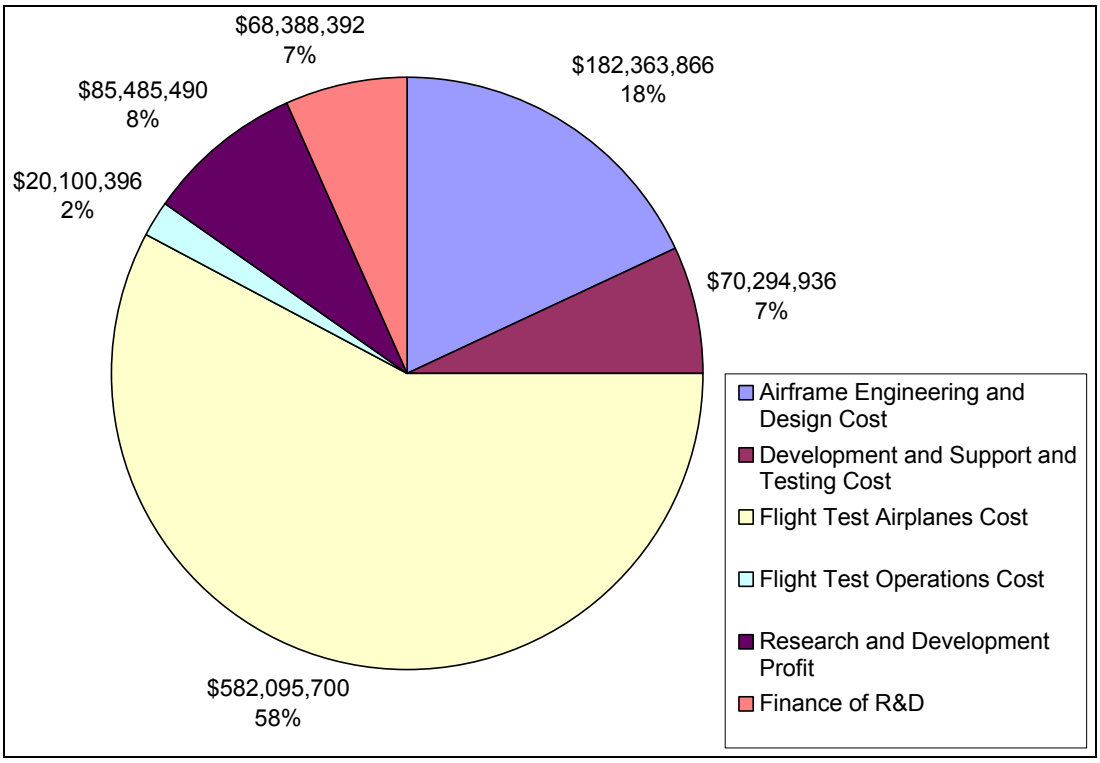

Figure 56. Breakdown of the Casper's R&D cost

13.2 Average Acquisition Cost

The average unit fly-away cost was estimated by summing the total R&D, profit, and manufacturing costs and dividing by the total number of aircraft produced. As the number of aircraft produced increases, the cost per aircraft decreases. Figure 57 shows the cost per aircraft for multiple production runs. A production run of 100 aircraft leads to a cost per aircraft of $32.7 million. A production run of 200 leads to a cost of $24.2 million per

aircraft. A production run of 400 leads to a cost of $18.9 million. The adaptability of the Casper for alternate missions encourages a larger production run, thus reducing the cost per aircraft.

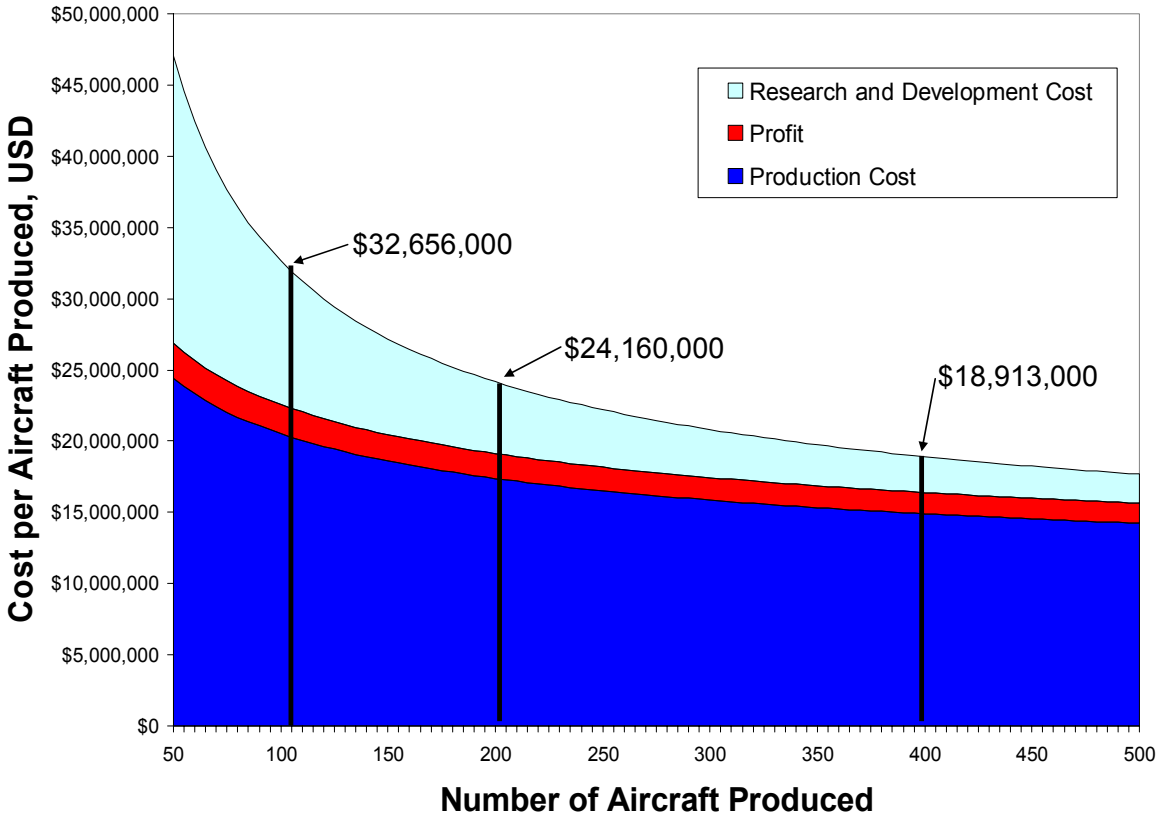

Figure 57. Average acquisition cost per aircraft produced

13.3 Operational Cost

Figure 58 shows the operating cost breakdown of the Casper. All operational cost analysis is based on a 30 year lifecycle. The simplicity of the airframe reduces the operational cost because replacement parts are easily accessible. The Casper will cost $8,600 per hour to operate, taking into account all of the direct personnel, indirect personnel, spare parts, and other miscellaneous cost associated with the maintenance of the aircraft. This low operational cost will lead to a lower total life cycle cost.

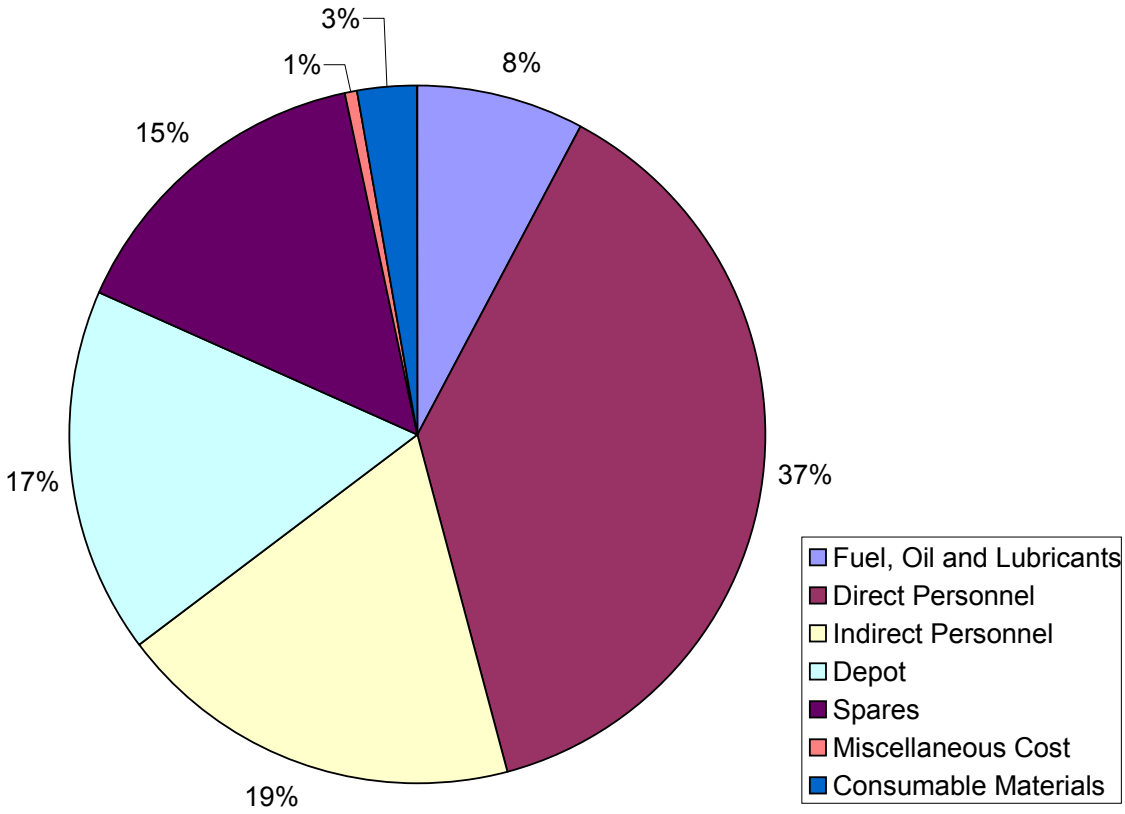

Figure 58. Breakdown of Operational Cost

13.4 Cost Summary

Table 29 summaries the cost analysis of the Casper in US dollars. The results of Table 29 show the funding required for the Casper is relatively low compared to current technology trends and military spending.

Table 29. Cost Summary

	Production Runs		
	100	200	400
Average fly-away Cost per Aircraft	$32.7 Million	$24.2 Million	$18.9 Million
Total Acquisition Cost	$2.1 Billion	$3.5 Billion	$6.1 Billion
Cost / Flight Hour	$8.6 Thousand	$8.6 Thousand	$8.6 Thousand

14. Corollary Missions and Aircraft Variants

The adaptability of the Casper allows it to be easily modified for alternate missions and variant designs. Primarily, the platform allows for flexibility in weapons selection. The bomb bay is capable of carrying both unguided and guided bombs of variable sizes and the aircraft is equipped with the electronic gear necessary to deliver the various types of munitions available in the US arsenal. In addition, the cannons can be replaced by newer systems as new technologies become available. As non-lethal and other non-traditional weapons become more available, the entire fuselage behind the pressurization bulkhead is capable of carrying these systems. With weapon and sensor adaptability, the Casper is capable of corollary missions, such as anti-submarine warfare, light bombing, and electronic warfare. For these new missions, no major airframe modification is necessary.

References

[1] Gambrell, Kathy. "Cost of unmanned aerial vehicle program triples." *GovExec.com*. 7 Dec. 2004. Retrieved 11 Dec. 2004 <http://www.govexec.com/dailyfed/1204/120704cdam2.htm>.

[2] "Unmanned Aerial Vehicles Roadmap, 2002-2027." *AcqWeb.* Office of the Secretary of Defense. Dec. 2002. Retrieved 11 Dec. 2004 <http://www.acq.osd.mil/usd/uav_roadmap.pdf>

[3] Raymer, D. Aircraft *Design: A Conceptual Approach, Third Edition*. Reston, VA

[4] IE. Pambagjo, K. Nakahashi, S. Obayashi and K. Matsushima. *Aerodynamic Design of A Medium Size Blended-Wing-Body Airplane,* AIAA2001-0129, Tohoku University, JAPAN

[5] Leibeck, R. "Design of the Blended Wing Body Subsonic Transport." *Journal of Aircraft,* Vol. 41, No. 1 (Jan. 2004): 10-25.

[6] Stinton, Darrol. *The Anatomy of the Airplane.* Oxford, UK: Blackwell Science 1998.

[7] Potsdam, M., Page, M., and Leibeck, R. "Blended Wing Body Analysis and Design." AIAA Paper 97-2317, 1997.

[8] Leibeck, R. "Blended Wing Body Design Challenges." AIAA Paper 2003-2659, 2003.

[9] Gorton, S., Owens, L., Jenkins, L., and Allen, B. "Active Flow Control on a Boundary-Layer-Ingesting Inlet." AIAA Paper 2004-1203, 2004.

[10] Anabtawi, A., Blackwelder, R., Lissaman, P., and Leibeck, R. "An Experimental Investigation of Boundary Layer Ingestion in a Diffusing S-Duct With and Without Passive Flow Control." AIAA Paper 99-0739, 1999.

[11] Roskam, Jan. *Airplane Cost Estimation: Design, Development, Manufacturing and Operation.* Airplane Design: Part VIII. Lawrence: Design Analysis and Research Corporation, 2003.

[12] *Federation of American Scientists.* Retrieved 11 Dec. 2004 <http://www.fas.org/>.

[13] "What is Synthetic Aperture Radar?" *Synthetic Aperture Radar*. Sandia National Laboratories. Retrieved 20 Jan. 2005. < http://www.sandia.gov/RADAR/whatis.html>.

[14] "44 mm Bofors." *Destroyer Escort Central.* USS Francis M. Robinson (DE-220) Association**.** Retrieved 11 Dec. 2004 <http://www.de220.com/Armament/40mm/40mm.htm>.

[15] Mulcahy, Paul. "40 mm Bofors L/70 Antiaircraft Guns." *Swedish Autocannons*. Retrieved 11 Dec. 2004. < http://www.pmulcahy.com/autocannons/swedish_autocannons.html>.

[16] "Naval Gun (40mm and 57mm), Mk3." *United Defense*. Retrieved 11 Dec. 2004. <http://www.uniteddefense.com/prod/ngun_mk3.htm>.

[17] "Naval and Optronic Sight." *Saab Systems*. Retrieved 12 Feb. 2005. <http://products.saab.se/PDBWeb/GetFile.aspx?pathtype=ProductFiles&filetype=Files&id=2313>.

[18] Parsch, Andreas. "AN/ASA to AN/ASK - Equipment Listing." Retrieved 13 Dec. 2004. <http://www.designation-systems.net/usmilav/jetds/an-asa2ask.html>.

[19] "AC-130U Spooky/Spectre Gunship." Retrieved 13 Dec. 2004. <http://www.mindfully.org/Technology/2004/AC-130U-Spooky-Spectre.htm>.

[20] Bedard, E.R. "Nonlethal Capabilities: Realizing the Opportunities." *Defense Horizons*. Center for Technology and National Security Policy. Retrieved 17 Jan. 2005. <http://www.ndu.edu/inss/DefHor/DH9/DH09.pdf>.

[21] Ball, Robert E. *The Fundamentals of Aircraft Combat Survivability Analysis and Design.* American Institute of Aeronautics and Astronautics Inc. 1985. New York, NY

[22] "Technical Commitees." *AIAA homepage*. American Institute for Aeronautics and Astronautics. Retrieved 11 Dec. 2004 <www.aiaa.org/tc/>.

[23] "Honeywell 'VIA 2000' Avionics." *Air Transport Avionics*. Honeywell. Retrieved 23 Oct. 2004. <http://www.cas.honeywell.com/ats/products/aims.cfm>.

[24] "Fly-by-Light: The Future of Flight Control Technology." *Technology Horizons*. Air Force Research Laboratory. Retrieved 05 Dec. 2004. <http://www.afrlhorizons.com/Briefs/Apr05/VA0412.html>.

[25] Adams, Charlotte. "Military/Civil Interoperability Extended Scope for CNS/ATM." *Newsstand*. Aviation Today. Retrieved 15 Feb. 2005. <http://www.aviationtoday.com >.

[26] "Navigation/Inertial Reference/GPS Systems." *Air Transport Avionics*. Honeywell. Retrieved 23 Oct. 2004. <http://www.cas.honeywell.com/ats/products/nav.cfm>.

[27] Roskam, Jan. *Layout Design of Landing Gear and Systems.* Airplane Design: Part IV. Lawrence: Design Analysis and Research Corporation, 2003.

[28] "Breakthroughs in Military Sensors." *Newsstand*. Aviation Today. Retrieved 15 Feb. 2005. <http://www.aviationtoday.com >.

[29] Tirpak, John A. "The New Way of Electron War." *Air Force Magazine Online*. Retrieved 17 Jan. 2005. <http://www.afa.org/magazine/dec2004/1204electron.html>.

[30] "Deicing and Anti-Icing Unite." *Tech Briefs*. Retrieved 17 Jan. 2005. <http://www.techbriefs.com/spinoff/spinoff2002/ps_1.html>.

[31] "Aerial Refueling Systems." *Aerospace Web*. Retrieved 15 Mar. 2005. <http://www.aerospaceweb.org/question/design/q0213.shtml>.

[32] *Material Property Data*. MatWeb. Retrieved 23 Feb. 2005. <http://www.matweb.com/index.asp?ckck=1>.

[33] "Look For LEXAN Resin." GE Plastics. Retrieved 23 Feb. 2005. <http://www.gelexan.com/gelexan/>.

[34] Roskam, Jan. *Layout Design of Cockpit, Fuselage, Wing and Empennage: Cutaways and Inboard Profiles.* Airplane Design: Part III. Lawrence: Design Analysis and Research Corporation, 2003.

[35] Roskam, Jan. *Component Weight Estimation.* Airplane Design: Part V. Lawrence: Design Analysis and Research Corporation, 2003.

[36] Harris, Charles D.: "Aerodynamic Characteristics of a 14-Percent-Thick NASA Supercritical Airfoil Designed for a Normal-Force Coefficient of 0.7", NASA TM X-72712, 1975.

[37] Mineck, Raymond E,; and Lawing , Pierce L.: "High Reynolds Number Tests of the NASA SC(2)-0012 Airfoil in the Langley 0.3-Meter Transonic Cryogenic Tunnel", NASA TM-89102, 1987

[38] Roskam, J. *Airplane Design:Part VI, Preliminary Calculation of Aerodynamic, Thrust and Power Characteristics.* Roskam Aviation and Engineering Corporation, 2003

[39] Harris, Charles: "NASA Supercritical Airfoils", NASA-TP 2969, Mar. 1990

[40] Yechout, Thomas R, et al, "Setting the Foundation for Flight Test – The AC-130U Gunship Drag Reduction Program", AIAA Paper 98-5532

[41] Hoak, D.E., et al, USAF Stability and Control Datcom, Airforce Flight Dynamics Laboratory, 1978

[42] Roskam, J. *Determination of Stability, Control and Performance Characteristics: FAR and Military Requirements.* Roskam Aviation and Engineering Corporation, 2003

[43] Drela, Mark and Harold Youngren. *Athena Vortex Lattice Method*. MIT. Retrieved 05 Oct. 2004. <http://raphael.mit.edu/avl/>.

[44] *AIAA Engine Deck*. Undergraduate Team Aircraft Design Competition. Retrieved 01 Dec. 2004. <http://www.aiaa.org/documents/student/enginedeck.xls>.

[45] Lutze, Dr.Frederick. "AOE 3104 Vehicle Performance." Virginia Polytechnic Institute and State University. Retrieved 07 Feb. 2005. <http://www.aoe.vt.edu/~lutze/AOE3104/>.